The mauC gene encodes a versatile signal sequence and redox protein that can be utilized in native and non-native protein expression and electron trnasfer systems

2016

Brian Dow
University of Central Florida

THE MAUC GENE ENCODES A VERSATILE SIGNAL SEQUENCE AND REDOX PROTEIN THAT CAN BE UTILIZED IN NATIVE AND NON-NATIVE PROTEIN EXPRESSION AND ELECTRON TRANSFER SYSTEMS

by

BRIAN ALDEN DOW
M.S. University of Central Florida, 2013
B.S. Missouri Western State University, 2011

A dissertation submitted in partial fulfillment for the requirements
for the degree of Doctor of Philosophy
in the Burnett School of Biomedical Sciences
in the College of Medicine
at the University of Central Florida
Orlando, Florida

Spring Term
2016

Major Professor: Victor L. Davidson

ABSTRACT

The redox-active type 1 copper site of amicyanin is composed of a single copper ion that is coordinated by two histidines, a methionine, and a cysteine residue. This redox site has a potential of +265 mV at pH7.5. Over ten angstroms away from the copper site resides a tryptophan residue whose fluorescence is quenched by the copper. The effects of the tryptophan on the electron transfer (ET) properties were investigated by site-directed mutagenesis. Lessons learned about the hydrogen bonding network of amicyanin from the aforementioned study were attempted to be used as a model to increase the stability of another beta barrel protein, the immunoglobulin light chain variable domain (V_L). In addition, amicyanin was used as an alternative redox partner with MauG. MauG is a diheme protein from the *mau* gene cluster that catalyzes the biogenesis of the tryptophan tryptophylquinone cofactor of methylamine dehydrogenase (MADH). The amicyanin-MauG complex was used to study the free energy dependence and impact of reorganization energy in biological electron transfer reactions.

The sole tryptophan of amicyanin was converted to a tyrosine via site-directed mutagenesis. This mutation had no effect on the electron transfer parameters with its redox partners, methylamine dehydrogenase and cytochrome *c*-551i. However, the pKa of the pH-dependence of the redox potential of the copper site was shifted +0.5 pH units. This was a result of an additional hydrogen bond between Met51 and the copper coordinating residue His95 in the reduced form of amicyanin. This additional hydrogen bond stabilizes the reduced form. Also, the stability of the copper site and the protein overall was significantly decreased, as seen by the temperature dependence of the visible spectrum of the copper site and the circular dichroism spectrum of the protein. This destabilization is attributed to the loss of an interior, cross-barrel hydrogen bond.

The V_L is structurally similar to amicyanin, but it does not contain any cross-barrel hydrogen bonds. The importance of the cross-barrel hydrogen bond in stabilizing amicyanin is evident. A homologous bond in

V_L was attempted to be engineered by using site-directed mutagenesis to insert neutral residues with protonatable groups into the core of the protein. Wild-type (WT) V_L was purified from the periplasm and found to be properly folded as determined by circular dichroism and size exclusion chromatography. Mutants were expressed in *E.* coli using the amicyanin signal sequence for periplasmic expression. Folded mutant protein could not be purified from the periplasm.

When amicyanin is used in complex with MauG, it retains the pH-dependence of the redox potential of its copper site due to the looseness of the interprotein interface. The free energy of the reaction was manipulated by variation in pH from pH 5.8 to 8.0. The ET parameters are reorganization energy of 2.34 eV and an electronic coupling constant of 0.6 cm^{-1}. P94A amicyanin has a potential that is 120 mV higher than WT amicyanin and was used to extend the range of the free energy dependence studied. The ET parameters of the reaction of WT and P94A amicyanin with MauG were within error of each other. This is significant because the ET reaction of P94A amicyanin with its natural electron acceptor was not able to be studied due to a kinetic coupling of the ET step with a non-ET step. This kinetic coupling obscured the parameters of the ET step because it is not kinetically distinguishable from the ET step.

A Y294H MauG mutant was also studied. This mutation replaced the axial tyrosine ligand of the six-coordinate heme of MauG with a histidine. No reaction is observed with Y294H MauG in its native reaction. However, the high valent oxidation state of the five-coordinate heme of Y294H MauG reacts with reduced amicyanin. The ET rate was analyzed by ET theory to study the high valent heme in Y294H MauG. The reorganization energy of Y294H MauG was calculated to be nearly 20% lower as compared to the same reaction with WT MauG. These results provide insight into the obscured nature of reorganization energy of large redox cofactors in proteins, particularly heme cofactors, as well as to how the active sites of enzymes are optimized to perform long range ET vs catalysis with regard to balancing redox potential and reorganization energy.

Dedicated to my family who has always supported me through every challenge
Keishla, Danica
Walt, Dianne, & Matt

ACKNOWLEDGMENTS

I express my deepest gratitude and appreciation to my famous, expert advisor and mentor, Dr. Victor L. Davidson for his guidance, patience, and example. In a world of fluorescent microscopes, he has been able to show me the utility and advantage of studying basic biochemistry and enzyme kinetics. Also I thank him for emphasizing the principle of Ockham's razor and not letting me (or anyone else in the lab) get swept away by overly complicated or unprecedented ideas.

I thank my committee members, Suren Tatulian, William Self, and Kyle Rohde for technical support in performing experiments and also for supporting me and my work in the Burnett School of Biomedical Sciences. I also appreciate and thank Dr. Griff Parks, Dr. Sampath Parthasarathy, and Dr. Richard Peppler for their vision, guidance, and support of our lab and department as a whole.

Particular thanks go to the rest of our lab group who have helped me keep my sanity, and, at times, tolerate my insanity. Specifically to Esha Sehanobish for her camaraderie, empathy, and teamwork; Heather Williamson for being a readily accessible font of biochemistry trivia; Yu Tang for her understanding and selfless willingness to express and purify proteins and provide buffers solutions, gels, and more. She is a most valuable anchor in the lab; Moonsung Choi and Sooim Shin for welcoming me to the lab and providing expertise in designing and performing experiments.

Throughout my tenure at UCF, I have also enjoyed the company and friendship of many of my fellow students, especially Jason O. Matos, Aladdin Riad, and Richard Barrett, and everyone in the Biomedical Sciences Graduate Student Association. I thank them as well for helping me maintain my sanity.

Finally, I thank my love, Keishla, and our beautiful daughter, Danica. They have always been on my mind or literally looking over my shoulder, demanding hard work, precision, integrity, and excellence. They have also both had unbelievable patience and understanding with me during my studies. Gracias.

TABLE OF CONTENTS

LIST OF FIGURES

LIST OF TABLES

LIST OF ABBREVIATIONS

λ ..... reorganization energy

CD ..... circular dichroism

Em ..... oxidation-reduction midpoint potential

ET ..... electron transfer

H_{AB} ..... electronic coupling

MADH ..... methylamine dehydrogenase

preMADH ..... precursor protein of MADH with incompletely synthesized TTQ

RMSD ..... root mean square deviation

SVD ..... singular value decomposition

Tm ..... midpoint temperature for a spectroscopic transition

TTQ ..... tryptophan tryptophylquinone

V_L ..... light chain variable domain

WT ..... wild-type

1 GENERAL INTRODUCTION

It is of great interest to further the general understanding of protein structure-stability relationships and how enzymatic reactions are optimized by the protein and its cofactor. The structure-function relationships of proteins have long been studied and well characterized. However, as more proteins and enzymes find applications in biotechnology, it is important to understand the limits of the stability of a protein and also how to improve the stability. Also, as more enzymes are being pursued for new enzymatic chemistries, it is beneficial to understand how cofactors are optimized for their reactions. By understanding the nature of the cofactors of existing enzymes, rational methods can be used to modify existing enzymes for new reactions, instead of attempting to design and fold *de novo* enzymes. This dissertation will use amicyanin as a model protein for studying protein structure-stability relationships and also as a tool for studying the nature of the diheme cofactor and its associated enzymatic reactions in MauG.

Amicyanin is a small blue copper protein from the cupredoxin family of proteins. It consists of a single beta barrel domain, which is composed strictly of beta sheets and loops with no helices. The "cupredoxin-like" fold of amicyanin is structurally conserved and similar to many protein superfamilies, such as the "immunoglobulin-like fold" of the V_L. It can be recombinantly expressed and purified from the periplasm of *E. coli*. Due to its relatively simple fold and evolutionary conserved and shared structure, as well as its ability to be easily expressed and purified, it is a prime candidate for extending our basic understanding of protein structure, intramolecular forces, and their relation to the stability of the active site and overall fold of the protein.

Site-directed mutagenesis is a versatile tool for exploring protein structure and stability and for understanding the relation between the structure and stability of evolutionarily conserved protein structures. Site-directed mutagenesis is utilized in this dissertation as a means of investigating the sole tryptophan residue of amicyanin. This tryptophan, Trp45, is over ten angstroms away from the redox site. However, its

fluorescence is affected by the copper in the redox site. This may occur either by electron transfer or by energy transfer. A W45Y mutation is introduced to study any effects the tryptophan may reciprocate to the copper. Trp45 is seen to play a role in the stability of amicyanin, and site-directed mutagenesis is used in an attempt to engineer a homologous tryptophan or similar residue within a structurally similar protein to recreate its effect in amicyanin within a different protein.

Amicyanin is also used as an enzymatic tool to probe the reactivity and parameters of the cofactor of WT and Y294H MauG. In complex with MADH, the redox potential of amicyanin is pH-independent. However, in complex with MauG, the redox site has a pH-dependent redox potential. His95 provides the pH-dependence of the redox potential by flipping out of coordination with the copper ion, when it is protonated. By varying the pH, the redox potential of amicyanin can be altered in order to study the free energy dependence of k_{ET} between reduced amicyanin and the high valence redox state of the diheme cofactor in MauG by stopped-flow spectroscopy. The free energy dependence is preferable over studying the temperature dependence for many reasons, including the ability to study the ET parameters of only the ET step in the kinetic mechanisms of the reaction. Temperature can alter kinetic reaction mechanisms and several of the ET parameters, while varying the free energy of the reaction does not. Despite the preference for studying the free energy dependence of ET, this is a very rare feat performed in proteins due to the technical limitations in selectively modifying the redox site to alter its redox potential. Thus, the ability to study the free energy dependence of k_{ET} in this complex will add to the relatively sparse data describing the free energy dependence of interprotein electron transfer reactions in the literature. Studying high valent heme species is also a difficult feat due to their inherent high reactivity and transiency, but in the unique case of MauG, this is possible to do. In MauG the high valent state is unusually stable and degrades on a time scale of several minutes, instead of seconds, like in other peroxidases. In addition to studying the free energy

dependence of biological interprotein ET reactions and gaining insight into the high valent diheme cofactor of MauG, this reaction scheme can be used to study the Y294H mutation in MauG.

Y294H MauG was not able to be studied in its native system because no reaction was observed. This is hypothesized to result from an inactivation of the six-coordinate heme. This inactivation resulted in a prohibitively large ET distance, around 40 Å, between the five-coordinate heme and its substrate, preMADH. This mutant does however react with reduced amicyanin. In complex with amicyanin, the ET distance between the five-coordinate hem and the copper site of amicyanin is around 14 Å. In this dissertation, reduced amicyanin will be used with Y294H MauG in order to further characterize the effect of this mutation on the high valent heme cofactor of MauG. The results and implications from this study will be presented and discussed with regard to the function, optimization, and design of cofactors for catalysis vs electron transfer, how these results impact our understanding of the nature of redox cofactors in ET theory, and also to the further insight gained about high valent heme species.

2 LITERATURE REVIEW

2.1 Cupredoxins

2.1.1 Type 1 Copper Site Structure and Spectra

Cupredoxins are a family of proteins from bacteria, fungi, and plants which mediate interprotein electron transfer via their type 1 copper site. The type 1 copper site is composed of a single copper ion coordinated by four residues. These residues include a cysteine, two histidines, and a weaker variable axial ligand. This variable ligand is a methionine in amicyanin[1], pseudoazurin, rusticyanin, and plastocyanin, while in stellacyanin it is a glutamine[2]. In the case of azurin, it is a methionine and also the backbone carbonyl of Gly45[3, 4]. The strong interaction between the sulfur of the cysteine and the Cu(II) ion produces an intense visible absorbance feature centered around 600 nm. This results from the S(Cys)π—>Cu(II)d_{X2-y2} ligand-to-metal charge transfer transition. Electron paramagnetic resonance (EPR) spectra exhibit very narrow hyperfine splitting in the parallel region[5].

In type 1 copper proteins, these amino acid ligands hold the copper ion in specified geometries which determine the redox potential of the copper ion. The geometry of the copper ion can also be influenced by the oxidation state of the copper, as well as the pKa of the amino acid ligands, which may affect the coordination of the copper ion. When the copper in amicyanin is coordinated by four amino acid ligands, the copper is pulled out of the trigonal planar geometry by the weaker ligand into a distorted rhombic configuration. Another variation of the type 1 copper site is seen in ceruloplasmin. Ceruloplasmin is a eukaryotic multi-copper protein with six cupredoxin-like domains and multiple types of copper centers. In one of the type 1 sites of ceruloplasmin, one of the ligands is replaced by a Leu residue, which cannot coordinate copper. Despite this, the site retains the spectral features of a type 1 copper site[6].

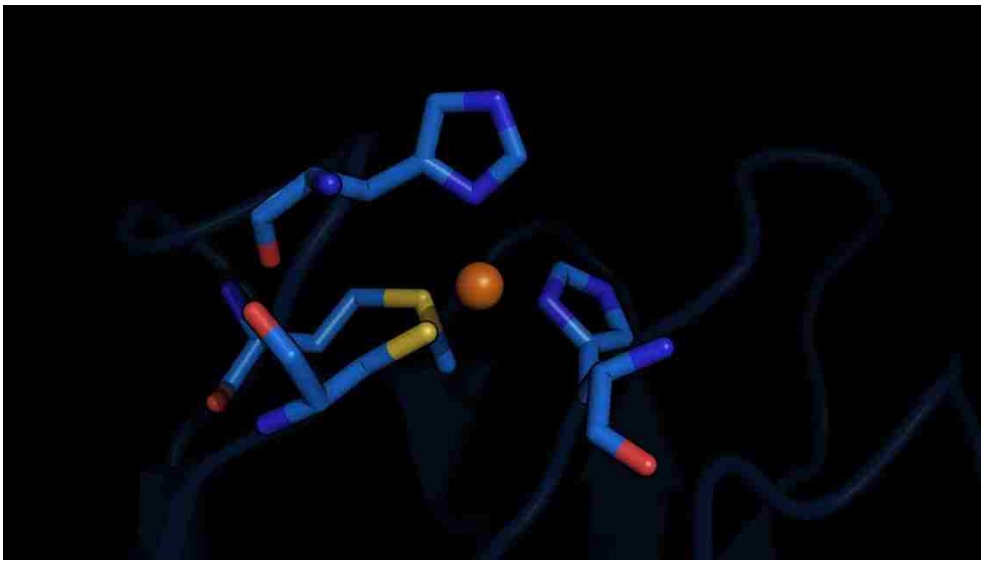

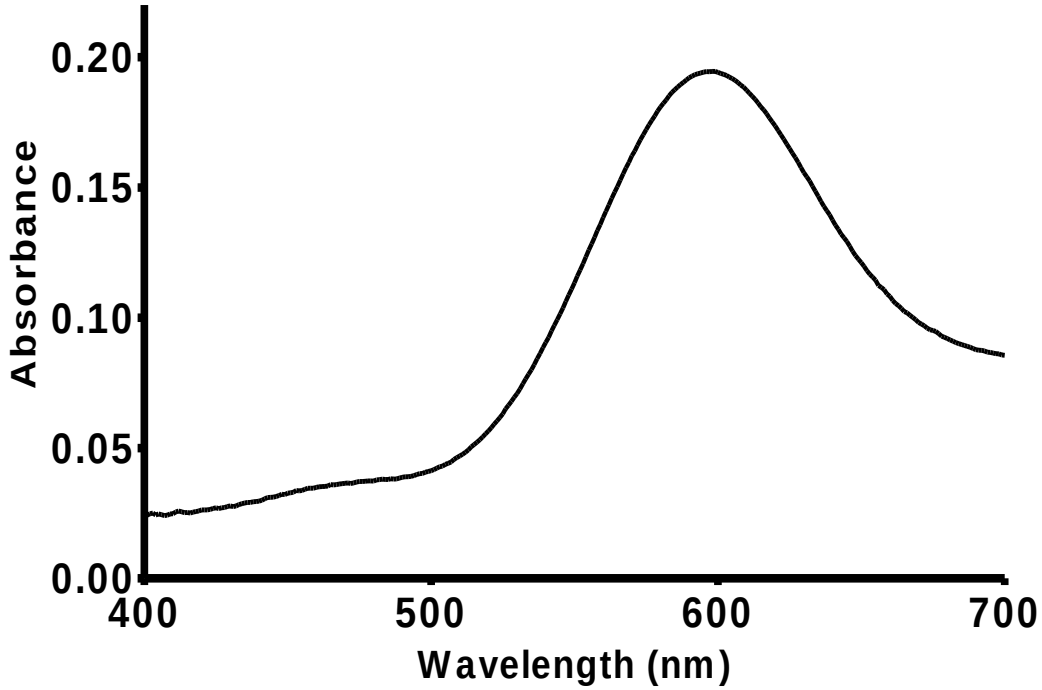

Figure 2.1.1 Structure and Spectra of the Type 1 copper site in amicyanin. Top) Structure of the Type 1 copper site of amicyanin. The copper is shown as a sphere, and its ligands are represented as sticks. Bottom) Visible absorbance spectra of the type 1 copper site in amicyanin.

2.1.2 Redox Potential

Cupredoxins exhibit a wide range of natural redox potentials of approximately +200 to +700 mV at pH 7. Through site-directed mutagenesis, this range has been increased to approximately -1000 mV to +1000 mV. This redox potential is influenced primarily by the coordination and conformation of the copper ion. In the case of amicyanin, the oxidized copper ion is held in a distorted tetrahedral conformation, when coordinated by all four ligands. One of the histidine ligands has a pKa near pH 7.7. Below this pKa, the histidine is protonated and the nitrogen which provides the copper ligand is flipped away from the copper ion. As the pH decreases, the redox potential increases. However, when amicyanin is in complex with MADH, its natural redox partner, this histidine is sterically hindered and held into the coordination sphere of the copper[7]. Thus, the redox potential is pH independent, when amicyanin is in complex with MADH. A similar "histidine flip" is seen in spinach plastocyanin at pH 4.9. The pKa for the histidine in amicyanin and plastocyanin are both near their respective physiologic pH in the periplasmic space and thylakoid space.

The relative hydrophobicity or hydrophilicity of the copper site also influences the redox potential. Most copper centers are surrounded by a hydrophobic pocket. This increases the redox potential because the copper site will prefer the less charged Cu(I) oxidation state. In this way, second sphere ligands, which are residues that make contacts with the copper ligating residues, can also impact the redox potential or pKa of the pH dependence of the redox potential. A P94A mutation in amicyanin of *P. denitrificans* was shown to increase the redox potential by approximately 120 mV, and this mutation also shifted the pKa to a more acidic pH[8]. These changes resulted from an additional hydrogen bond formed between the thiolate of the cysteine that coordinates with the copper ion as a result of the mutation. Similar results have also been seen in a P80I mutation in pseudoazurin of *Alcaligenes faecali*[9]*s* and a N47S mutation in azurin[10]. An F114G and F114P mutation in azurin also resulted in the gain and loss of a hydrogen bond in the copper site. This resulted in the increase and decrease of the redox potential, respectively[2, 10].

Table 2.1.1 Redox potential of various cupredoxins.

Protein	Redox Potential (mV) at pH 7.0	Reference
Stellacyanin	184	[11]
Azurin	265	[12]
Pseudoazurin	270	[13]
Amicyanin	294	[14]
Plastocyanin	370	[15]
Rusticyanin	680	[16]

2.1.3 Structure

2.1.3.1 *Beta Barrel Fold*

The beta barrel protein fold is one of the most ubiquitous and versatile in nature. Proteins with this fold are composed of one or more beta-sheets, which themselves are composed of antiparallel beta strands. Typically the residues on each strand alternate in hydrophilicity and hydrophobicity so that either mostly hydrophilic residues are on the inside and mostly hydrophobic residues are on the outside, such as in membrane channels, or vice-versa, such as in water-soluble proteins[17].

Beta barrels are generally composed of successive antiparallel strands which are bonded via hydrogen bonds to preceding and following strands. Usually the strands are bonded together to form two beta sheets. These beta sheets pack face-to-face to form a beta sandwich motif. This simple type of beta barrel can be seen in porins and retinol binding protein, for example[18, 19]. The Greek key motif is characterized by a series of antiparallel strands which are hydrogen bound to the preceding and following strand. One of the strands is bound to a strand on the opposite side of the barrel by a long loop[20, 21].

Several Greek key motifs can be formed in the same barrel. Two overlapping Greek key motifs can be formed into a "jelly roll" barrel. These are common in domains of spherical viruses, such as the rhinovirus[22]. A final beta barrel motif is the chymotrypsin-like fold, which is found in chymotrypsin and all other serine proteases. This fold is characterized by four strands that form a Greek key motif immediately followed by two antiparallel strands[23].

Proteins with the beta barrel Greek key motif have a wide variety of functions and come from a wide variety of organisms as referenced above. This alludes to the evolutionary basicness of this fold, and explains its widespread presence throughout biology. Examples of beta-barrel proteins with the Greek key motif span

from the cupredoxin family of electron transfer mediating proteins to the immunoglobulin variable domain of mammalian antibodies[24]. Cupredoxins are widespread throughout biology and can be found in bacteria, fungi, and plants[25]. Cupredoxin-like domains can also be found in various mammalian enzymes, such as complex IV of the electron transport chain[26]. Understadning the amino acids and bonding structure involved in developing and maintaining these folds is just as important as the redox active site. These folds determine the stability and longevity of these proteins *in vivo*, and also nearby residues involved in the fold can also affect the surrounding environment of the redox center, which tunes its ET properties.

2.1.3.2 *Amicyanin*

Amicyanin is a 12.5 kDa beta barrel protein in a Greek key motif composed of beta sheets and loops with no alpha helices. It has a series of interior hydrophobic residues in a diagonal pattern that are conserved amongst cupredoxins and other beta barrel proteins, such as the immunoglobulin light chain variable domain[27]. One peculiarity of this feature is a tryptophan residue that is semi-conserved amongst cupredoxins. Neutron diffraction coupled to hydrogen-deuterium exchange studies have shown that this residue is one of relatively few that does not exchange hydrogens in amicyanin[28]. This tryptophan is also implied in influencing the catalytic site of amicyanin due to the possibility of Förster energy transfer or electron transfer between the residue and the copper ion of the active site[29, 30]. Thus, this residue may be implied in either structural or functional effects of the protein, or both. Effects in either of these categories may have broad implications for ET proteins or beta barrel proteins in general, since this residue is part of a series of conserved residues.

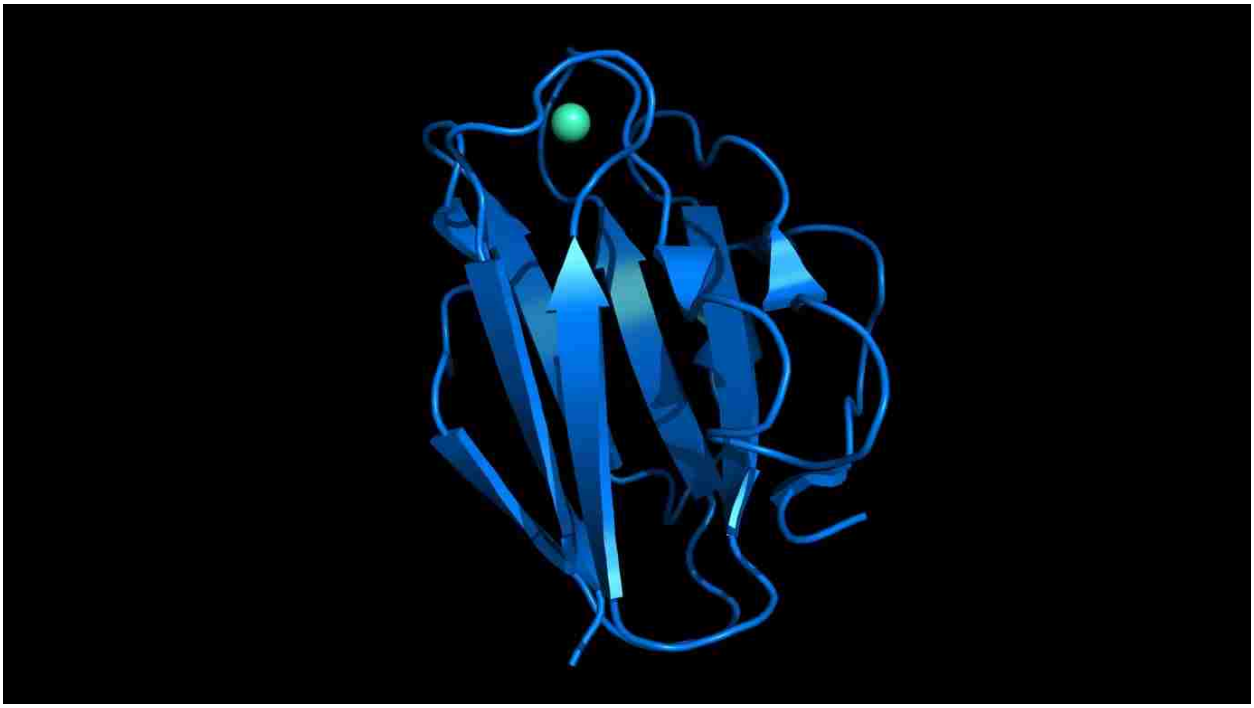

Figure 2.1.2 Structure of amicyanin. The overall structure of amicyanin is presented with the copper ion shown as a light green sphere.

2.2 Immunoglobulin Light Chain Variable Domain (V_L)

2.2.1 Structure

The Ig V_L is composed of nine β-strands packed tightly against each other in two face-to-face antiparallel β-sheets in the form of a Greek key beta barrel[31]. The majority of the Ig V_L is highly conserved. There are three regions known as the complementarity determining regions (CDR), which are hypervariable. These regions are the part which recognize and bind to the epitope of antigens. The CDRs consist of three loops at the N-terminus of the protein. The fold of the Ig V_L, known as the "immunoglobulin-like fold" has conserved structural feature shared with many protein families.

One of the protein families that share conserved structural features with the V_L is the cupredoxin family of proteins. They consist of a beta-barrel structure with two beta sheets in a Greek key motif with little or no alpha helical secondary structure[27]. When the beta sheets and a conserved beta loop are structurally aligned using the RCSB Pairwise FATCAT flexible or rigid alignment algorithms, the resulting alignment RMSD is 1.68 angstroms[32]. Also, the V_L has a single disulfide bond in the same position as the metal center in cupredoxins. Amongst all the cupredoxins, the V_L has the most similarity with amicyanin. Both of them lack alpha helices and contain a homologous interaction at nearly the same spatial position in the amino terminus (a disulfide bond in the V_L and a strong Cu-S bond in the metal center of amicyanin) without any additional disulfide bonds near the C-terminus (Fig. 2.2.1) [1, 33].

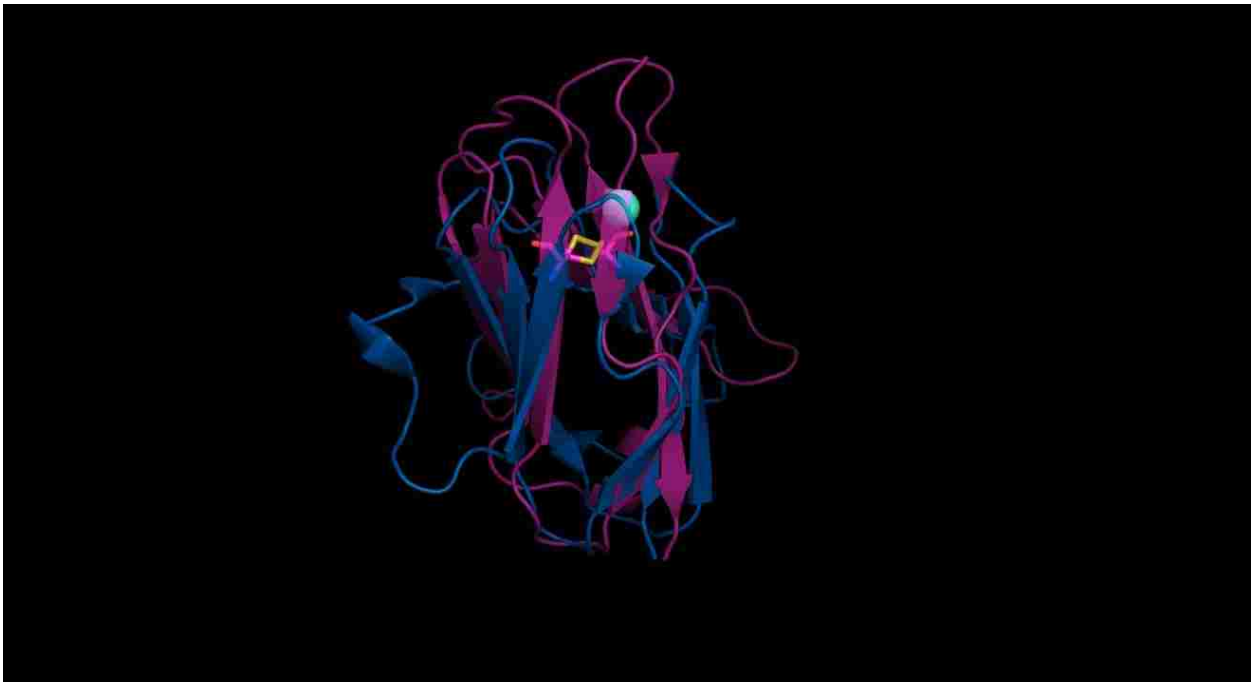

Figure 2.2.1 Structural alignment of an immunoglobulin light chain variable domain and amicyanin. Amicyanin is represented in blue with the copper ion as a light green sphere. The light chain variable domain is represented in pink with the disulfide bond represented as sticks.

2.2.2 Stability

It is widely believed that the aggregation characteristics of antibody based therapeutics are determined by the stability of the light and heavy chain variable domains. Antibodies which vary exclusively in their variable domains have been shown to have very different aggregation rates[34]. The heavy chain variable domain (V_H) has been successfully engineered to exhibit more favorable biophysical properties by studying the factors which contribute to the high stability and low aggregation propensity of the antibodies of camelids, such as camels and llamas. However, these improvements have been attributed to significant conformational changes in the interface with the light chain variable domain (V_L) that increases the hydrophilicity of the heavy chain variable domain[35, 36]. These structural changes are not a problem in camelids because they are naturally devoid of light chains. This is however a problem for engineered human antibodies because their heavy and light chain domains must be able to successfully pair up.

The intra-domain interactions responsible for the decreased stability and unfolding of the V_L remain to be elucidated. Identification of these factors has proven difficult due to the high sequence diversity in the CDR and the need to maintain antigen binding. Some recent efforts have been aimed at identifying conserved key positions in the area of the antigen binding loops by the use of phage display. These studies utilized the monoclonal antibody found in the anti-breast cancer therapeutic Herceptin and identified key positions in the CDR that mediate aggregation but did not alter binding with the Herceptin target molecule. Although these mutations did not affect the Herceptin immune complex, these same mutations may affect binding in other antibody-antigen complexes[37]. Other groups have been using phage display in combination with high temperatures or denaturing conditions to identify mutants with high stability[38, 39]. However, some of these mutations are also located in the CDR. Another method involves calculation of a new parameter, Spatial Aggregation Propensity (SAP), which determines the effective dynamically exposed hydrophobic patches, which are prone to aggregation. These patches are subsequently mutated by targeted mutagenesis

to increase the hydrophillicity[40]. The binding affinity for these mutants also needs to be checked for each specific antibody. It is much more desirable to identify a global method to engineer increased stability without altering the antigen binding loops. This method should be aimed at increasing the stability of the beta barrel fold of the V_L.

2.2.3 Applications

An increasing number of recombinant monoclonal antibodies and human single chain fragments (scFV) therapeutics are currently in clinical trials and are being approved. scFVs are fusion proteins consisting only of the variable domains of the heavy and light chains connected by a short linker peptide. They especially are of increasing interest in biotechnology for medical imaging and tumor targeting applications. Despite the increasing trend toward the use of therapeutic biologics, protein aggregation represents a major technical challenge in the manufacture, storage, and use of antibody based therapeutics. Antibodies are resistant to *in vivo* environmental stressors. However, during purification, concentration, formulation, storage, and final filling, they are subjected to extreme temperatures, pH, and mechanical strain. The ability to store and administer antibodies at high concentrations (~100 mg ml^{-1}) is necessary for therapeutic administration both in a medical care facility and at-home [41-43]. An anti-idiotype response to the antigen binding region of humanized monoclonal antibodies can be elicited upon the second exposure to the therapeutic[44]. This necessitates that the first exposure be as concentrated as possible for maximal efficacy during first exposure. Also, at-home administration requires the therapeutic to be able to be administered in a relatively small volume. High concentrations during administration also increase the risk for *in vivo* antibody aggregation. This could mimic light chain deposition disease, in which aggregates cause pathological depositions on organs, which lead to organ failure and eventually death[45]. Another key consideration for at-home administration is the viscosity of the solution. The viscosity must be kept as low as

possible to prevent mechanical strain to the antibody, to prevent discomfort to the patient, and also to provide as accurate as possible dosing in pre-filled syringes[34]. For these reasons, antibodies must be stored and used at high concentrations. However, the high concentration increases the probability of aggregation and unfolding. The innate instability of these molecules leads to significantly decreased shelf life, even at low temperatures. Antibody solutions with a population of partially unfolded or aggregated antibodies have decreased efficacy and can even be immunogenic when administered in the body.

2.3 Heme Proteins

2.3.1 Heme Types

A heme is a cofactor that contains an iron ion coordinated by a large heterocyclic ring made of four conjoined pyrroles known as a porphyrin. There are several different types of hemes, which are distinguished by the substituent groups on the porphyrin. The three most common heme types are A, B, and C. Heme B is the most biologically common heme. It is found in hemoglobin, myoglobin, catalase, various peroxidases, cyclooxygenase-1/2, and cytochrome P450. The iron ion in Heme B is generally coordinated by a single residue. Typically this residue is a histidine or a cysteine, as seen in hemoglobin and cytochrome P450, respectively[46]. The structure of heme A is derived from that of heme B with the addition of a hydroxyethylfarnesyl group and the conversion of a methyl group to a formyl group. Heme A can be found in cytochrome c oxidase of the electron transport chain. Cytochrome c oxidase has two a-type hemes. These hemes readily exchange electrons between themselves and neighboring copper sites[47]. C-type hemes are covalently bound to the protein via one or two thioether bonds with cysteine residues. These residues are found in a conserved CXXCH motif, where the two cysteines bind the porphyrin and the histidine provides an axial ligand for the iron ion. C-type cytochromes, which function as electron carriers, are a common example of this type of heme in nature[46].

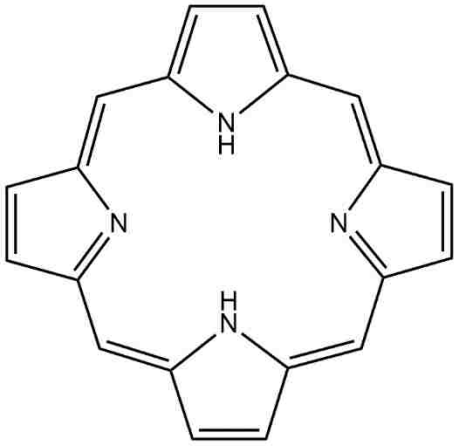

Figure 2.3.1 Basic porphyrin ring

Table 2.3.1 Substituents of Hemes A, B, & C

	Heme A	Heme B	Heme C
Functional Group at C3	-CH(OH)CH_2Farnesene	-CH=CH_2	-CH(cysteine-S-yl)CH_3
Functional Group at C8	-CH=CH_2	-CH=CH_2	-CH(cysteine-S-yl)CH_3
Functional Group at C18	-CH=O	-CH_3	-CH_3

2.3.2 Heme Redox Properties & Function

Hemes can exist in a variety of oxidation states, ranging from Fe(II) to an Fe(V) equivalent. The various oxidation states of the heme play indirect and direct roles in the catalytic and electron transfer mechanism of the protein. For example, the catalytic cycle of heme-dependent peroxidases involve three consecutive redox states; two of them involve high valent oxidation states s (compound I and compound II), which perform the H_2O_2-mediated catalytic oxidation of substrate. Thus, the steady state kinetics of the catalytic cycle are affected by the oxidation-reduction potentials of three redox couples: compound I/Fe(III), compound I/compound II and compound II/Fe3+. Even though the catalytic mechanism relies on the reduction of the high valent states, generation of the H_2O_2 oxidation of peroxidases to compound I requires that the heme be able to stabilize the ferric state in physiologic conditions. Thus, the catalytic mechanism depends on and can be gated by the reduction potential of the Fe(III)/Fe(II) couple[48, 49].

In heme peroxidases, the Fe(III)/Fe(II) redox couple is negative. This helps to ensure that the iron is in the ferric state in physiologic conditions. As discussed earlier, this is a prerequisite for the *in vivo* function of the enzymes. Although the potentials are all negative, there is significant variability in the potentials. This indicates that the individual microenvironments of the hemes in the various enzymes adjust the potential of the hemes. Specifically, the Fe(III)/Fe(II) couple is affected by the electronic properties of the electron donating axial iron ligand(s), the polarity of the heme pocket, and the electrostatic interactions between solvent, protein residues, and the heme center[50-52].

The same five-coordinate iron ligation is shared by peroxidases and globins. The iron is coordinated by four nitrogens in the porphyrin heterocycle and a nitrogen from a histidine ligand. Despite this commonality, peroxidases have a negative Fe(III)/Fe(II) redox couple, while globins have a positive couple. The positive redox potential ensures the ferrous form is maintained under physiologic conditions[53, 54]. This

form is able to bind oxygen, which is essential to the function of many globins, such as hemoglobin and myoglobin. This positive potential is made possible by the neutral electronic character of the axial histidine. The neutral charge is an effect of weaker hydrogen bonding between the histidine and a neighboring backbone carbonyl group as compared to peroxidases and reduces the amount of electron sharing between the histidine and iron, and this raises the redox potential of the iron.

It is important to understand the molecular details of the mechanism of peroxidases and other heme-depedent enzymes whose catalytic cycle involve oxyferryl intermediates. This can be seen in the catalytic cycle of cytochrome P450cam (Figure 1.4.2). Some examples of these enzymes include cytochrome *c* oxidase, catalase, and cytochrome P450. However, it is very technically difficult to study these intermediates due to their inherent instability and side reactions which may occur due to their high reactivity. Despite this technical challenge, the compound I/compound II and compound I/Fe(III) couples of a few different plant and bacterial peroxidases have been determined experimentally. However, it is still very evident that there is a lack in the understanding of these high valent heme species in biology due to the vast diversity of heme-dependent enzymes throughout all kingdoms of biology which catalyze an equally diverse number of different reactions.

Horseradish peroxidase was determined by Farhangrazi et al. to have a compound I/compound II couple of 898 mV and a compound II/ Fe(III) couple of 869 mV[55]. Whereas in Cytochrome *c* peroxidase, only the compound I/ Fe(III) couple has been determined. This was found to be 717 mV[56]. *Anthromyces ramosus* peroxidase has a compound I/compound II and compound II/Fe(III) couple of 915 mV and 982 mV, respectively[57]. This peroxidase is the only one known to date to have a higher compound II/ Fe(III) couple than its compound I/compound II couple. This reversal in order of redox potentials can have implications with regard to its reactivity and what reactions it can catalyze.

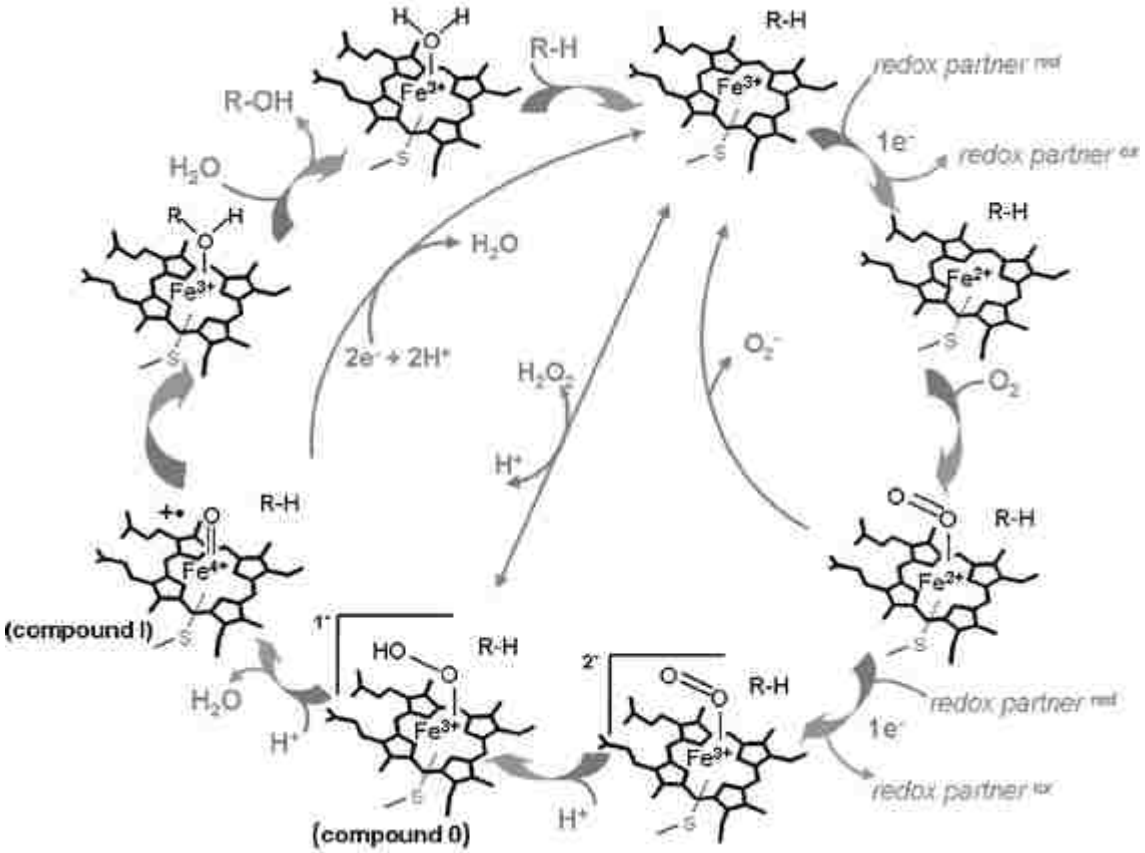

Figure 2.3.2 Catalytic cycle of cytochrome P450[58]

Table 2.3.2 Reduction potentials and heme types of various heme-dependent enzymes

Protein	Fe(III)/Fe(II) Potential (mV)	CpdI/CpdII Potential (mV)	CpdII/Fe(III) Potential (mV)	Heme type	Reference
Soybean APX	-159	1156	752	b	[59]
S. cerevisiae CcP	-194	717[1]	717[1]	a	[60]
M. tuberculosis KatG	-60			a	[61]
A. ramosus peroxidase	-183	915	982	b	[62]
C. cinereus peroxidase	-219			b	[63]
HRP A_2	-190	920	880	c	[64]
HRP-C	-270	898	869		[65]

[1] Represents average of CpdI/CpdII couple and CpdII/Fe(III) couple

2.3.3 MauG

MauG is a 42.3 kDa protein from the mauG gene of the mau gene cluster from *Paracoccus denitrificans*. Its active site is composed of two covalently bound *c*-type hemes with an intervening tryptophan residue. These hemes display cooperativity and function as a single redox site. It is the first enzyme described that utilizes a diheme center to catalyze a monooxygenation reaction, however it does not exhibit peroxidase activity. Instead, it has been shown that the diheme is responsible for the posttranslational modification of MADH that generates the protein-derived cofactor, TTQ.

In MADH, TTQ is formed from residues βTrp57 and βTrp108. The substrate for this reaction is a monohydroxylated precursor (preMADH) in which one oxygen atom has been inserted into the in mV and -dole ring of βTrp57. Maturation of the TTQ cofactor is a six-electron oxidation process comprised of three two-electron oxidations. These two-electron oxidation reactions require the formation of a high-valent *bis*-Fe(IV) MauG intermediate in which one heme is present as Fe(IV)=O with an axial ligand provided by a His and the other is present as Fe(IV) with His-Tyr axial ligation and no exogenous ligand. This redox state is stabilized even though the two heme irons are separated by 21.1 Å. This has been shown to occur through an ultrafast ET between the two hemes via an intermediate Trp residue, Trp93. This ultrafast ET provides for a resonance-like equilibrium between a variety of charge states on the two hemes and Trp93[66-68].

The Fe(III)/Fe(II) redox couple for the two electron transfers has been shown to be -159 and -244 mV. This was done by spectrochemical titration with sodium dithionite and potassium ferricyanide using FMN and safranin T as electron mediators. Cyclic voltammetry determined a midpoint potential of -198 mV. This method is not able to distinguish the two electron reductions. However, this value correlates well with the average of the two potentials determined from the spectrochemical titration[69]. The redox potential of the higher oxidation state of *bis*-Fe(IV) has not yet been determined experimentally. However, comparison of

the reorganization energies of the reaction of the ferrous form of MauG with the TTQ of quinone MADH showed that the redox potential of *bis*-Fe(IV) MauG should be near +700 to +800 mV[70].

2.4 Interprotein Electron Transfer Reactions

2.4.1 Electron Transfer Theory

Long range electron transfer (ET) is a fundamental metabolic process that is necessary for respiration and catalysis. Although this is a fundamental biochemical process, there is still a lot to learn regarding different ET mechanisms and how ET is regulated and optimized by nature for the specific reactions.

The electron transfer rate (k_{ET}) can be described by electron transfer theory. In electron transfer theory, several parameters, including the free energy ($\Delta G°$), electronic coupling (H_{AB}), and the reorganization energy (λ) of the reaction determine k_{ET}. The free energy is the difference in redox potential of the donor and acceptor redox sites. If the electron acceptor is more electronegative than the electron donor, the reaction is more thermodynamically favorable. The H_{AB} is a combined expression of the intervening protein medium with regard to its ability to conduct electrons and the distance the electron travels. The reorganization energy reflects the amount of energy needed to rearrange the reactant states of the molecules to their product states. An alternative equation can also be used to predict the direct edge to edge ET distance from the donor and acceptor redox sites. This equation takes into account the exponential decrease in k_{ET} over distance[71, 72].

2.4.2 Defining Reorganization Energy

In particular, reorganization energy in interprotein electron transfer reactions can become obscured by interactions of solvent and other nearby residues with the redox center. Reorganization energy has two spheres. The inner sphere is composed of the energy needed to optimize bond angles and lengths of the

redox cofactors, while the outer sphere is the energy needed to change bulk solvation and/or the orientation of solvent molecules. In small molecules, these two terms are well distinguished. However, these lines blur in proteins as the cofactors become larger with an asymmetrical electron density. In general, there are relatively few protein complexes for which the reorganization energy has been determined either experimentally or theoretically using computational methods. QM/MM (Quantum mechanical/ molecular mechanics) methods have been used to determine λ for protein ET reactions. In these calculations, the methods tend to focus on the contributions of the protein medium[7, 73]. Reorganization energy has also been calculated for interprotein reactions between the redox cofactor and an added redox active tag such as Ruthenium complexes[74, 75]. Lasers have also been used to generate disulfide radicals which act as electron donors for other intraprotein reactions. The reorganization energies for these reactions have also been determined[76]. The reactions of amicyanin with MADH[77] and cytochrome c-551i[78], and the reactions between MauG and preMADH and MADH[79] are amongst the few native biologic reactions for which reorganization energy has been described.

2.4.3 Free Energy Dependence of Electron Transfer Reactions

It is preferable to study the free energy dependence of an ET reaction in order to ascertain its true ET parameters. When using the temperature dependence, it is important to keep in mind that the parameters obtained using this method can contain contributions from preceding non-ET steps such as a conformational change, if these steps limit the ET step and/or are affected differently at various temperatures. Also, the temperature can affect the K_d of the complex and the redox potential of the redox site. However, when one uses the free energy dependence of the reaction, these considerations do not need to be taken into account because they are unaffected by the free energy of the reaction. This is rarely ever able to be achieved, though, due to the technical difficulty to specifically modify the redox potential of a cofactor in a protein.

Usually this can be done by site-directed mutagenesis, however, more often than not various other properties are also affected.

2.4.4 Kinetic Complexity of Interprotein Electron Transfer Reactions

ET theory can only be used to accurately describe the electron transfer step. However, there are three different kinetic mechanisms that can describe electron transfer reactions. These mechanisms are known as: True, Gated, and Coupled. In a true ET event, the observed rate constant (k_{obs}) and k_{ET} are equal. In this reaction scheme, K_{ET} is thermodynamically favorable. However it is much slower than any preceding non-ET reaction steps. Examples of these steps can include conformational changes or changes in the orientation of solvent molecules. The combined rate and equilibrium for any and all of the preceding non-ET step(s) is described by k_X and K_X, respectively. In a gated ET mechanism, k_X is prohibitively slower than k_{ET}. In this case k_{Obs} is k_X[80, 81] . However, in the case where the preceding non-ET step is rapid but not thermodynamically favorable, the ET step is kinetically coupled to the non-ET step(s). In coupled ET reactions, k_{Obs} is the product of K_X and k_{ET}.[82]

3 SECTION I: STRUCTURE AND STABILITY OF AMICYANIN AND AN IMMUNOGLOBULIN LIGHT CHAIN VARIABLE DOMAIN

3.1 Section I Introduction

One of amicyanin's interesting features is that it contains one tryptophan residue, Trp45, which is located over ten angstroms away from the copper center. Despite this large distance, the fluorescence of the tryptophan is quenched, when the copper site is constituted with a copper ion. This same quenching phenomenon is exhibited in other cupredoxins, such as pseudoazurin[83], but it is not known if this tryptophan residue has any effect on the electronic and redox properties of the copper site. The effect of mutating this tryptophan residue on the structure, function, and stability of amicyanin are evaluated in this study. Information gained from this particular mutant about the stability of amicyanin and possibly beta barrel proteins in general was attempted to be utilized in a structurally similar protein, an immunoglobulin light chain variable domain (V_L).

Despite having a relatively low sequence similarity, the V_L has a high structural similarity to amicyanin. When aligned together, there is a 2.9 Å RMSD between the two proteins. In light of this high structural similarity, it is conceivable that one could engineer the V_L to have similar structural features as amicyanin in an effort to increase the stability of the V_L. Increasing the stability of the V_L is of particular interest in biotechnology and therapeutic applications because the V_L is the main determinant of aggregation in molecules which contain the V_L domain. Results from attempts to express and purify V_L mutants are presented and discussed.

3.2 The Sole Tryptophan of Amicyanin Enhances its Thermal Stability but does not Influence the Electronic Properties of the Type I Copper Site

3.2.1 Introduction

Type 1 copper sites are found in a wide range of redox proteins in bacteria, plants and animals, and function as electron transfer mediators [25, 84]. In the type 1 site a single copper is coordinated by three equatorial ligands that are provided by a Cys and two His residues, and by a fourth weak axial ligand, usually provided by a Met. These ligands hold the copper in a distorted tetrahedral geometry. Cupredoxins are small soluble type 1 copper proteins with a single copper site which are characterized by an intense blue color and absorption centered near 600 nm that results from a S(Cys)π→Cu(II)dx2-y2 ligand-to-metal charge transfer transition [5]. Amicyanin from Paracoccus denitrificans [85, 86] is a cupredoxin which mediates electron transfer from methylamine dehydrogenase (MADH) [87] to cytochrome *c*-551i [88]. Crystal structures of amicyanin alone [1] and in complex with its redox partner proteins [89, 90] have been determined, and spectroscopic, redox, kinetic and site-directed mutagenesis studies have described structure-function relationships that define the roles of specific amino acid residues of amicyanin in recognition of redox partners and mediation of interprotein electron transfer [91-97].

An interesting feature of Paracoccus denitrificans amicyanin is that it contains a single tryptophan residue, Trp45 which resides in the hydrophobic core of the protein. While Trp45 is 10.1 Å from the copper, the intrinsic fluorescence from this tryptophan is quenched when copper is bound relative to the fluorescence that is observed with apoamicyanin from which copper has been removed [98]. The cupredoxins azurin [99] and stellacyanin [2] also possess a tryptophan residue located within 10 Å of the copper ion and each exhibits the phenomenon of tryptophan fluorescence quenching upon metal ion binding [100, 101]. This metal

dependent fluorescence quenching has been attributed to either Forster energy transfer or electron transfer[29, 30, 102]. In azurin, a structurally analogous Trp residue has been shown to participate in hopping-mediated electron transfer between a rhenium ion attached to the protein surface and the copper of the type 1 site [103]. The finding that the copper of the type 1 site in amicyanin influences the electronic properties of Trp45, and the evidence that this Trp could participate in hopping-mediated electron transfer, raise the question of whether or not the presence of tryptophan in this position influences the properties of the type 1 copper site of amicyanin.

It has been suggested that this tryptophan in cupredoxins is part of an interior core of hydrophobic residue pairs. The spatial orientation of the hydrophobic residue pairs is conserved in azurin, amicyanin, rusticyanin, nitrocyanin, pseudoazurin, plastocyanin, stellacyanin, and auracyanin [104]. The roles of several of these hydrophobic residues in the protein folding behavior of azurin from Pseudomonas aeruginosa was studied by site-directed mutagenesis, however Trp was not one of the residues that was altered [104]. Thus, another question regarding Trp45 of amicyanin is whether this residue is an important determinant of the overall structure and stability of this type 1 copper protein.

To address these questions, Trp45 was altered by site-directed mutagenesis and the effects of this change on the structure and function of amicyanin were assessed. W45A, W45F, W45L and W45K mutations resulted in no detectable protein from the expression system. Only a W45Y mutation was tolerated by the protein. The effects of this mutation on the structure of the protein, the spectroscopic and redox properties of copper site, the affinity of the protein for copper, and the thermal stability of the protein were determined.

3.2.2 Materials and Methods

3.2.2.1 *Protein expression and purification.*

Methods for the expression and purification of MADH [105], cytochrome *c*-551i [88] and wild-type (WT) amicyanin [85] from P. denitrificans were as described previously. The Phusion site-directed mutagenesis kit was used to create W45A, W45F, W45L, W45K, and W45Y amicyanin variants. The forward primers for Trp45 mutations (mutated nucleotides are underlined) were W45A, 5'-CGTCACCGCGATCAAC-3'; W45F, 5'-CGTCACCTTCATCAACCG-3'; W45Y, 5'-CGTCACCTACATCAACCGC-3'; W45L, 5'-CGTCACCCTAATCAACCG-3'; W45K, 5'-CGTCACCAAGATCAACCG-3'. In each case the reverse primer was 5'-GTGTCGCCGACCTTCAC-3'. Mutagenesis was performed using pMEG201 [92] which contains the mauC gene [106] which encodes amicyanin. The entire 555-base mauC-containing fragment was sequenced to ensure that no second site mutations were present, and in each case none were found. Amicyanin variant proteins were expressed in E. coli BL21 cells and isolated from the periplasmic fraction as described for other recombinant amicyanin variants [92].

Reduced amicyanin was prepared by titration with sodium dithionite until absorbance at 595 nm was completely lost. Apoamicyanin was prepared as previously described [98] by dialyzing reduced amicyanin against 0.1 M potassium cyanide in 0.1 M Tris-HCl buffer (pH 8.0) for 20 hr, followed by dialysis against 10 mM potassium phosphate buffer (pH 7.1) for four hr.

3.2.2.2 *Protein crystallization and X-ray structure determination.*

All new crystal structures were obtained by Dr. Narayanasami Sukumar at Argonne National Laboratory. The name of the structures and references are listed.

W45Y amicyanin was washed with 5 mM Na/K phosphate buffer, pH 6.6 before the crystallization trials following the protocol used previously for WT amicyanin and some amicyanin variants [86, 107, 108]. The Hampton Research's ammonium sulfate screen (HR2-211) was used to get initial crystals. These crystals were used as seeds to grow crystals suitable for x-ray data collection using 90:10 mixture of 3.2 M monobasic sodium:dibasic potassium phosphate solution. The reduced form of W45Y amicyanin was produced by soaking the crystals in an artificial reservoir solution containing 80 mM sodium ascorbate in the same buffer solution for 20 min. Both the oxidized and reduced crystals were cryo-protected with krytox oil for data collection.

X-ray data from crystals of oxidized and reduced W45Y amicyanin were recorded at the 24lD-E and 24lD-C beamlines of NECAT, Advanced Photon Source (APS), equipped with Microdiffractometer-MD2 and ADSC Quantum 315 CCD detector (24IDE)/ Pilastus6MF (24IDC). These data were processed using DENZO and scalepack, as a part of the HKL2000 package [109]. A fluorescence scan was carried out at the Cu absorption energy at 24lDC, NECAT, APS to confirm the presence of Cu ion in both oxidized and reduced forms.

The structures of oxidized and reduced W45Y amicyanin were solved by molecular replacement method using PHASER [110] of PHENIX [111] using the coordinates for native amicyanin (PDB entry lAAC) with Trp45 mutated to Ala. There was a single molecule in the asymmetric unit. Based on difference Fourier electron density maps using COOT [112], Ala was changed to Tyr45. To monitor the refinement, a random subset of all reflections (5%; 1661 reflections for oxidized state and 1985 reflections for reduced state) was set aside for Rfree calculation [113]. An anomalous difference Fourier map was computed for both oxidized and reduced forms to confirm the presence of copper. The refinement of W45Y amicyanin was carried out using PHENIX by subjecting the model to alternative positional and B-factor refinement. A simulated annealing refinement was performed at the beginning of the refinement. No restraints were applied to the metal, ligand distances or bond angles. A total of 174 and 171 water molecules were added to the oxidized and

reduced W45Y model. The final R/Rfree values of the model are 12.7/15.4 for oxidized and 13.4/15.0 for reduced forms, respectively. The final models contain one copper and one sodium ion for the oxidized form and only copper ion for reduced form. For the oxidized form, the average temperature factor is 8.2 Å2 for all protein atoms, 15.6 Å2 for water molecules and 5.2 Å2/ 10.4 Å2 for copper/ sodium ions. For the reduced form, the average temperature factor is 8.8Å2 for all protein atoms, 19.4 Å2 for water molecules and 7 Å2 for copper ion. A significant negative density along with positive density observed around the copper position in the reduced form (Figure 3.2.2C). The Ramachandran map calculated for both oxidized and reduced forms using PROCHECK [114] show that all the non-glycine residues are either in most favored or in additional allowed regions. The rms deviation calculation and structure analysis were carried out using the programs COOT [112], CCP4MG [115] and CCP4 [116].

3.2.2.3 *Resonance Raman spectroscopy*

Resonance Raman analysis was performed by Dr. Alfons Schulte at the University of Central Florida.

Resonance Raman spectra of 2 mM WT and W45Y amicyanin were measured with a micro-Raman system (Horiba Jobin Yvon, LabRam HR) at an excitation wavelength of 632.8 nm. Spectra were recorded with a back-thinned CCD detector at a spectra resolution of 2 cm-1. Calibration was performed with silicon and naphthalene standards.

3.2.2.4 *Redox potential determinations*

Oxidation-reduction midpoint potential (Em) values were determined by spectrochemical titration as described previously for amicyanin [7]. The ambient potential was measured directly with a redox electrode which was calibrated using quinhydrone (a 1:1 mixture of hydroquinone and benzoquinone) as a standard

with an E_m value of 286 mV at pH 7.0 [117]. The titrations were performed in 10 mM potassium phosphate buffer at the indicated pH, at 25 °C. The mixture was titrated by addition of incremental amounts of a reductant, ascorbate, or an oxidant, ferricyanide. The concentrations of oxidized and reduced amicyanin were determined by comparison with the spectra of the completely oxidized and reduced forms. The data were analyzed according to eq 1 to determine the E_m value. The pH-dependence of the E_m value was determined by eq 2, where EmAlk is the most alkaline E_m measured that is in the pH-independent region [7], R is the gas constant, T is temperature (K), n is the number of electrons, K_a is the acid dissociation constant and F is Faraday's constant.

$$E = E_m + \left(\frac{2.3RT}{nF}\right)\log\left(\frac{[Amicyanin_{oxidized}]}{[Amicyanin_{reduced}]}\right) \quad (3.2.1)$$

$$E = E_{mAlk} + \left(\frac{2.3RT}{nF}\right)\log\left(\frac{1+[H+]}{Ka}\right) \quad (3.2.2)$$

3.2.2.5 *Kinetic studies*

The steady-state kinetic parameters for amicyanin with its natural redox partner proteins were determined as previously described for two different reactions. One reaction is the methylamine-dependent reduction of amicyanin by MADH [118]. The other is the methylamine-dependent reduction of cytochrome *c*-551 by the MADH-amicyanin complex [119]. These reactions were performed in 10 mM potassium phosphate pH 7.5 buffer at 30° C.

3.2.2.6 *Temperature dependence of amicyanin absorbance (optical melt)*

Absorbance measurements of oxidized amicyanin were made with an HP diode array 8452 spectrophotometer equipped with a programmable Peltier cell holder controlled by a Quantum TC1 thermostat controller. Absorbance measurements at 595 nm were recorded as the cell increased in temperature 1°C/min. Absorbance values were normalized with the maximum absorbance set to 1.0 and the minimum absorbance set to zero. After creating a first derivative curve from the raw data, the midpoint temperature of the optical transition (Tm) was determined from the minimum of that curve as described by La Rosa et al [120]. All experiments were performed in 10 mM potassium phosphate buffer, pH 7.5 using 30 µM WT or W45Y amicyanin.

3.2.2.7 *Circular dichroism*

CD measurements were conducted on WT and W45Y amicyanins in 10 mM potassium phosphate buffer, pH 7.5, for the oxidized and reduced forms, and in 100 mM buffer, for the apo forms because the latter undergoes aggregation at low ionic strength conditions [121]. A 0.4 cm×0.4 cm rectangular quartz cuvette was used and the measurements were done on a J-810 spectropolarimeter equipped with a Peltier temperature controller (Jasco corp., Tokyo, Japan). CD measurements were recorded consecutively on samples which were equilibrated at each temperature for 3 min before measurements. The protein concentration in these experiments was 3 or 7 µM to obtain reasonable signal intensity and still avoid excessive light scattering in the far UV region. The measured ellipticity, θmeas, was converted to mean residue molar ellipticity [θ], through the formula [θ] = θmeas/nlc, where n = 105 is the number of amino acid residues in the protein, l is the optical pathlength in mm, and c is the molar concentration of the protein. Thermal unfolding of the protein secondary structure was determined from the increase in the negative CD signal at 205 nm which results from an increase in the fraction of unordered structure [122]. Changes in the

protein tertiary structure were determined from changes in the signal intensity around 280 nm, generated by the aromatic side chains. In all cases, the value of Tm was determined as the inflection point of the sigmoidal temperature-dependence curves of the corresponding ellipticity, which was identified as the extremum of the first derivative with respect to the temperature.

3.2.3 Results

3.2.3.1 *Protein expression*

Trp45 of amicyanin was converted to alanine, phenylalanine, leucine, lysine, and tyrosine by site-directed mutagenesis. However, only the W45Y amicyanin variant could be isolated from the transformed E. coli cells. This suggests that the W45A, W45F, W45L and W45K mutations either disrupted the biosynthesis of amicyanin or decreased its stability such that it could not be expressed or isolated.

3.2.3.2 *Spectroscopic properties*

The absorption spectrum of W45Y amicyanin was very similar to that of WT amicyanin. A notable difference is the decrease in absorption at 280 nm and shift of the maximum to 278 nm in the spectrum of W45Y amicyanin (Figure 3.2.1A). This is a consequence of the loss of the sole Trp residue in the protein. Each spectrum exhibits an absorption maximum at 595 nm. The extinction coefficient at 595 nm was determined by a quantitative redox titration with a standardized solution of ascorbate and determined to be 4,520 M-1cm-1 compared to 4,610 M-1cm-1 for WT amicyanin. Thus, the mutation has negligible effect on the visible absorption. The retention of the strong absorbance at 595 nm is consistent with retention of the type 1 site and strong interaction of Cu(II) with the Cys92 ligand.

Resonance Raman spectroscopy is a sensitive probe of the type 1 copper site and WT amicyanin has been previously characterized by this technique [123]. Excitation of the chromophore produces strong

enhancement of fundamental vibrational modes in the 350-450 nm region which have been attributed to Cu-S interaction, as well as overtone and combination bands in the 750-900 nm region [124]. Comparison of the resonance Raman spectra of WT and W45Y amicyanin indicate that they are essentially identical (Figure 3.2.1B). This indicates that the mutation has had no apparent effect on the strong Cu(II)-Cys interaction in the type 1 site.

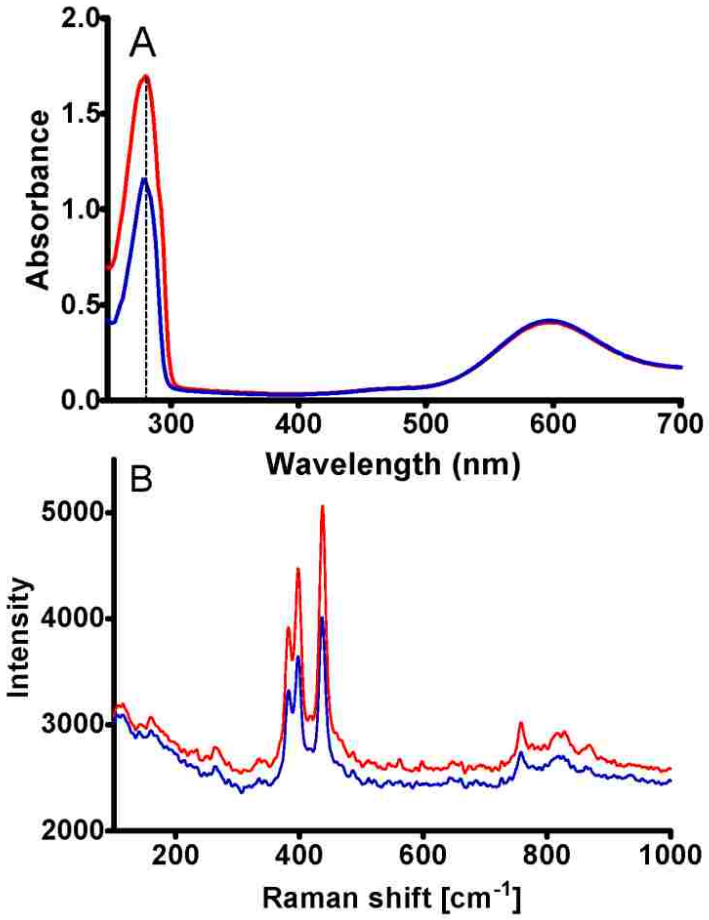

Figure 3.2.1 A. UV-Visible absorbance spectra of 100 μM WT (red) and W45Y (blue) amicyanin.

Figure 3.2.2B. Resonance Raman spectra of 2 mM WT (red) and W45Y (blue) amicyanin.

Each spectrum was recorded in 10 mM potassium phosphate, pH 7.5. The dashed line in A highlights the fact the absorbance maximum at 280 nm of WT amicyanin shifts in W45Y amicyanin.

3.2.3.3 *X-ray crystal structures of oxidized and reduced W45Y amicyanin.*

The X-ray crystal structures of the oxidized and reduced states of W45Y amicyanin were determined to 1.09 Å and 1.02 Å resolution, respectively. Each of these forms was crystallized in the monoclinic space group P21, as has been the case for WT and most other amicyanin variants. Table 1 lists the data collection, refinement and model parameters. The very high-resolution electron density map clearly showed the presence of mutated Tyr45, both in oxidized and reduced forms. The Tyr45 adopts an identical conformation in both forms. The rms deviation between the oxidized forms of native amicyanin (PDB entry 2OV0) and W45Y amicyanin is 0.08Å with 105 matched Cα atoms (Figure 3.2.3A) based on the secondary structure matching [125], calculated using CCP4 [116]. The RMSD between oxidized and reduced forms of W45Y amicyanin is 0.15 Å. The copper differs by 0.75 Å between oxidized and reduced forms of W45Y amicyanin. The RMSD between W45Y reduced and WT amicyanin reduced at pH 4.4 and pH 7.7 is 0.32 Å and 0.27 Å respectively (Figure 3.2.4B). There is a presence of negative electron density along with positive density close to His95 ligand around the copper ion site at the reduced state which indicates heightened mobility for the copper ion (~2.2 Å from its present position) towards the direction of His95. However, the electron density for each of the ligands of copper ion is well ordered. Attempts to create dual positions for copper ion were not successful (Figure 3.2.5C).

The copper coordination distances of WT and W45Y amicyanin at the oxidized and reduced states are shown in Table 2. The positions of Cu(II) and the four ligands are nearly identical in WT and W45Y oxidized amicyanin (Fig. 3.2.6A). The β-factors of Cu(II) and Cu(I) are 5.2 Å and 7.0 Å respectively.

On reduction of amicyanin, His95 which serves as a ligand for Cu(II), rotates by 180° about the Cβ-Cγ bond relative to its position in oxidized amicyanin and is no longer in the copper coordination sphere 7. This accounts for the pH dependence of the Em value of amicyanin. In the structure of reduced W45Y amicyanin a hydrogen bond between an imidazole nitrogen of His95 and the sulfur of Met51 (3.5 Å) is observed; a feature

that is not seen in WT amicyanin (Figure 3.2.7). This may account for the change in the pH-dependence of the Em value of amicyanin that is caused by the W45Y mutation (discussed later).

In WT amicyanin, the indole ε1-nitrogen of Trp45 is hydrogen bonded with the hydroxyl η-oxygen of Tyr90 (2.6 Å). This hydrogen bond connects two of the nine β-strands that comprise amicyanin and in doing so may stabilize the overall tertiary structure of the protein. In W45Y amicyanin, this hydrogen bond is lost (Figure 3.2.8). In W45Y amicyanin there is a C-H...O hydrogen bond between methyl group of Val102 and hydroxyl group of Tyr45 (3.4 Å), although this is likely a weaker interaction. These observations may be relevant to the effect of the W45Y mutation on the thermal stability of amicyanin (discussed later).

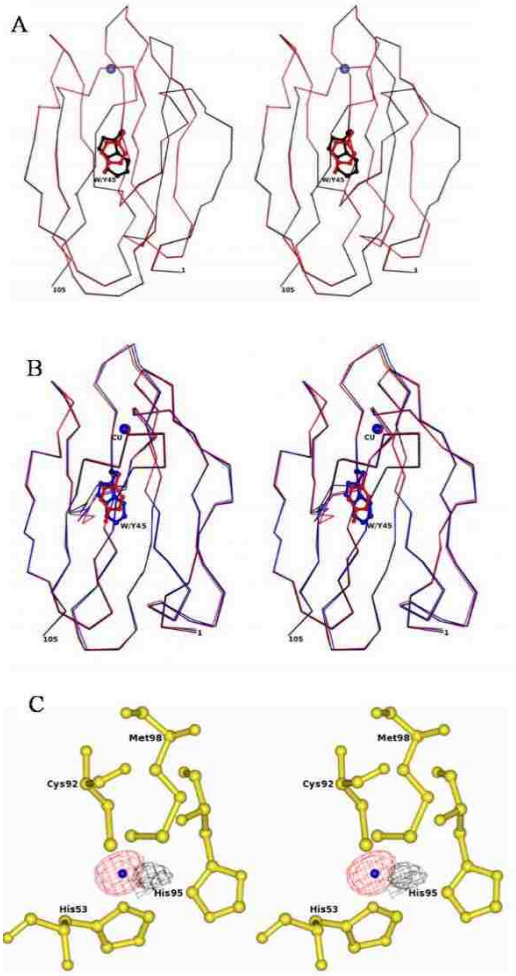

Figure 3.2.3A. Stereoview of the superposition of oxidized W45Y amicyanin with WT amicyanin (red and PDB code 2OV0; black, respectively). The Cu(II) ion is shown as a sphere in blue. Residue 45 of each protein is shown as a ball and stick in respective colors.

Figure 3.2.4B. Stereoview of the superposition of reduced W45Y amicyanin (red) with WT reduced amicyanin pH 4.4 and pH 7.7 (PDB code 1BXA, black; 2RAC, blue). The Cu(I) ion is shown as a sphere in respective colors. Residue 45 of each protein is shown as ball and stick in respective colors.

Figure 3.2.5C. Stereoview of negative density of the Cu(I) site in reduced W45Y amicyanin. The negative and positive densities are at 2.5 sigma level are shown in red and black respectively, Cu(I) is shown as a blue sphere and the copper ligands are yellow ball and stick models.

Table 3.2.1 Data Collection and Structure Determination and Refinement

Crystal	W45Y amicyanin (oxidized)	W45Yamicyanin (reduced)
Data collection		
Wavelength (Å)	0.98	0.98
Space group	$P2_1$	$P2_1$
Unit cell dimensions		
a,b,c (Å)	27.2,56.2,28.9	27.2,56.7,28.7
α,β,γ (°)	90,95.9,90	90,96.7,90
Res. limit (Å)	50-1.09 (1.13-1.09)	57-1.02 (1.06-1.02)
I/Sigma(I)	31.8 (15.2)	34.1(11.8)
R_{merge} (%)	5.0 (11.6)	4.4(13.6)
Completeness (%)	93.2 (78.0)	91.7(76.1)
Redundancy	6.8	5.9
Refinement		
resolution range (Å)	25.4-1.09	28-1.02
R-work (%)	12.7	13.4
R_{free} (%)	15.4	15.0
R (working + test) (%)	12.9	13.5
No. of Reflections	33258	40205
Model		
No. of amino acids	105	105
No. of water molecules	174	171
No. of Copper/Sodium	1/1	1/0
Residues in generously allowed region	0	0
Residues in disallowed regions	0	0
No. of residues with alternate conformation	10	2
Stereo-chemical ideality		
bonds (Å)	0.016	0.014
angles (deg)	1.82	1.85
dihedral angles (deg)	10.92	10.63
Planarity (Å)	0.012	0.011

Table 3.2.2 Copper coordination distances in W45Y and native amicyanin at oxidized and reduced state.

Ligands	W45Y amicyanin oxidized (Å)	[2]Native amicyanin oxidized (Å)	W45Y amicyanin reduced (Å)	[3]Native amicyanin reduced pH 4.4 (Å)	[4]Native amicyanin reduced pH 7.7 (Å)
Cu-SG/Cys92	2.16	2.17	2.11	2.09	2.12
Cu-ND1/His95	2.02	2.05	5.53	5.45	5.33
Cu-ND1/His53	1.97	1.99	1.91	1.91	1.90
Cu-SD/Met98	3.05	3.07	2.99	2.90	2.91

[2] PDB 2OV0
[3] PDB 1BXA
[4] PDB 2RAC

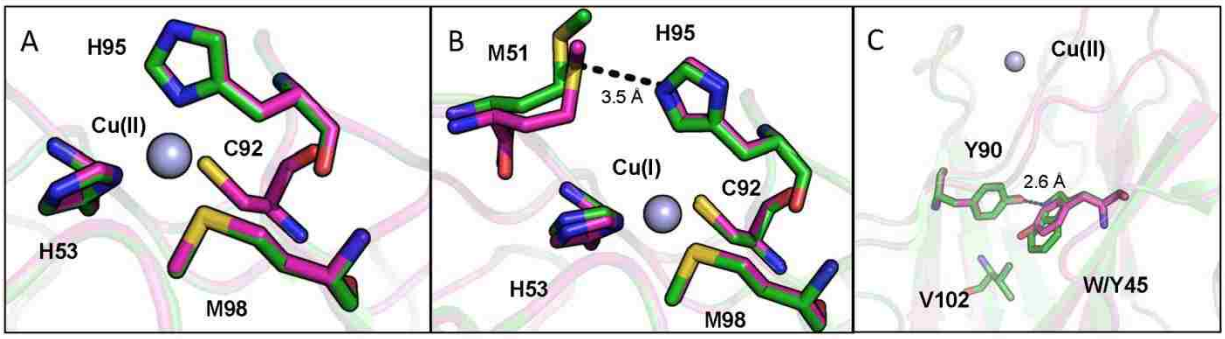

Figure 3.2.6 A. Overlay of the copper sites in oxidized WT amicyanin and W45Y amicyanin (green, PDB code 2OV0 and purple, respectively). The copper ion is shown as a blue sphere.

Figure 3.2.7B. Overlay of the copper sites in reduced WT amicyanin and W45Y amicyanin (green, PDB code 2RAC and purple, respectively). The copper ion is shown as a blue sphere. The hydrogen bond between His91 and M51 which is observed only in W45Y amicyanin is shown as a dashed line.

Figure 3.2.8C. Overlay of the sites surrounding residue 45 in oxidized WT amicyanin and W45Y amicyanin (green, PDB code 2RAC and purple, respectively). The copper ion is shown as a blue sphere. The hydrogen bond between Trp45 and Tyr90 which is observed only in WT amicyanin is shown as a dashed line. Figures were produced using PyMOL (http://www.pymol.org/).

3.2.3.4 *Redox properties*

The E_m value of WT amicyanin was previously shown to be pH-dependent and exhibit a pKa value of 7.5 ± 0.3. The E_m value becomes independent of pH at high pH where it exhibits an alkaline pH-independent value of 240 ± 7 mV [7]. The E_m values of W45Y amicyanin was determined by spectrochemical titration over a range of pH values from 6.0-9.0 (Figure 3.2.9). The fit of these data to eq 2 yielded a pKa value of 8.0 ± 0.2 and an alkaline pH-independent value of 236 ± 6 mV, respectively. Thus, it can be concluded that the mutation has caused a small shift in the pH-dependence of the E_m value but has negligible effect on the intrinsic pH-independent E_m value.

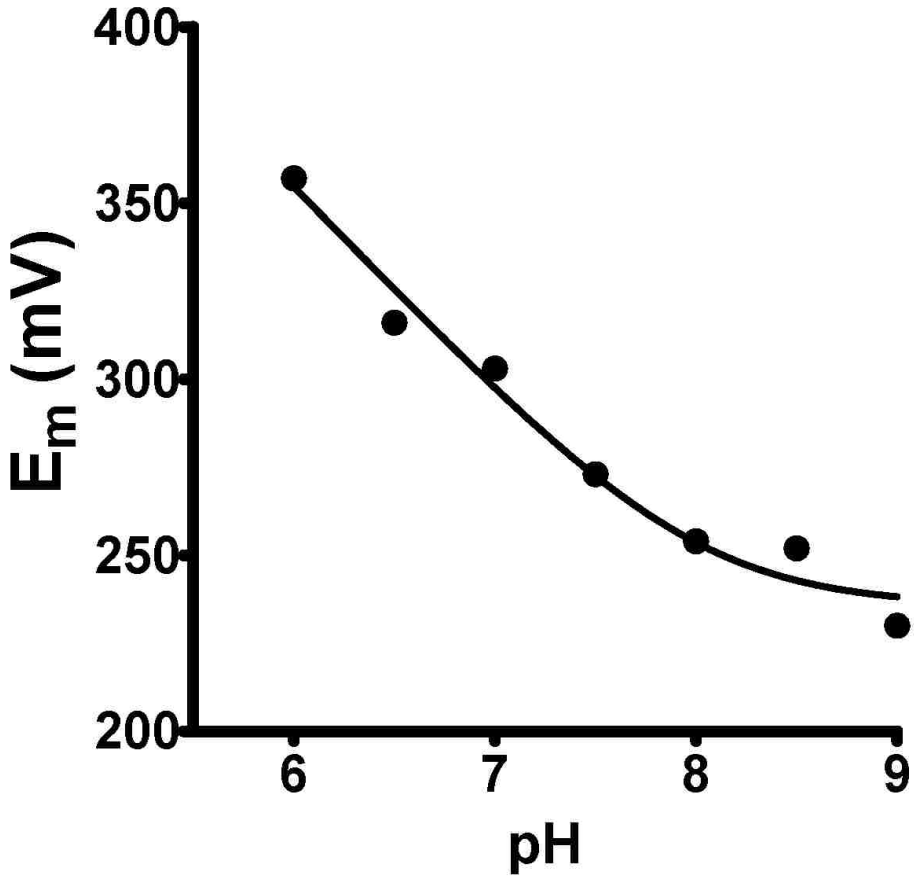

Figure 3.2.9 Dependence of the E_m value of W45Y amicyanin on pH. Em values were determined in 10 mM potassium phosphate buffer at the indicated pH at 25 ºC. The line is the fit of the data by eq 2.

3.2.3.5 *Reactivity of W45Y amicyanin with its natural redox partners*

The steady-state kinetic parameters for the reactions of W45Y amicyanin with the natural redox partners of WT amicyanin, MADH and cytochrome *c*-551i, were determined and compared with those for the reactions with WT amicyanin. In the reaction of methylamine-dependent reduction of W45Y amicyanin by MADH, values of kcat = 65.5 ± 2.8 s-1 and Km= 3.2 ± 0.5 µM for W45Y amicyanin were obtained. These were essentially the same as those obtained when the reaction was performed with WT amicyanin which yielded values of kcat = 60.9 ± 2.1 s-1 and Km= 2.3 ± 0.3 M. In the reaction of methylamine-dependent reduction of cytochrome *c*-551i by the MADH-W45Y amicyanin complex, values of kcat = 12.8 ± 1.2 s-1 and Km= 1.0 ± 0.2 µM for W45Y amicyanin were obtained. These values were similar to those obtained when the reaction was performed with WT amicyanin which yielded values of kcat = 18.3 ± 1.7 s-1 and Km= 1.3 ± 0.2 µM. Given the kinetic complexity of this steady-state reaction [119] these data suggest that the W45Y mutation has not significantly affected the reactivity of amicyanin with its natural redox partners.

3.2.3.6 *Effect of the W45Y mutation on the thermal stability of amicyanin*

It was previously shown that the temperature dependent bleaching of the visible absorption spectrum of oxidized amicyanin corresponded to the native to unfolded state transition [126]. The loss of absorbance at 595 nm is attributed to the disruption of the type 1 Cu(II) site which gives rise to the strong visible absorption of the oxidized protein. An optical melt experiment was performed with W45Y amicyanin and the results compared with that for WT amicyanin (Figure 3.2.10). The W45Y mutation decreased the midpoint temperature at which the loss of visible absorbance occurred from 66.4 ± 0.2° C in WT amicyanin to 53.9 ± 0.1° C in W45Y amicyanin.

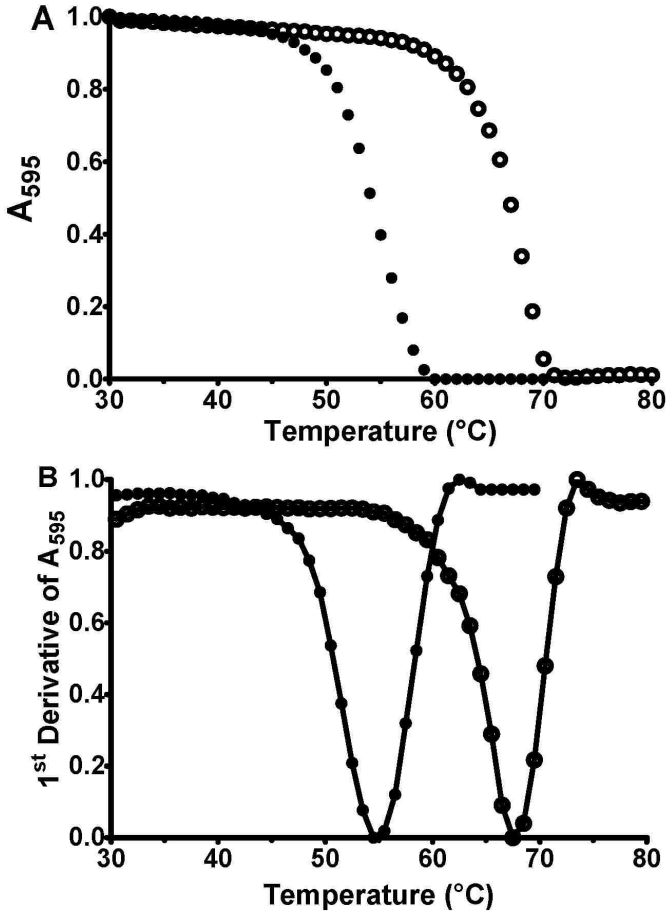

Figure 3.2.10 The change in absorbance at 595 nm of WT and W45Y amicyanin with increasing temperature (WT open circles; W45Y closed circles). For ease of comparison, the absorbance values were normalized so that the maximum absorbance of each is set to 1.0. The data were obtained with 30μM protein 10 mM potassium phosphate buffer at pH 7.5. The absorbance data are shown in A and the first derivative of the absorbance versus temperature is shown in B.

3.2.3.7 Circular dichroism analysis of the thermal stability of WT and W45Y amicyanins

In order to obtain more detailed information on the structural changes associated with the increase in temperature, temperature-induced changes in the CD spectra of WT and W45Y amicyanins were monitored. The structure of amicyanin consists of β-sheets and short (<10 amino acid residues) loops and turns with no α-helix [1]. As such, the changes in the CD spectrum are relatively simple to interpret and make this an ideal approach to examine the unfolding of the protein. It also allows examination of the reduced and apo forms of the protein which have no absorbance in the visible region. CD has been previously used to monitor the temperature-dependent unfolding of oxidized amicyanin [120].

The CD spectra of both WT and W45Y mutant amicyanin at T $\leq$37 ^{o}C display a minimum near 218-220 nm and a maximum of comparable intensity around 195-198 nm, indicative of a β-sheet secondary structure [122] (Figure 3.2.11). In addition, a weaker minimum around 280 nm is present that is generated by the aromatic side-chains [127]. A negative CD signal appeared around 200 nm and gained intensity with increasing temperature, in parallel with a reduction of the aromatic side-chain signal at 280 nm, indicating thermal unfolding of the secondary and tertiary structures [122, 127]. The decrease in the β-sheet nπ* transition intensity around 218 nm was not always clearly displayed because this effect was largely offset by the substantial increase in the unordered structure band around 200 nm (Figure 3.2.11). The thermal transition temperatures (T_m) of the protein secondary structure, as determined from the temperature-dependencies of the CD signal at 205 nm (insets in Figure 3.2.11), are summarized in Table 3. This wavelength (205 nm) was chosen to avoid excessive noise in the CD spectra at lower wavelengths, especially in case of apo proteins which were studied at a higher ionic strength to prevent protein aggregation [121]. Secondary structure unfolding occurred at 60 ^{o}C for the oxidized WT amicyanin and 53-55 ^{o}C for the reduced and apo forms (Table 3). The W45Y mutation caused significant thermal instability in the oxidized and apo forms of the protein, i.e. a decrease in T_m from 60 ^{o}C to 46 ^{o}C and from 55 ^{o}C to 34 ^{o}C, respectively, but had less effect on the thermal

transition of the reduced protein, from 53 ^{o}C to 50 ^{o}C. These data indicate that the W45Y mutation itself exerts strong effect on the thermal stability of the protein's secondary structure.

Tertiary structural transitions are manifested by the decrease in the CD signal at 280 nm, which is generated by the aromatic side chains in the chiral environment of the protein backbone Cα atoms [127]. As the tertiary structure opens up with increasing temperature, the chirality of the microenvironment of the aromatic residues and, subsequently, the CD intensity at 280 nm decrease. Temperature-induced changes in the signal at 280 nm paralleled those at 205 nm (Figure 3.2.11). Precise interpretation of these effects is complicated by the fact that the unfolded copper-free amicyanin may undergo additional bimolecular reactions. It is known that apoamicyanin has a tendency to form aggregates, particularly at low ionic strength [121] and that the denatured amicyanin may form disulfide dimers between molecules since the lone cysteine residue is free when no longer binding copper [128]. This also affects the thermal reversibility of the unfolding transition [126]. Thus there may be more than one "unfolded" structure and the aromatic residues could have different microenvironments in each structure. Nonetheless, temperature-dependent decrease in the negative ellipticity at 280 nm (Figure 3.2.11) indicates thermal unwrapping of the protein's tertiary structure and the analysis showed that these changes precede the secondary structural unfolding.

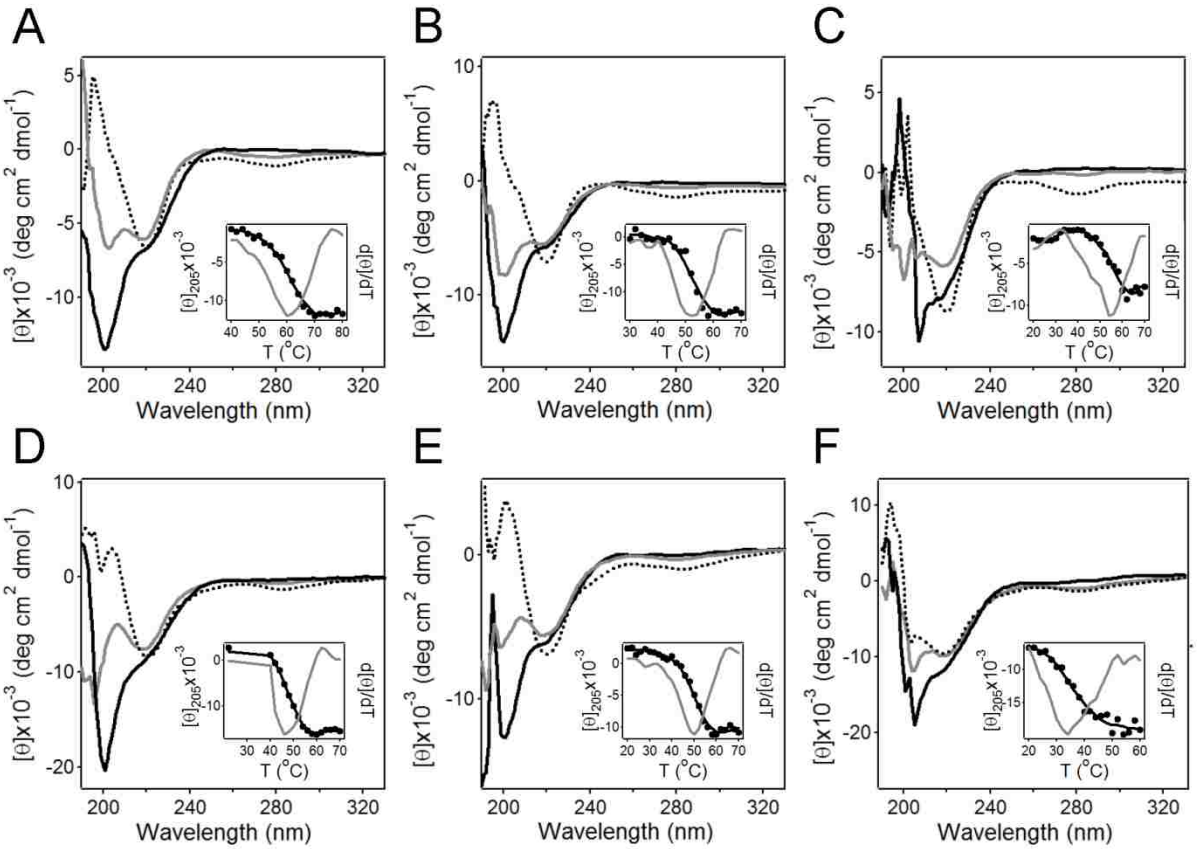

Figure 3.2.11 CD spectra of WT (A, B, C) and W45Y (D, E, F) amicyanin as a function of temperature. The protein was in oxidized (A, D), or reduced (B, E), or apo (copper-less) form (C, F). In each case three spectra are shown, those recorded at the lowest temperature (dotted line) the T_m (gray solid line) and highest temperature measured (black solid line). Data for all spectra recorded over the complete range of temperatures are shown in the insets, which present the temperature dependence of the mean residue molar ellipticity at 205 nm (black) and the 1st derivative with respect to temperature (gray).

Table 3.2.3 Tm values determined from the temperature dependent decrease at 205 nm in the CD spectrum of amicyanin

Amicyanin form	WT amicyanin	W45Y amicyanin
Oxidized	60±1[5] °C (66.4±0.2)[6]	46 ± 2 °C (53.9±0.1)
Reduced	53 ± 2 ºC	50 ± 1 ºC
Apo[7]	55 ± 1 ºC	34 ± 2 ºC

[5] Standard deviations indicate deviations in T_m values in two to three independent experiments.

[6] Values in parentheses are T_m values obtained from the optical melt in Figure 4 for comparison.

[7] Studies with apoamicyanins were performed in 100 mM buffer to minimize aggregation of the apo forms which occurs in 10 mM buffer, the condition used for the studies of oxidized and reduced amicyanin.

3.2.4 Discussion

Despite the fact that the copper in the type 1 copper site of amicyanin quenches the fluorescence of Trp45, the replacement of Trp with Tyr has no detectable effect on the electronic or spectroscopic properties of the type 1 copper site. The visible absorbance and resonance Raman spectra, and the pH-independent intrinsic redox potential are unchanged. The structure of the type 1 site with respect to the positions of Cu(II) and the four copper ligands is essentially unchanged. Thus, it appears that Trp45 does not reciprocate any form of electronic communication to the copper. One physical parameter of the type 1 site that is altered by the mutation is the pH dependence of the E_m value. The pH-dependence has been attributed to the fact that His95, which serves as a ligand for Cu(II), when protonated rotates by 180° about the C_β-C_γ bond and is no longer in the copper coordination sphere of Cu(I) in the reduced protein. The pK_a of W45Y amicyanin is increased by approximated 0.5 pH units. This may be explained by the observation that a hydrogen bond is formed between the rotated and protonated His95 and Met51 in reduced W45Y amicyanin but not in reduced WT amicyanin. This hydrogen bond could stabilize the reduced form in W45Y amicyanin relative to WT amicyanin in a pH-dependent manner thus altering the pK_a value. Flexibility of the ligand loop has been shown to effect the redox and pH-dependent equilibria of cupredoxins [129, 130].This same structural feature could account for the decreased occupancy of the Cu(I) ion and mobility towards the CD2-His95 ligand to as close as ~1.8 Å, in the crystal structure of reduced W45Y amicyanin (Figure 3.2.5C). This structural perturbation may also account for the similar thermal stability of the reduced and oxidized forms of W45Y amicyanin compared to WT amicyanin in which the reduced form is less stable since the hydrogen bond will decrease the mobility of this loop which connects two β- strands.

The most significant effect of the W45Y mutation is on the thermal stability of amicyanin. Decreased thermal stabilities of the oxidized, reduced and apo forms of the W45Y mutant as compared to WT amicyanin were determined from the downshifts in transition temperatures of secondary structure unfolding. The T_m

values obtained from the loss of absorbance are approximately 6-7º C higher than those obtained from the secondary structure unfolding determined by CD for both WT and W45Y amicyanin (Table 3). These data suggest that in both the WT and W45Y amicyanin heating first causes tertiary structural distortion when the β-strands move relative to each other, followed by secondary structure disordering, followed by disruption of the type 1 site with loss of copper. From comparison of the crystal structures of WT and W45Y amicyanin it can be inferred that the decrease in overall thermal stability of W45Y amicyanin can most likely be attributed to the loss of a strong interior hydrogen bond between Trp45 and Tyr90 (2.6 Å) in WT amicyanin which links two of the β-sheets.

The importance of the hydrogen bond between Trp45 and Tyr90 is consistent with previous results of a joint x-ray/neutron diffraction study of amicyanin which determined the extent of hydrogen/deuterium exchange and related this to the flexibility and dynamic nature of amicyanin [28]. Trp45 and Tyr90 were among only 14 residues of amicyanin with non-exchangeable hydrogen atoms. Hydrogen bonding to the analogous Trp residue is seen in other cupredoxins. In cucumber stellacyanin (PDB entry 1JER) the indole N of Trp13 is 2.9 Å from the backbone O of Asn47 [2]. In pseudoazurin from *Hyphomicrobium denitrificans* (PDB entry 3EF4) the indole N of Trp50 is within 3.1 Å of the backbone O of Val54 and within 3.2 Å of the backbone O of Ala55 [131]. It was also shown that mutation of Trp48 of *Pseudomonas aeruginosa* azurin decreased the stability of the protein towards guanidine hydrochloride-induced unfolding [132]. The stability afforded to amicyanin by interactions involving Trp45 may be a general feature of β-sheet proteins. For example, the variable domains of immunoglobulins have two β-sheets which are folded face-to-face and have conserved hydrophobic residues clustered along a diagonal pattern of each β-sheet, a feature which has been linked to cupredoxins including amicyanin [27, 133]. The importance of Trp45 in maintaining the structure of amicyanin can further be inferred from the observation that when this residue was mutated to other residues, alanine, phenylalanine,

leucine and lysine, no protein could be isolated. This is likely due to an inability to stabilize the properly folded protein.

3.3 Translating the Cross-Barrel Bond from Amicyanin

As seen in the previous study, the cross-barrel hydrogen bond between Y90 and W45 is very important to the thermal stability of amicyanin, and this may be a general feature of β-sheet proteins. Amicyanin is part of the cupredoxin family of proteins with a "cupredoxin-like" fold. A near cousin of this protein/fold family is the "immunoglobulin-like" fold family. Both of these protein folds are characterized by a Greek key beta barrel formation with seven beta strands. Some members of the cupredoxin family have additional strands with alpha-helices, however neither amicyanin nor immunoglobulin domains have helices. In this way, amicyanin is more similar to the proteins with the "immunoglobulin-Like" fold, such as the immunoglobulin light chain variable domain (V_L), than other cupredoxins. As expected, there is a high structural similarity between the two proteins, and the V_L contains a disulfide bond near where the copper site is in amicyanin, providing a similar stabilizing mechanism. However, the V_L does not contain any cross-barrel hydrogen bonds, as seen in amicyanin, which helps improve its thermal stability.

It makes sense that a homologous cross-barrel hydrogen bond could be engineered into the V_L to increase its stability. This would allow the use of the V_L for more effective therapies and biotechnological applications, such as monoclonal antibodies and radioisotope labelled antibody fragments for in vivo imaging. The following chapter will detail efforts made to express and purify the V_L using the amicyanin signal sequence, which itself is novel, and to engineer a cross-barrel hydrogen bond into the V_L via site-directed mutagenesis.

3.4 Use of the Amicyanin Signal Sequence for Efficient Periplasmic Expression in E. coli of a Human Antibody Light Chain Variable Domain

3.4.1 Introduction

Escherichia coli is widely used in the production of recombinant proteins, including approximately 30% of therapeutic proteins that have been approved by the FDA [1]. Problems associated with protein expression in *E. coli* include degradation by intracellular proteases and the correct formation of disulfide bonds in the cytoplasm. The correct formation of disulfide bonds is especially important in biological therapeutics, where inefficient disulfide formation has been shown to limit the yield of the expressed protein [2]. High levels of cytoplasmic expression of recombinant proteins can also lead to formation of inclusion bodies and mis-folding of the proteins. This is especially prevalent during the expression of recombinant immunoglobulin domains [3], [4],[5] and [6]. These problems can be circumvented by translocation of the recombinant proteins into the periplasm of *E. coli.* The periplasm is an oxidizing environment compared to the cytoplasm. This facilitates formation of disulfide bonds that are often required for correct protein folding. The periplasm has a lower concentration of proteolytic enzymes and host cell proteins in general [7]. Thus, the periplasm is enriched in the relative concentration of the recombinant protein which facilitates its purification. For the above reasons the formation of inclusion bodies in the periplasm is much less likely than in the cytoplasm. Recombinant proteins are translocated to the periplasm via membrane-associated secretion systems that recognize an N-terminal signal sequence. The cleavage of the signal peptide during export of the recombinant protein to the periplasm yields a protein with its correct N-terminal residue. A variety of signal peptides have been used for this purpose. Some of the most widely used signal peptides are pelB from *Erwinia carotovora* and ompA, DsbA, and TolB from *E. coli* [8], [9] and [10].

Amicyanin [11] is a periplasmic type I copper protein, referred to as a cupredoxin [12], which is encoded by the *mauC* gene [13] of *Paracoccus denitrificans*. Recombinant amicyanin was previously

expressed in *E. coli* at high levels [14]. In this study, we describe the use of the N-terminal signal sequence of amicyanin to express the light chain variable domain (*V*L) 1 of a human antibody in the periplasm of *E. coli*. The κI O8/O18 germline antibody *V*L was chosen for expression as it is a well characterized member of this family [15]. Correct folding of this protein requires formation of a disulfide bond and as with many antibodies and single chain fragments, aggregation and incorrect folding of these recombinant proteins has been problematic [16]. The folding and stability of this *V*L has previously been characterized by circular dichroism (CD) and thermal stability studies [15]. Thus, it was possible to assess the integrity of the recombinant protein that was expressed in this study by comparison to those results. The results of this study demonstrate the utility of the amicyanin signal sequence as an alternative for recombinant protein expression in *E. coli*. It should also be noted that an increasing number of recombinant human single chain fragments are being developed for therapeutics and so there may be additional applications of the results which are presented.

3.4.2 Materials and Methods

3.4.2.1 Protein expression

DNA encoding the κI O8/O18 germline VL with the N-terminal signal sequence of mauC from P. denitrificans and a C-terminal hexahistidine tag was codon-optimized for expression in E. coli, and synthesized by GenScript (Piscataway, NJ). The sequence of the DNA and the amino acid sequence of the protein that it encodes are shown in Table 1. The synthetic gene was cloned into a pET11a expression plasmid at the Nde1 and BamH1 restriction sites (Table 3.4.1). E. coli BL21(DE3) cells were transformed with this plasmid, and cells were cultured in LB media at 37° C in the presence of 100 μg/ml ampicillin. When the A_{600} of the culture reached 0.6, 0.4 mM IPTG was added to the culture to induce expression and incubation was continued at 30° C for 12 hours.

The QuickChange II site-directed mutagenesis kit was used to create I21W/T, Q37L, L47T, F62W/Y, G64S/Y, G66Y, F71Y, F73A/W/Y, and T102Y V_L variants.. The entire V_L-containing fragment was sequenced to ensure that no second site mutations were present, and in each case none were found.

Table 3.4.1 Sequences of the synthetic gene used to express κI O18/O8 V_L and the protein that is encoded by the gene. (Top) The DNA sequence of the gene encoding κIO18/O8 V_L with the N-terminal mauC signal sequence and the sequence encoding the C-terminal hexahistidine tag underlined. (Bottom) The amino acid sequence encoded from this gene is shown. The N-terminal signal sequence which is cleaved during expression and hexahisidine tag that is used for affinity purification are underlined.

ATGATTTCCGCTACCAAAATCCGCTCATGCCTCGCGGCCTGTGTCTTGGCTGCCTTTGGAGCCACCGGAGCCCTTGCCTCGACA
TTCAAATGACTCAATCCCCGTCATCCCTGTCAGCGAGTGTCGGTGATCGCGTCACGATCACGTGCCAGGCGTCTCAAGACATTAGCA
ACTACCTGAATTGGTACCAGCAGAAACCAGGTAAGGCCCCGAAACTCTTGATCTACGACGCGTCCAATTTGGAAACAGGCGTGCCG
AGTCGCTTTAGCGGTAGCG
GAAGCGGCACCGATTTCACCTTCACCATCAGTTCCCTTCAGCCGGAAGACATCGCCACCTACTATTGTCAACAGTATGACAATCTGC
CATATACGTTTGGCCAGGGCACCAAACTGGAAATCAAG**CACCATCATCATCATCAT**TAG

M I S A T K I R S C L A A C V L A A F G A T G A L A D I Q M T Q S P S S L S A S V G D R V T I T C Q A S Q D I S N Y L

N W Y Q Q K P G K A P K L L I Y D A S N L E T G V P S R F S G S G S G T D F T F T I S S L Q P E D I A T Y Y C Q Q Y D

N L P Y T F G Q G T K L E I K **H H H H H H**

3.4.2.2 *Protein purification*

The recombinant κI O8/O18 V_L was purified from the periplasmic fraction of the E. coli cells. The periplasmic fraction was obtained using a lysozyme/osmotic shock method [85, 134]. The harvested cells were resuspended in 10 mM Tris-HCl buffer, pH 8.0, at a ratio of 6 mL/g of wet cell weight. The buffer also contained 20% w/v sucrose, 0.7 mM EDTA, 2 mg/mL of lysozyme, 1 mM MgCl2, 0.01 mg/mL of DNase and 200 μM phenylmethylsulfonyl fluoride. After incubation for 20 min at 30° C with shaking, an equal volume of H_2O was added and incubation continued for a total of one hour. The spheroplasts were then removed by centrifugation and the periplasmic fraction was the supernatant. The His-tagged κI O8/O18 V_L was purified from the periplasmic fraction by affinity chromatography using a Ni-NTA column (Qiagen). Protein concentration was determined from absorbance of the pure protein at 280 nm and the amino acid composition of the protein, which yielded an extinction coefficient of 16,055 M^{-1} cm^{-1}. This was calculated using the Expasy ProtParam tool (http://web.expasy.org/protparam/) [135].

3.4.2.3 *Protein characterization*

Size exclusion chromatography was performed with a HiPrep 16/60 Sephacryl S-300 HR column (GE Healthcare). The equilibration and elution buffer was 10 mM potassium phosphate, pH 7.5, with 150 mM NaCl. The flow rate was 1.0 mL/min. Methylamine dehydrogenase, cytochrome *c*-553, cytochrome *c*-551i, and amicyanin with molecular weights of 124, 30, 22, and 11.5 kDa, respectively, were used as standards.

CD spectra were recorded using a J-810 spectropolarimeter equipped with a Peltier temperature controller (Jasco corp., Tokyo, Japan). Samples contained 3 μM protein in 10 mM potassium phosphate buffer, pH 7.5. For temperature-dependence studies, samples were equilibrated at each temperature for 2 min before CD measurements were recorded. The measured ellipticity, θmeas, was converted to mean

residue molar ellipticity [θ], through the formula [θ] = θmeas/nlc, where n = 113 is the number of amino acid residues in the protein, l is the optical pathlength in mm, and c is the molar concentration of the protein. Thermal unfolding of the protein secondary structure was determined from the increase in the negative CD signal at 205 nm which results from an increase in the fraction of unordered structure [122]. The value of the thermal transition temperature (Tm) was determined as the inflection point of the sigmoidal temperature-dependence curves of the corresponding normalized signal intensity (fraction folded), which was identified as the extremum of the first derivative with respect to the temperature. To determine fraction folded greatest signal intensity at 205 nm at the lower temperatures was defined as 100% of the protein is in its native folded conformation and the lowest signal intensity at high temperatures was defined as 0% of the protein is in its native folded conformation.

$$Fraction\ Folded = \frac{[\theta]_T - [\theta]_{70}}{[\theta]_{40} - [\theta]_{70}} \qquad (3.4.1)$$

3.4.3 Results

3.4.3.1 *Protein expression and purification*

The recombinant κI O18/O8 germline V_L was successfully expressed in E. coli and purified. The yield of pure WT protein was 70 mg/L of cell culture. Of the variants, none resulted in protein expressed in the periplasm, except for Q37L, whose yield was 60 mg/L of cell culture. The Q37L variant was not used in any further assays. This variant was previously found to decrease the thermal stability[136]. From here on, all results are in reference to the WT protein. The purified protein ran as a single band on SDS-PAGE (Figure 3.4.1A). When the protein was subjected to size exclusion chromatography it eluted as a single peak consistent with it being present exclusively as a monomer (Figure 3.4.1B). Comparison of the elution volume

of the V_L to other protein standards indicated that it eluted at a position corresponding to a molecular mass lower than that determined by SDS-PAGE and calculated from the amino acid sequence of 12.8 kDa. However, this observation is consistent with anomalously lower values for molecular mass determined by size exclusion chromatography that have been previously observed with V_L domains [37, 137, 138]. The identity of the purified protein was further confirmed by demonstration that it binds to protein L resin, which is often used for affinity purification of immunoglobulins [139]. In this study we chose to add a His-tag for purification because the Ni-NTA superflow resin used for purification has a much higher capacity for bound protein than the protein L resin. It was also confirmed by Western blot that the purified protein reacted with an anti-His-tag antibody. These results show that use of the amicyanin signal sequence allowed for expression of high levels of monomeric V_L in the periplasm, which could be easily purified in a single step with no evidence of aggregation or inclusion bodies.

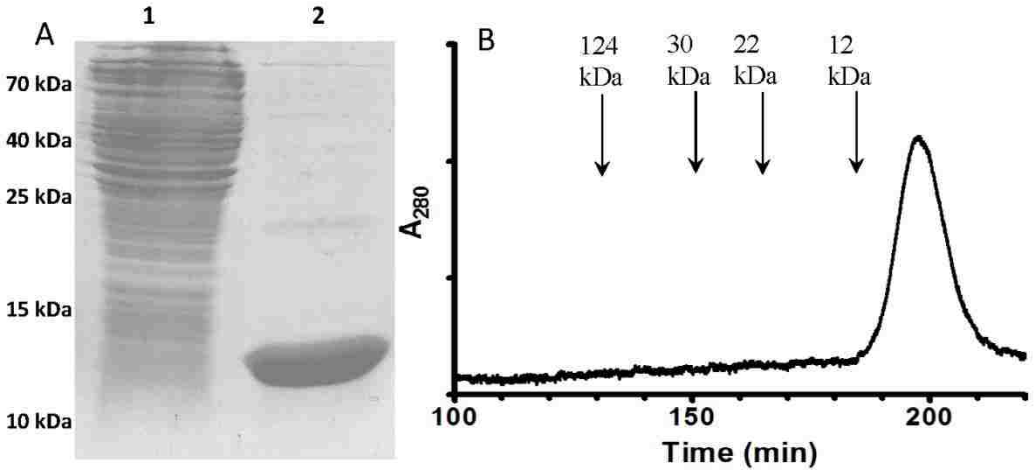

Figure 3.4.1 SDS-PAGE and size exclusion chromatography of the expressed and purified κIO18/O8 V_L. A. SDS-PAGE was performed using a 12.5% gel. Lane 1 is a whole cell extract of the E. coli cells from which the recombinant VL was purified. Lane 2 is the protein that was purified from the periplasmic fraction of the cells. The positions of MW markers which were also run on the gel are indicated. B. The elution profile obtained when the purified recombinant VL was subjected to size exclusion chromatography is shown with the positions of elution of other proteins of known molecular weight indicated.

3.4.3.2 *Protein structure and stability*

The secondary structure of the κI O18/O8 V_L has previously been characterized by CD spectroscopy [33]. As such, the CD spectrum of the purified recombinant protein was obtained and compared with the published data. The spectrum shown in Figure 3.4.2A (solid line) is essentially identical to that previously reported for κIO18/O8 V_L. It has a β-sheet secondary structure as indicated by the minimum around 216 nm. The spectrum also exhibits a second minimum at 232 nm, which can be assigned to type I β -turn structure [140]. The maximum at 205 nm is indicative of β -turns. The minimum between 200-205 nm that appears at higher temperatures (Figure 3.4.2A, dashed line) is generated by unordered structure [122]. These features of the CD spectrum are essentially identical to those reported for the native protein and are consistent with the x-ray crystal structure of the germline Vk1 O18/O8 V_L [33] (PDB entry 2Q20).

These results indicate that the recombinant V_L protein that was expressed in the periplasm using the amicyanin signal sequence is properly folded with regard to secondary and tertiary structures. It is also important to assess the thermal stability of this recombinant protein. CD Spectra were recorded at temperatures from 40° C to 70° C. In Figure 3.4.2A the spectra of the native protein at 40° C, completely denatured protein at 70° C, and the protein at the T_m are shown. The Tm of the protein, as determined from the temperature-dependent perturbations of the CD signal at 205 nm was 53° C (Figure 3.4.2B). This value is in agreement with the previously reported value of 56° C for κI O18/O8 V_L [33].

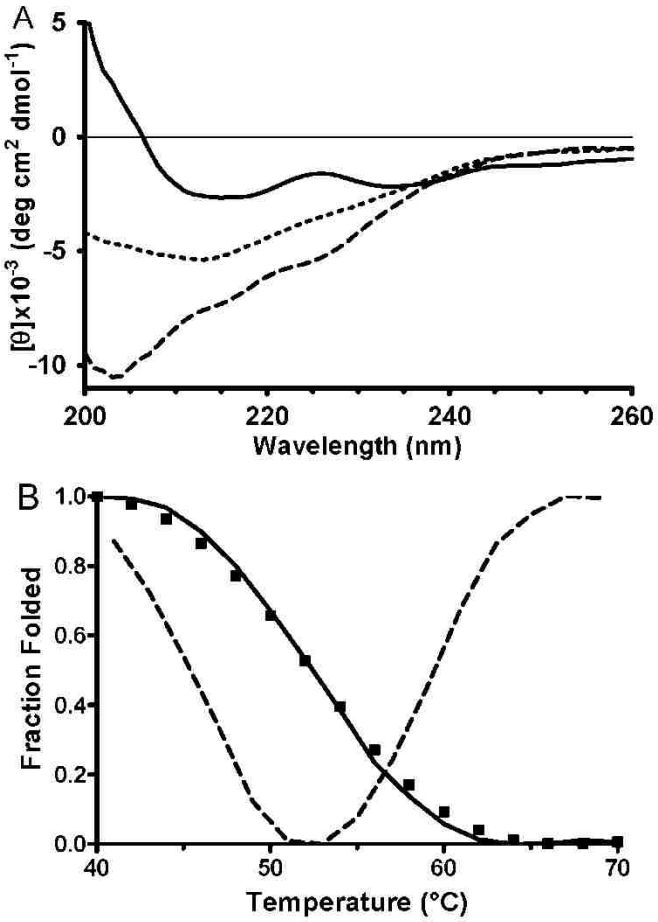

Figure 3.4.2 CD spectra of purified recombinant κI O18/O8 V_L and determination of the T_m for the protein. CD spectra of the protein were recorded at a range of temperatures up to 70º C. **A.** For clarity only three spectra are shown which were recorded at 40º C (solid line), 53º C (short dashed line) and 70º C (long dashed line). **B.** The values of mean residue molar ellipticity at 205 nm for the temperature range are shown (solid line) as well as the 1st derivative of that line which was used to determine the T_m (dashed line).

3.4.4 Discussion

As stated earlier, there are certain advantages to expressing recombinant proteins in the periplasm of E. coli rather than the in the cytoplasm. The amicyanin signal sequence is shown to be an efficient leader sequence for periplasmic recombinant protein expression. It may also be particularly useful for expression of proteins which are prone to misfolding or formation of inclusion bodies. The mauC gene encodes amicyanin, a Type I copper protein that is localized in the periplasm [85]. It was shown that incorporation of the very tightly bound copper occurs during the folding of amicyanin in the periplasm [141]. In cases such as this, the timing of the translocation of the protein is important to avoid misfolding and aggregation that can result from unavailability of copper at the critical point in protein folding. Recombinant expression of VL proteins and immunoglobulins has also been problematic due to the tendency to form inclusion bodies. For expression of some protein such amicyanin and κI O18/O8 V_L, as well as many others, the level of recombinant protein expression may not necessarily be as important as the timing and rate at which the protein is being expressed and co-translationally translocated into the periplasm. In cases such as this the amicyanin signal sequence may be a useful alternative to other commonly used signal sequences for expression of proteins in E. coli and other prokaryotes.

3.5 Section I Conclusion

Due to the efficiency of the translocation of the amicyanin leader sequence, it can be concluded that the attempted mutations in the V_L resulted in very unstable proteins. The presence of hydrophilic or polar residues in the interior core of proteins is generally uncommon, as this can lead to a destabilization of van der Waals forces resulting from the hydrophobic packing of the core. Also, the insertion of rather large residues such as tryptophan and tyrosine can lead to distortions in the shape of the protein. This can affect the

function as well as the structure and stability. Given these general insights along with the experimental results related to the W45Y mutation of amicyanin and expression of V_L mutants, it is interesting that an interior tryptophan residue is key to increasing the stability of amicyanin and possibly other cupredoxins, who also retain this semi-conserved interior tryptophan residue.

4 SECTION II: USING A NON-PHYSIOLOGIC ENZYME COMPLEX TO STUDY PHYSIOLOGIC BIOCHEMISTRY

4.1 Section II Introduction

In analyzing k_{ET} according to ET theory, it is preferable to measure the free energy dependence of the reaction, rather than the temperature dependence. This is because variations in temperature can affect the kinetic mechanism of the ET reaction, redox potential of the donor and acceptor sites, as well as the reorganization energy needed to optimize the molecules to perform ET. However, measuring the free energy dependence is usually technically not possible due to limited technologies available to specifically alter the functional groups and substituents of amino acids in proteins in order to alter the redox potential of the cofactor. By using amicyanin and MauG together in a non-physiologic complex, it is possible to easily alter the free energy of the reaction using pH variation and site-directed mutagenesis. This is the first time this has been described, and it also provides a proof of concept mechanism that could be applied to other proteins that have a redox site that exhibits pH dependence of its redox potential.

A P94A mutation in the copper site of amicyanin also allowed expansion of the range of interprotein free energy dependence of ET that could be studied. These studies using this complex also describe the first time an alternate redox partner has been used to study a true ET reaction, which is kinetically coupled in its physiologic complex. The effect of relaxation of the conformational constraint of the copper ligands on k_{ET} in P94A amicyanin was obscured in its native complex. However, by using MauG, these effects have been uncovered. The implications of these results with regard to the design and engineering of redox site coordination are discussed.

This complex has also granted an opportunity to study interprotein ET and gain insight into two different high valent heme redox site variations of MauG. WT MauG contains a di-*c*-type heme redox site that can be oxidized to the *bis*-Fe(IV) redox state, where one heme is present as an Fe(IV)=O with an axial

ligand provided by a His and the other is present as an Fe(IV) with His-Tyr axial ligation and no exogenous ligand. In most heme-dependent enzymes which use a high valence intermediate, it is too short lived in order to study well. In MauG, it is unusually stable and decays over a period of several minutes, instead of a fraction of a second, as seen in other enzymes, such as peroxidases. This is long enough for study in a stopped flow spectrophotometer.

Using site-directed mutagenesis, a high valence state single heme redox site can also be produced in Y294H MauG. This redox site, known as "compound I", is one of the typical high valence intermediates in heme-dependent enzymes because many of these enzymes contain only one heme. Thus, the amicyanin-MauG complex provides a unique opportunity to not only study these two different, highly reactive, and elusive intermediates, but also, to study them within the same protein matrix.

This section demonstrates how alternate redox partners can be used to complement and enhance our understanding of the mechanisms and optimization of cofactors that perform catalytic and long-range ET reactions. These studies help to provide further insight regarding the design and nature of alternative mechanisms to stabilize and utilize long-range ET and catalytic cofactors in high valent heme-dependent enzymes and which factors contribute to the magnitude of reorganization energy in proteins in order to optimize the function of the enzyme.

4.2 Characterization of the Free Energy Dependence of an Interprotein Electron Transfer Reaction by Variation of pH and Site-Directed Mutagenesis

4.2.1 Introduction

Long range electron transfer (ET) is a fundamental cellular process necessary for respiration, photosynthesis and redox reactions of intermediary metabolism. Although this is a fundamental biochemical process, there is still much to be understood with regard to the different ET mechanisms and how ET is

controlled to direct the flow of electrons within the cell. Dysfunctional ET can cause disastrous cellular consequences, including increased production of reactive oxygen species. The rate of an ET reaction (k_{ET}) can be described by ET theory, often termed Marcus theory [142]. In this formalism the parameters that determine k_{ET} are temperature (T), free energy (ΔG°), electronic coupling (H_{AB}), and the reorganization energy (λ). The free energy is determined by the difference in the oxidation-reduction midpoint potential (Em) values of the donor and acceptor redox sites. H_{AB} describes the extent of overlap of the wave functions of the reactant and product state and is dependent upon the ET distance and the nature of the intervening medium[71, 72, 143]. λ reflects the amount of energy needed to optimize the system for ET; i.e., the energy required to bring the reactant and product states to the state in which the ET event occurs. In principle, one could experimentally determine H_{AB} and λ values by examining the dependence of k_{ET} on either ΔG° or temperature. However, application of ET theory to interprotein ET reactions is challenging. The kinetic complexity of these reactions may mask the true k_{ET} [144, 145]. Even when it is possible to monitor k_{ET}, in contrast to ET reactions involving small molecules, it is difficult and usually impossible to systematically alter the ΔG° for the reaction. It is possible to examine the temperature dependence of protein ET reactions, although one is limited to studies over a fairly narrow range of temperatures given the relative instability of proteins.

Amicyanin from Paracoccus denitrificans [85] is a blue copper protein that mediates ET from the protein-derived tryptophan tryptophylquinone (TTQ) [146] cofactor of methylamine dehydrogenase (MADH) [147] to the heme of cytochrome *c*-551i [148] via its type 1 copper site [149]. The type 1 copper site consists of a single copper ion coordinated by His53, His95, Cys92, and Met98 [1]. The complex of MADH, amicyanin, and cytochrome *c*-551i is one of the best characterized physiological protein ET systems. The proteins have been structurally characterized by x-ray crystallography of the binary complex of MADH and amicyanin [150] and the ternary protein complex, which includes cytochrome *c*-551i [89]. The protein complexes were shown to be catalytically active and able to perform ET in the crystalline state [151-153]. The ET reactions to [154-157] and from

[149] the type I copper center of amicyanin within the ternary protein complex have been studied in solution by stopped-flow spectroscopy, and many of these reactions have been analyzed by ET theory.

A curious feature of the reactivity of amicyanin in this system is that while these three proteins are isolated from P. denitrificans as individual soluble proteins, they must form the ternary protein complex in order to catalyze methylamine-dependent cytochrome *c*-551i reduction [149, 158]. Although it is a thermodynamically favorable reaction, MADH does not directly reduce cytochrome *c*-551i in the absence of amicyanin. Furthermore, reduced free amicyanin does not reduce oxidized cytochrome *c*-551i in the absence of MADH at physiologic pH because the E_m value of free amicyanin is much more positive than that of the cytochrome [7]. The redox properties of amicyanin are altered on complex formation with MADH so as to facilitate the reaction by lowering the E_m value of amicyanin in the complex under physiological conditions [7]. This phenomenon is related to the pH-dependence of the E_m value of free amicyanin which is due to a change in the geometry of the reduced form of the copper site upon deprotonation of the surface exposed His95 copper ligand (Figure 4.2.1). When His95 is deprotonated the imidazole nitrogen points towards the copper ion to form a ligand. When it is protonated, the imidazole side chain rotates 180° out of the coordination sphere of the copper ion. Thus, the Cu(I) is three-coordinate while the Cu(II) is four coordinate. There is no evidence that within the pH range of this study the Cu(II) ever becomes three-coordinate. As such, since the E_m value of amicyanin is pH-dependent, one would expect the ΔG° for the ET reactions of amicyanin to be pH-dependent. However, when amicyanin is in complex with MADH, this rotation of His95 is sterically hindered by MADH and so the Cu(I) remains four-coordinate and the E_m value of amicyanin in complex is now independent of pH [7]. In the present study, ET is studied from amicyanin to an alternative protein electron acceptor, the diheme enzyme MauG [159]. In the amicyanin-MauG complex, the pH-dependence of the E_m value of amicyanin is retained allowing the characterization of the dependence of kET on ΔG° for this interprotein ET reaction.

The complexity of biological ET reactions must also be considered when attempting to apply ET theory to protein ET reactions. ET reactions may be either gated [80, 160, 161] or coupled [144]. In these cases, the observed rate of the ET reaction is not a true k_{ET} and therefore the true λ and H_{AB} associated with the ET event cannot be determined by ET theory. A P94A mutation of amicyanin altered its E_m value [8, 81]. In addition to altering the E_m value, the P94A mutation also converted the ET from the reduced copper site to cytochrome *c*-551i from a true ET reaction to one which was kinetically coupled [97]. It is shown herein that the ET reaction of reduced P94A amicyanin to MauG is not coupled and so the effect of the mutation on the ET parameters of P94A amicyanin can now be characterized in the amicyanin-MauG system.

MauG is a di-c-type heme enzyme responsible for the posttranslational modification of a precursor of MADH (preMADH) to generate the protein-derived TTQ cofactor [66-68]. These oxidative biosynthetic reactions require the formation of a high-valent *bis*-Fe(IV) redox state of MauG in which one heme is present as Fe(IV)=O with an axial ligand provided by a His and the other is present as Fe(IV) with His-Tyr axial ligation and no exogenous ligand [66, 162]. This *bis*-Fe(IV) form of MauG is used as the electron acceptor for reduced amicyanin in the present study. The studies of this ET reaction with amicyanin also provide an opportunity to further examine and gain insight into the ET properties of this unique high-valent heme species.

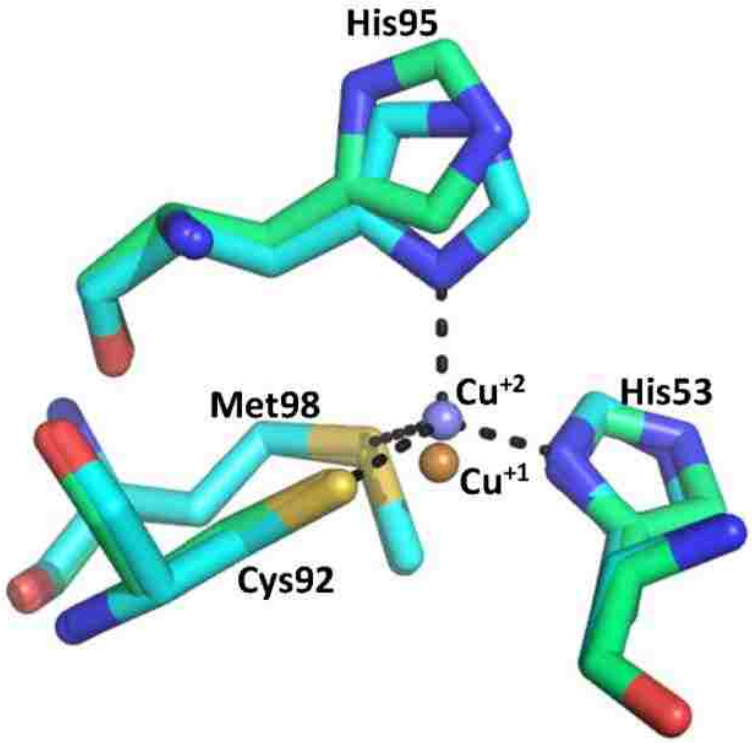

Figure 4.2.1 The type 1 copper site of amicyanin. An overlay is shown of the structures of the oxidized protein (PDB ID: 2OV0) (carbons colored cyan) and the reduced protein (PDB ID: 2RAC) (carbons colored green) below the pKa for the pH-dependence of the E_m value.

4.2.2 Materials and Methods'

4.2.2.1 *Protein purification.*

Recombinant amicyanin was expressed in Escherichia coli BL21 (DE3) and purified from the periplasmic fraction as described previously for WT [92] and P94A [97] amicyanins. Recombinant MauG was expressed in and purified from Paracoccus denitrficans as described previously [159].

4.2.2.2 *Determination of kET.*

The rates of the ET reactions from reduced amicyanin to *bis*-Fe(IV) MauG were determined using an On-Line Instruments (OLIS, Bogart, GA) RSM1000 stopped-flow rapid scanning spectrophotometer. Each reaction was performed in 10 mM potassium phosphate buffer, pH 7.5 (unless otherwise specified), at the indicated temperature. One syringe contained the limiting reactant, 1-2 µM *bis*-Fe(IV) MauG, and the second syringe contained varying concentrations of reduced amicyanin. The concentration of amicyanin was always in at least 10-fold excess. Amicyanins were reduced by addition of a stoichiometric amount of sodium dithionite [98]. The *bis*-Fe(IV) MauG was generated by addition of equimolar hydrogen peroxide [162]. After rapid mixing the reactions were monitored over the range from 365 to 435 nm to observe the conversion of *bis*-Fe(IV) MauG to diferric MauG. Kinetic data were reduced by factor analysis using the singular-value decomposition (SVD) algorithm and then globally fit using the fitting routines of OLIS Global Fit.

4.2.2.3 *Analysis of kET by ET theory*.

Data for the temperature-dependence of kET and the ΔG°-dependence of kET were each analyzed using eq 4.2.1. The other terms in this equation are Planck's constant (h) and the gas constant (R). An alternative equation (eq 4.2.2) was also used which takes into account the exponential decrease in k_{ET} over

distance. This equation can be used to predict the ET distance between the donor and acceptor redox sites [71, 72, 143]. The parameter β is used to quantitate the nature of the intervening medium with respect to its efficiency to mediate ET. The donor to acceptor distance is r, and r_0 is the close contact distance (3Å). k_0 is the characteristic frequency of nuclei ($k_0 = 10^{13}$ s-1) which is the maximum ET rate when donor and acceptor are in van der Waals' contact and λ=-ΔG°.

$$k_{ET} = \left[\frac{4\pi^2 HAB^2}{h\sqrt{(4\pi\lambda RT)}}\right] e^{\left[-\frac{(\Delta G^\circ + \lambda)2}{4\lambda RT}\right]} \quad (4.2.1)$$

$$k_{ET} \approx k_o \exp[-\beta(r - r_0)] \exp\left[-\frac{(\Delta G^\circ + \lambda)2}{4\lambda RT}\right] \quad (4.2.2)$$

Kinetic data were analyzed using the model described in eq 4.2.3 where A and B are amicyanin and MauG, respectively. In each of the single-turnover kinetic experiments, the observed rate constant (kobs) was best fit to a single-exponential relaxation. The limiting first-order rate constant for each reaction was determined from the concentration dependence of k_{obs} using eq 4.2.4.

$$A(Cu(I)) + B(Fe(IV)) \overset{K_d}{\rightleftharpoons} A(Cu(I)) - B(Fe(IV)) \overset{k_{ET}}{\underset{k_{-ET}}{\rightleftharpoons}} A(Cu(II)) + B(Fe(III)) \quad (4.2.3)$$

$$k_{obs} = \frac{k_{ET}[A(CuI)]}{[A(CuI)] + K_d} + k_{-ET} \quad (4.2.4)$$

4.2.2.4 *In Silico Docking of WT amicyanin and MauG.*

A docking model of WT amicyanin with MauG was constructed by using the ZDOCK utility version 3.02 and server (http://zdock.umassmed.edu) [163]. The PDB files of WT amicyanin (PDB ID: 2OV0) and MauG (PDB ID: 3L4M, chain A) were used in model building. All residues of both chains were used to explicitly search the rotational space, and the translational space was searched using fast Fourier transform. No residues were blocked from the binding site during docking, and no specific residues were selected for filtering binding site predictions.

4.2.3 Results

4.2.3.1 *Determination of kET for of the reaction of bis-Fe(IV) MauG with reduced amicyanin.*

The reaction of *bis*-Fe(IV) MauG with varied concentrations of reduced amicyanin at pH 7.5 at 25º C exhibited saturation behavior (Figure 4.2.2). The fit of this data to eq 4.2.2 yielded a limiting first-order rate constant (k_{ET}) of 22 ± 2 s-1 and a Kd of 165 ± 50 µM. It should be noted that reduction of *bis*-Fe(IV) MauG to diferric MauG requires two electrons and that oxidation of Cu(I) amicyanin requires one electron. Thus two molecules of Cu(I) amicyanin must be oxidized to observe the complete reaction. In each reaction, the change in absorbance fit best to a single exponential. This means that after the first Cu(I) amicyanin reacts it dissociates and then a second Cu(I) amicyanin binds and reacts. The fact that a single exponential relaxation is observed means that the dissociation/association steps are very rapid relative to k_{ET} and since excess Cu(I) amicyanin is present, rebinding of the Cu(II) amicyanin after the single turnover is not a factor.

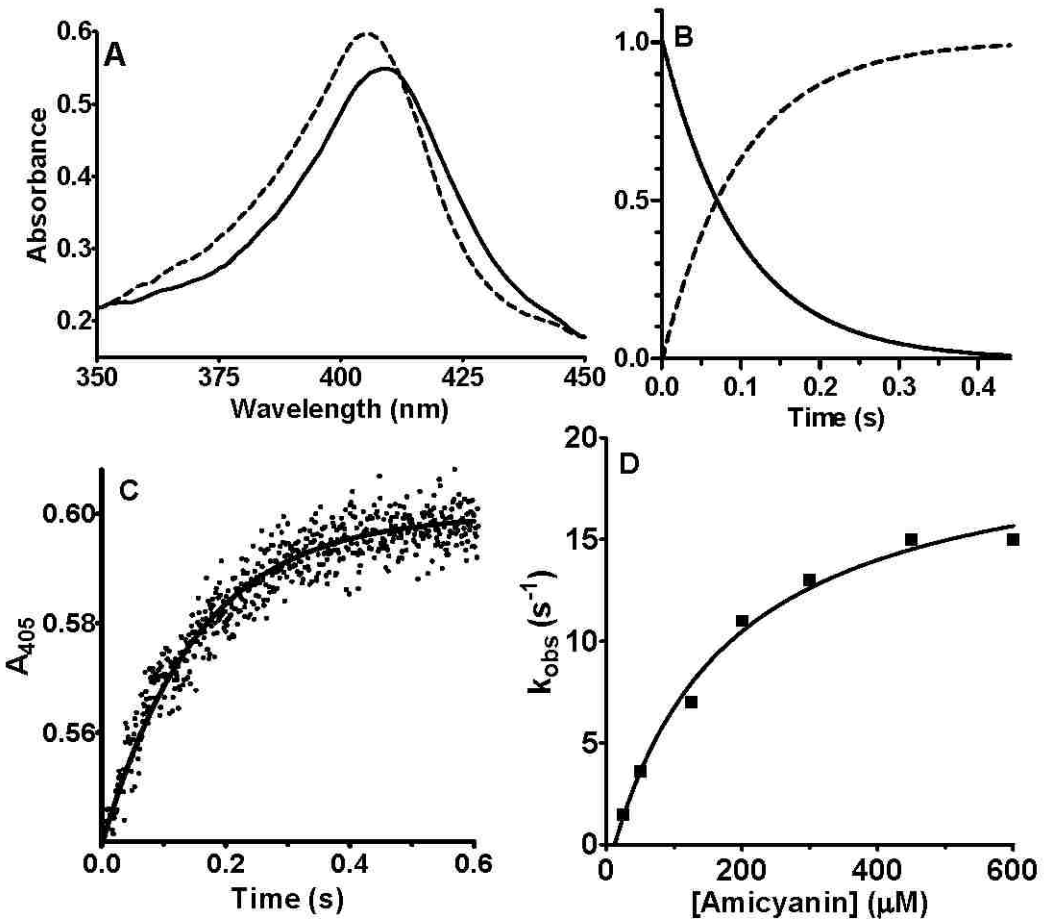

Figure 4.2.2 The reduction of *bis*-Fe(IV) MauG by reduced amicyanin. A. Spectral changes associated with the ET reaction. The visible spectrum of the Soret region of the hemes of *bis*-Fe(IV) before (solid line) and after (dashed line) reaction with reduced amicyanin. B. The kinetic plots depict global fits of the most statistically significant eigenvector of the SVD reduced three-dimensional data. The time courses for the disappearance of the initial species (solid line) and appearance of the final species (dashed line) are displayed. C. The time course for the change in absorbance at 405 nm after formation of the *bis*-Fe(IV) state. The solid line is the fit of the data by a single exponential transition. D. The concentration dependence of observed rate of ET from reduced amicyanin to *bis*-Fe(IV). The line is a fit of the data by eq. 4.

4.2.3.2 *Temperature dependence of k_{ET} for the reaction of bis-Fe(IV) MauG with reduced amicyanin.*

The k_{ET} for the ET reaction from reduced amicyanin to *bis*-Fe(IV) MauG was determined at temperatures from 10° C to 30° C (Figure 4.2.3). The *bis*-Fe(IV) MauG was unstable at higher temperatures and so this limited the range that could be studied. The E_m value for the *bis*-Fe(IV)/diferric couple of MauG is unknown. E_m values for Fe(IV)/Fe(III) couples in heme-dependent peroxidases have been determined and these values range from 724-1160 mV [164]. The results of previous studies of the ET reaction of *bis*-Fe(IV) MauG with preMADH determined that the reduction of the *bis*-Fe(IV) center during hopping-mediated ET via a Trp radical was endergonic by ~200-300 mV [70]. E_m values for the Trp radical/Trp redox couple have been determined to be in the range of 890-1080 mV [165, 166]. This suggested that the E_m value for the Fe(IV)/Fe(III) couple in MauG is at the low end of what has been reported for similar systems. As such, for the analysis of the temperature-dependence of the ET rates the E_m value of 724 mV for MauG and the known E_m value of amicyanin at pH 7.5 of 265 mV [7] were used to determine the ΔGº for the reaction to input into eq 3. The fit of the data to eq 3 yielded values of $\lambda = 2.3 \pm 0.1$ eV and $H_{AB} = 0.6 \pm 0.1$ cm-1. Using eq 4 it is also possible to obtain an experimentally-determined estimate of the ET distance. In analyzing protein ET reactions by eq 4, average β values of 0.7-1.4 Å-1 have been used to describe the nature of the intervening protein medium between the redox centers [71, 72, 143]. Analysis of these data inputting β values in this range yielded a range of ET distances of 12-21 Å.

In order to gain insight into the relative orientations of the redox centers in the amicyanin-MauG complex, a protein docking model was constructed using the ZDOCK program [163] from the crystal structures of amicyanin and MauG (Figure 4.2.4). This model places the amicyanin copper approximately 16.7 Å from the porphyrin ring edge of the ferryl heme and 17.9 Å from the ferryl heme iron. These distances correlate well with the experimentally-determined range of ET distance obtained from analysis of the temperature-dependence of the ET rate using eq. 4.

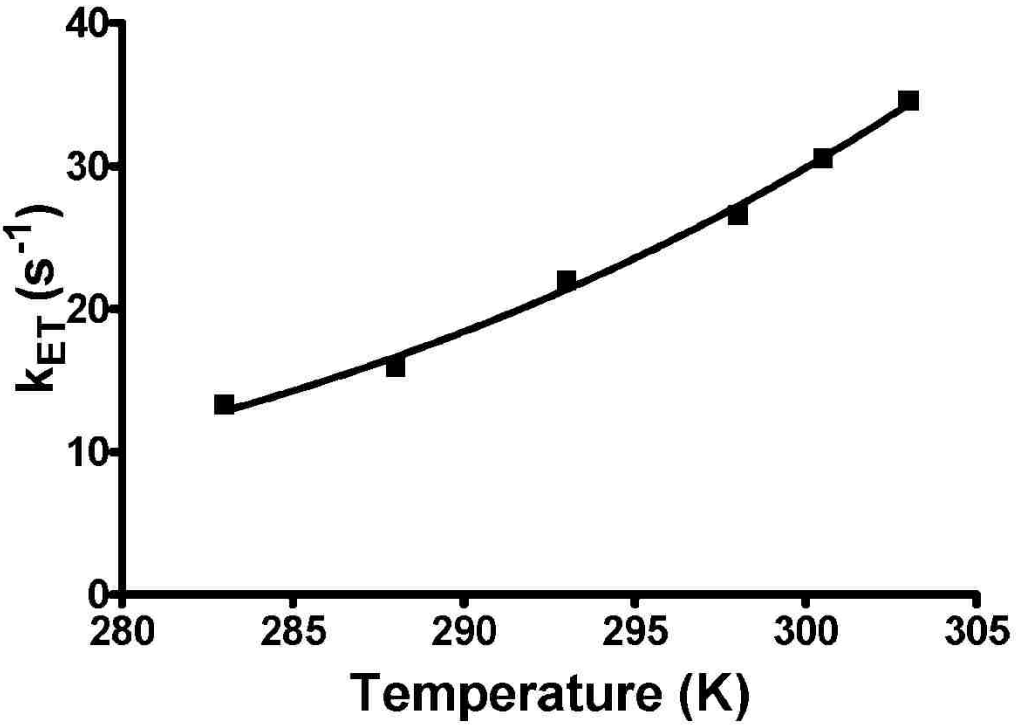

Figure 4.2.3 The temperature dependence of k_{ET} from reduced amicyanin to *bis*-Fe(IV). The line is a fit of the data by eqs. 1 and 2. Those two fits are superimposable.

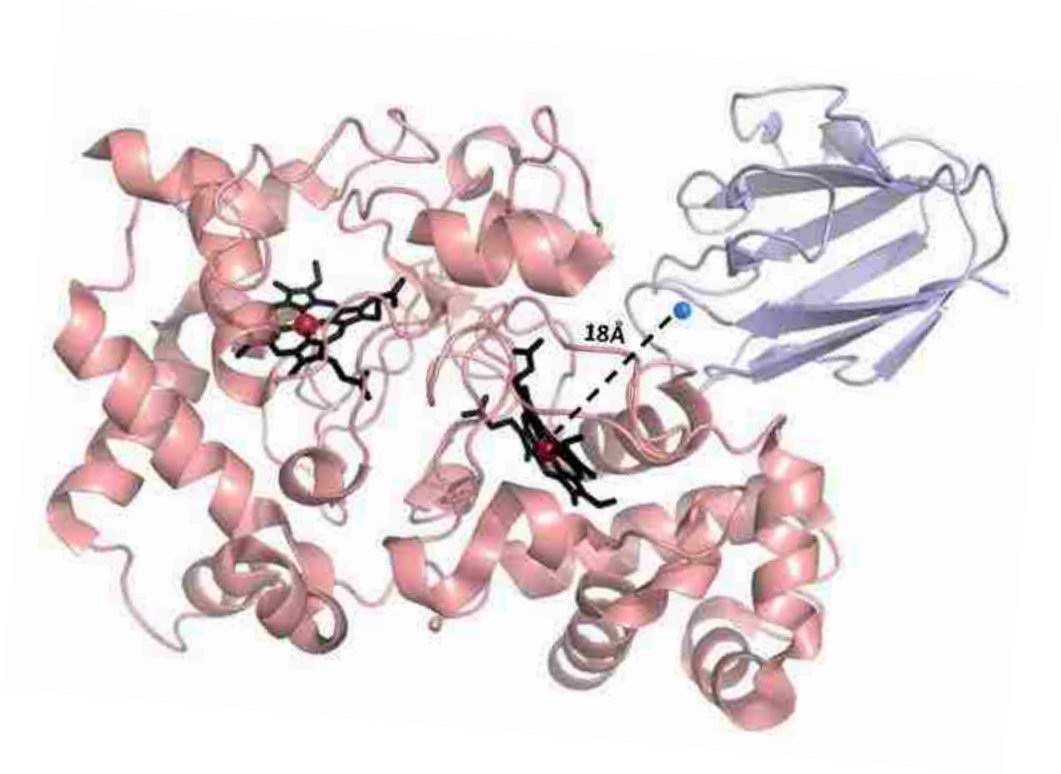

Figure 4.2.4 Docking model of the amicyanin-MauG complex. MauG is colored pink with the porphyrin rings black and irons red. Amicyanin is colored purple with the copper blue. The distance from the copper to the high-spin heme iron is indicated.

4.2.3.3 *ΔG°- dependence of k_{ET} from reduced amicyanin to bis-Fe(IV) MauG.*

As stated earlier, the E_m value of type I copper site of free amicyanin is pH-dependent due to the fact that the His95 ligand is lost when it is protonated (Figure 4.2.5). The pKa for this phenomenon is 7.5 [7]. This pH-dependence was not a factor in the ET reaction between MADH and amicyanin because when amicyanin is in complex with MADH the rotation of the His95 ligand out of the copper coordination sphere is sterically prevented. Thus, the E_m value of amicyanin in complex with MADH is pH-independent [7]. Inspection of the docking model for the amicyanin-MauG complex suggested that movement of His95 was not likely to be hindered in this complex, meaning that the E_m value of amicyanin in this complex should be the same as free amicyanin. To examine this further the ET reaction from reduced amicyanin to *bis*-Fe(IV) MauG was examined over a range of pH from 5.6 to 7.9. The range could not be extended further due to instability of the proteins. As can be seen in Figure 4.2.5, k_{ET} increased with increasing pH, consistent with the decrease in E_m value of amicyanin with increasing pH, and consequently an increasingly less negative ΔG° for the ET reaction.

In order to assess whether the dependence of k_{ET} on pH was truly reflecting the ΔG°- dependence of k_{ET}, and not some other effect of pH on the system, these data were analyzed using eq 1. A curve simulating the predicted ΔG°- dependence of k_{ET} was constructed using the values of λ and H_{AB} that were obtained from the fit of the data in Figure 3 at a fixed temperature of 25 °C at which the pH-dependence studies were performed. The values of ΔG° for the reactions at different values of pH were calculated using the known E_m values for free amicyanin at each pH and the E_m value of 724 mv for MauG. As can be seen in Figure 6, the data points fall nearly exactly on the predicted curve for the Δ°°- dependence of k_{ET}.

As stated above, the E_m value for MauG used in this analysis is an estimation. As per eq 4.2.3, uncertainty in this value could influence the fitted value of λ. The E_m value that was used was at the low end of literature values for similar systems. If the E_m value of MauG were more positive then the corresponding fitted value of λ would be proportionately greater; however the value of λ of 2.3 eV is at the high end of what

would be considered a λ value for a true ET reaction. The data in Figure 4.2.6 provide further evidence that this is λ value describes a true ET reaction is presented later. These data also provide evidence that the E_m value of MauG and λ for the reaction do not vary with pH since the change in ΔGº values determined solely from the pH-dependence of amicyanin fit so well to the curve that is described by pH-independent values for those parameters.

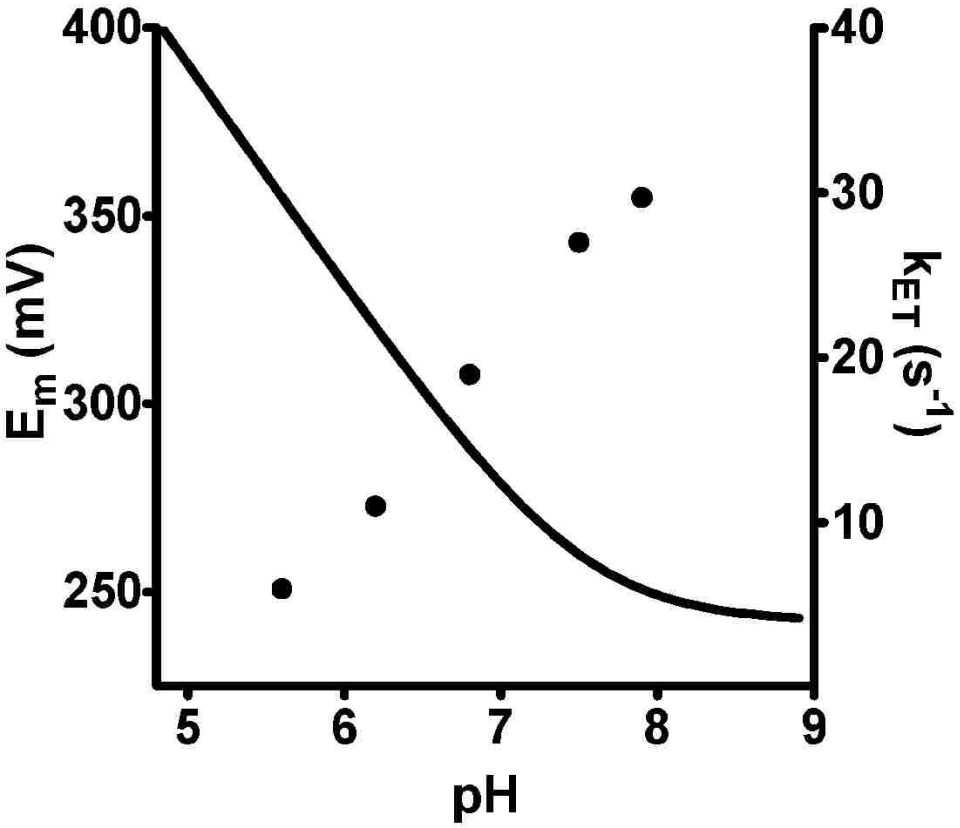

Figure 4.2.5 pH dependencies of the E_m value of amicyanin and k_{ET} from reduced amicyanin to *bis*-Fe(IV). The solid line describes the pH dependence of the E_m value of free amicyanin [7]. The circles are the k_{ET} values at the indicated pH.

4.2.3.4 *ET from reduced P94A amicyanin to bis-Fe(IV) MauG.*

To further explore the ΔGº- dependence of k_{ET} from reduced amicyanin to *bis*-Fe(IV) MauG, studies were performed with the P94A amicyanin variant [81]. The mutation of Pro94 to Ala increased its E_m value and shifted the pKa for the pH dependence of the E_m value to more acidic values [8]. The reaction of *bis*-Fe(IV) MauG with varied concentrations of reduced P94A amicyanin at pH 7.5 exhibited saturation behavior. The fit of this data to eq 2 yielded a k_{ET} of 7.8 ± 0.6 s-1 and a Kd of 240 ± 82 μM. The k_{ET} for the reaction of P94A amicyanin with *bis*-Fe(IV) MauG was also determined at pH 6.0. At pH 6.0 and 7.5 the E_m values of P94A amicyanin are 412 and 380 mV, respectively [8]. The ΔG° values for these reactions are less than any of those for the reactions of WT amicyanin so that the range of the ΔG°-dependence of the reaction could be expanded. As seen in Figure 4.2.6 these data points also fall on the predicted curve for the ΔG°- dependence of k_{ET}.

The ET reaction from reduced P94A amicyanin to cytochrome *c*-551i could not be analyzed by ET theory because the mutation converted this true ET reaction to a coupled ET reaction [97]. It is noteworthy that the k_{ET} values for the reactions reduced P94A amicyanin are consistent with those for a true ET reaction with λ and H_{AB} values identical to those of the reaction with WT amicyanin (discussed later).

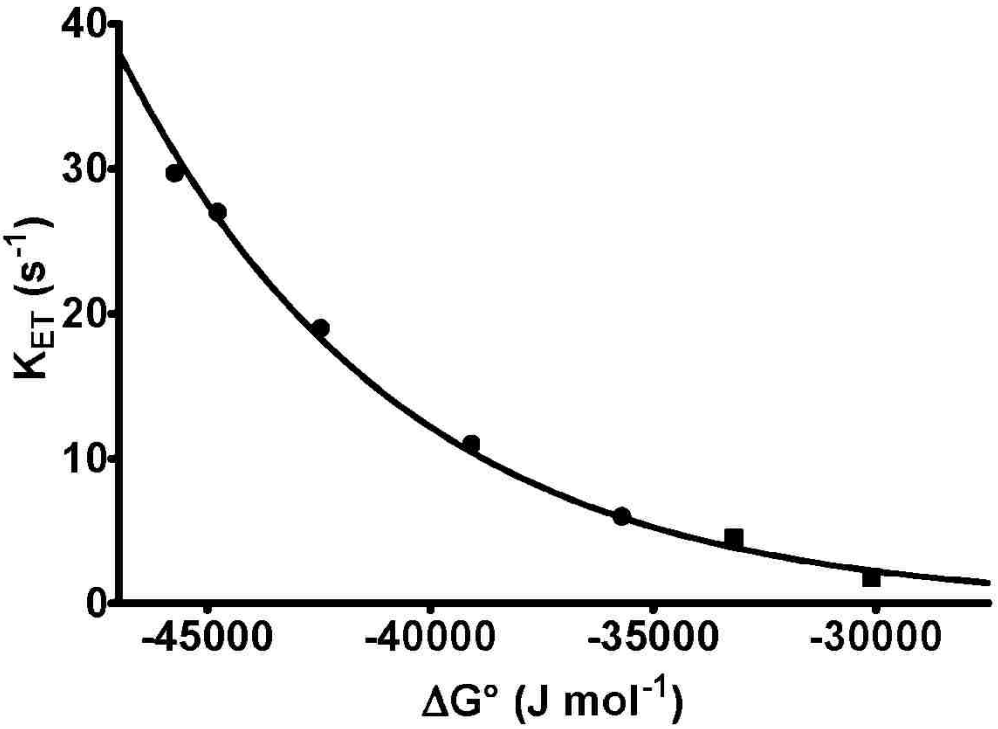

Figure 4.2.6 Free energy dependence of k_{ET} from reduced amicyanin to *bis*-Fe(IV). The line which was generated using eq 1 uses the experimentally-determined values of H_{AB} and λ that were determined from the data in Figure 4.2.3 to describe the predicted dependence of k_{ET} on ΔGº at 25 ºC. The experimentally determined k_{ET} values are shown for the reactions WT amicyanin (circles) and P94A amicyanin (squares) which were determined at different pH values to allow variation of ΔGº.

4.2.4 Discussion

There are relatively few examples of studies of protein ET reactions in which it was possible to examine the ΔGº-dependence of kET. Gunner and Dutton [167] were able to study the ΔGº dependence of the ET from bacteriochlorophyll to ubiquinone in the photosynthetic reaction center from Rhodobacter sphaeroides by substituting the native QA with quinones with different E_m values. Scott et al [168] studied intramolecular ET in cytochrome b5 labeled with Ruthenium(II) polypyridine complexes with different E_m values. Farver et al. [76] recently studied the intramolecular ET reactions between the copper of azurin a disulfide radical anion with several site-directed mutants that spanned a wide range of E_m values. The ΔGº-dependence of the ET reaction between MADH and amicyanin had previously been examined by looking at the rates of the forward and reverse reactions of amicyanin with different redox forms of MADH [155, 157]. The use of the pH-dependent variation of ΔGº that is described herein is a novel approach for analysis of an interprotein ET reaction by ET theory. This approach could be applied to other systems in which the electron donor or acceptor site has a pH-dependent E_m value. As in this study, it could also be possible to use amicyanin or a another protein with a pH-dependent E_m value to study the ET reactions with a non-physiologic redox protein of interest and gain information on the ET parameters associated with ET to or from its redox center.

In the present study, it is interesting to compare the value of λ obtained in this study of 2.3 eV with the λ values previously obtained for the reactions of amicyanin with MADH of 2.3 eV [155, 157] and with cytochrome *c*-551i of 1.1 eV [149]. While the ET reaction with the cytochrome may seem more similar to the reaction with MauG, in that the redox center is a heme, the λ values are quite different and more similar to the reaction with the TTQ cofactor of MADH. The redox center of MauG is not just a single heme, but two hemes with an intervening Trp residue that share spin and charge [169]. In this sense, the diheme redox center of MauG is more similar to TTQ. TTQ is comprised of two covalently-linked modified Trp residues which share

delocalized charge. Another similarity is that while the heme iron of cytochrome *c*-551i is shielded from solvent, the high-spin heme of MauG and the quinone moiety of TTQ are each exposed to solvent. The fact that the reorganization energies associated with the diheme site of MauG and the TTQ of MADH could require changes in lengths and angles of multiple bonds, as well as contributions from reorganization of solvent is likely reflected in the similar and relatively large values of λ for their respective reactions with amicyanin. The magnitude of these λ values is consistent with the contribution of these different processes that poise the system for the ET event and are kinetically indistinguishable from that event.

It is significant that whereas the mutation of Pro94 to Ala in amicyanin converts the true ET reaction from reduced amicyanin to cytochrome *c*-551i to a kinetically coupled ET reaction, the reaction of reduced P94A amicyanin with *bis*-Fe(IV) MauG remains a true ET reaction. This is evident from the results shown in Figure 4.2.6. The fact that the rates of reaction of P94A amicyanin with MauG lie on the ΔGº-dependence curve indicate that the λ and H_{AB} for the reaction with reduced amicyanin are not affected by the P94A mutation, despite the fact that the E_m value is significantly altered by the mutation. The basis for the change in the E_m value of the type 1 copper site of P94A amicyanin was that a consequence of the mutation was the introduction of a hydrogen-bond to the Cys thiolate ligand and alteration of the position of the Cu+ ion [81]. It is noteworthy that the λ associated with its ET reaction from the copper site was not altered in the reaction with MauG. This is information that could not be obtained from the physiologically relevant and well-studied MADH-amicyanin-cytochrome *c*-551i complex because the mutation altered the kinetic mechanism of that reaction such that it was coupled [97].

In true ET reactions, the ET event is the rate limiting step. Thus, k_{obs} is k_{ET}. However, gated and coupled ET reactions cannot be properly analyzed by ET theory. In a gated ET reaction a kinetically indistinguishable reaction step precedes and is required for ET, and the rate of that step (kx) is slower than k_{ET}. Thus, k_{obs} is k_X rather than k_{ET} [80, 161]. In a coupled ET reaction, k_x is faster than k_{ET} but thermodynamically

unfavorable such that the equilibrium constant for that step (K_x) is <1. In this case k_{obs} is the product of KX and k_{ET} [82]. The basis for the coupled reaction mechanism of ET from reduced P94A amicyanin to cytochrome *c*-551i in the ternary protein complex with MADH is as follows. The copper site in reduced P94A amicyanin was found to exist in an equilibrium between two different conformations. In one of these conformations, the Met98 copper ligand is replaced by a water molecule and the copper atom is displaced by 1.4 Å and disfavored for ET to the cytochrome. As such the observed rate of ET is influenced by the equilibrium constant for the interconversion of these two conformations [97]. This is evidently not the case for the reaction with *bis*-Fe(IV) MauG. This may be due to differences in the protein-protein interactions at the protein interface in the respective ET complexes. As discussed earlier, the movement of the His95 copper ligand is constrained at the amicyanin-MADH interface but it is not constrained when in complex with *bis*-Fe(IV) MauG. Residue 94 is also in this interface. The P94A mutation increased the Kd for complex formation with MADH [97] and with *bis*-Fe(IV) MauG (discussed earlier). It is possible that whereas the protein-protein interactions at the amicyanin-MADH interface shift the equilibrium to the conformation that disfavors ET, the protein-protein interactions at the P94A amicyanin-MauG interface shift the equilibrium strongly to the conformation that favors ET, resulting in a true ET reaction.

This study includes the first description of the use of variation of pH as a means to examine the free energy dependence of an interprotein ET reaction. The amicyanin-MauG system allowed study of the ET properties of amicyanin in this manner, which could not be studied this way in the native system with MADH and cytochrome *c*-551i. This study includes the first description of how an alternative redox protein partner can be used to study true ET from a redox cofactor which was obscured due to the kinetic complexity of its reaction with its native electron acceptor. This study also provides an opportunity to examine an interprotein ET reaction to the *bis*-Fe(IV) redox state of MauG. These results demonstrate how ET reactions with

alternative redox partner proteins can complement and enhance our understanding of the reactions with the natural redox partners, and further our understanding of mechanisms of protein ET reactions.

4.3 Utilizing the Amicyanin-MauG Complex to Study Y294H MauG

As seen in the previous study, the amicyanin-MauG complex was effectively able to be used to further study and characterize the ET properties of the *bis*-Fe(IV) diheme redox center of MauG. In addition to characterizing this uncommon and poorly understood redox center, the free energy dependence of interprotein electron transfer and also the effect of the P94A mutation on the redox and ET properties of amicyanin were also studied. Since this complex was effective in studying the redox center of P94A amicyanin, it may be useful in studying the effects of other mutations that could not be studied with their natural redox partners. One such example is Y294H MauG.

The effect of the Y294H mutation on the redox and ET properties of the diheme cofactor of MauG could not be studied with preMADH, its natural redox partner. This is because no reaction was observed. It is hypothesized that no reaction was observed due to a loss of function in the six-coordinate heme, which is spatially closer to the binding site of preMADH than the five-coordinate heme, to stabilize the high valence redox state necessary for reaction with the preTTQ cofactor of preMADH. As a result, both of the oxidizing equivalents of the high valence state are located on the five-coordinate heme forming a cofactor known as "compound I".

Compound I is a poorly characterized, transient intermediate in many catalytic mechanisms, and dysregulated ferryl heme is implied to be involved in the pathogenesis of many disease states, such as rhabdomyolysis[170], heme degradation and free iron release[171], lipid peroxidation[172], sickle cell disease[173], and superoxide generation. Like the *bis*-Fe(IV) redox state of the diheme cofactor in WT MauG, the compound I

cofactor in Y294H MauG is unusually stable. Amicyanin has already been shown to react with WT MauG, and docking models predicted that amicyanin reacts with WT MauG by binding close to the five-coordinate heme. Thus the compound I cofactor of Y294H MauG is an excellent candidate for study with amicyanin because amicyanin is likely to bind at the same position close to the five-coordinate heme, which appears to remain functional in the Y294H mutation in MauG based upon spectroscopic evidence.

4.4 Converting the Bis-Fe(IV) State of the Diheme Enzyme MauG to Compound I Decreases the Reorganization Energy for Electron Transfer

4.4.1 Introduction

High-valent hemes in proteins participate in a variety of important biological processes. They are used in the oxidation of substrates, as in oxygenases including cytochrome P450 enzymes [174, 175] and as intermediates in the breakdown of peroxides in peroxidases [176]. The hemes are usually present as compound I or compound ES, in which the ferryl heme iron is Fe(IV)=O with a cation radical present on the porphyrin ring or a nearby Trp or Tyr residue, respectively [177]. The *bis*-Fe(IV) state of MauG is an alternative strategy by which to stabilize a high-valent heme iron which utilizes two hemes [162]. In MauG from *Paracoccus denitrificans* this high-valent state has one heme present as Fe(IV)=O with an axial ligand provided by His35 and the other present as Fe(IV) with two axial ligands provided by His205 and Tyr294 and no exogenous ligand (Figure 4.4.1) [66, 178]. Ultrafast electron transfer (ET) between the hemes in the *bis*-Fe(IV) state is mediated by hopping through Trp93, which lies between the hemes. This leads to charge resonance stabilization of this high-valent heme species[169]. Trp93 is reversibly oxidized to a radical species during this process. It is believed that as a consequence of the CR stabilization, the high-valent state is actually comprised of an ensemble of resonance structures with the true *bis*-Fe(IV) state as the dominant species [169, 179]. The function of MauG is unique among other enzymes that use high-valent hemes as reaction intermediates. This di-*c*-type heme enzyme catalyzes the posttranslational modification of a precursor of

MADH (preMADH) to generate the protein-derived TTQ cofactor [180]. TTQ is generated by the six-electron oxidation by MauG of two Trp residues in preMADH. The oxidizing intermediate is the *bis*-Fe(IV) species. In contrast to the mechanism of heme-dependent oxygenases, the hemes of MauG make no direct contact with the substrate. Instead preMADH binds to the surface of MauG with the residues on preMADH that are oxidized at a distance of 40 Å and 19 Å, respectively, from the two heme irons [66]. Due to the long distance, the catalytic reactions require long range ET from the substrate to the hemes.

Hemes are also involved in many non-catalytic physiological ET reactions. Nearly all of these involve the Fe(II) and Fe(III) redox states as the electron donor and acceptor. The long range ET reaction from preMADH to the *bis*-Fe(IV) hemes of MauG, which is required as a part of the catalytic mechanism, has been studied and the ET parameters for this reaction have been determined[70]. Similar long range ET studies have not been performed with other types of high-valent hemes. In this study we present a direct comparison of the ET properties of the hemes in the *bis*-Fe(IV) and compound I redox states within the same protein framework of MauG.

Mutation of the Tyr294 axial ligand of the 6-coordinate heme of MauG resulted in a heme with His-His axial ligation rather than Tyr-His ligation [181]. The crystal structure of Y294H MauG showed that apart from the ligand substitution, this mutation did not significantly perturb the structure of the diheme region of MauG. Whereas addition of H_2O_2 to MauG results in formation of the *bis*-Fe(IV) state, addition of H_2O_2 to Y294H MauG resulted in formation of a compound I species because the six-coordinate heme with His-His ligation could not stabilize Fe(IV). The high-valent compound I species in Y294H MauG was unable to oxidize preMADH and catalyze TTQ biosynthesis. It was concluded that the inability of compound I in Y294H MauG to oxidize preMADH was because the ET distance from the substrate to this single heme was too great (~40 Å), whereas the delocalization of the oxidizing equivalent over both hemes in the *bis*-FeI(V) state of MauG reduced the ET distance to a more manageable distance (~19 Å). Thus, it appears that a major function of the

six-coordinate heme of MauG in TTQ biosynthesis is to shorten the ET distance, which exponentially increases the ET rate. Unfortunately, because of the inability of Y294H MauG to react with preMADH, this meant that it was not possible to compare the ET properties of the different high-valent redox states of wild-type (WT) and Y294 MauG.

Recently an inter-protein ET reaction between the cupredoxin amicyanin and MauG was described [182]. Amicyanin is a small beta-barrel protein from P. denitrificans with a type 1 copper center that consists of a single copper ion coordinated by His53, His95, Cys92, and Met98 [1]. The ET reaction that was studied was that from CuI amicyanin to *bis*-Fe(IV) MauG. A docking model of the MauG-amicyanin complex placed the copper of amicyanin 16.7 Å from the porphyrin ring and 17.9 Å from the heme iron of the five-coordinate heme of MauG [182]. This distance matched that estimated from analysis of the temperature-dependence of the rate of the ET reaction (k_{ET}). The shorter ET distance to the five-coordinate heme in MauG-amicyanin complex than in the preMADH-MauG complex suggested that it might be possible to study an ET reaction of the compound I redox state of Y294H MauG in complex with amicyanin. In this study the ET reaction between Y294H MauG and amicyanin is analyzed and compared to the reaction with WT MauG. This allows a direct comparison of the ET properties associated with the ET from the *bis*-Fe(IV) and compound I redox states. This provides a unique opportunity to study an inter-protein ET reaction involving a compound I redox center in the same protein matrix as the *bis*-Fe(IV) redox center, and it allows for direct comparison of the ET parameters, i.e. reorganization energy (λ) and electronic coupling (H_{AB}) associated with ET from these two different types of high-valent heme redox states.

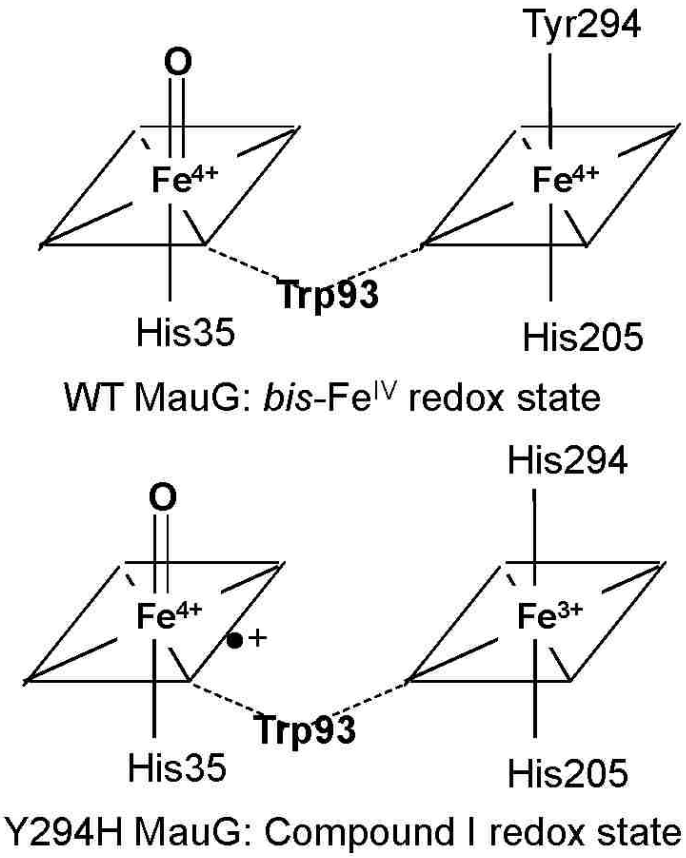

Figure 4.4.1 The structures of the *bis*-Fe(IV) redox state of WT MauG and the compound I redox state of Y294H MauG are illustrated. The porphyrin rings are represented as parallelograms with the iron and oxygen atoms, amino acid ligands indicated.

4.4.2 Materials and Methods

4.4.2.1 *Protein purification*

Recombinant amicyanin was expressed in Escherichia coli BL21 (DE3) and purified from the periplasmic fraction as described previously [92]. Recombinant Y294H MauG was expressed in and purified from Paracoccus denitrficans as described previously [159, 181].

4.4.2.2 *Determination of kET*

The rates of the ET reactions from reduced amicyanin to Compound-I Y294H MauG were determined using an On-Line Instruments (OLIS, Bogart, GA) RSM1000 stopped-flow rapid scanning spectrophotometer. Each reaction was performed in 10 mM potassium phosphate buffer, pH 7.5, at the indicated temperature. One syringe contained the limiting reactant, 2 μM Y294H MauG, and the second syringe contained varying concentrations of reduced amicyanin. Amicyanin was reduced by addition of an equimolar amount of sodium dithionite [98]. The high valent species of Y294H MauG was generated by addition of equimolar H2O2 [181]. After rapid mixing the reactions, the absorbance spectrum was monitored over the range from 365 to 435 nm to observe the conversion of Compound-I Y294H MauG to diferric Y294H MauG. Kinetic data were reduced by factor analysis using the singular-value decomposition (SVD) algorithm and then globally fit using the fitting routines of OLIS GlobalWorks software. In each of the reactions that were performed, the observed rate constant (kobs) was best fit to a single-exponential relaxation. The rate constants that were obtained at different concentrations of amicyanin were analyzed by eq 1 to determine the limiting first-order rate constant (kET) for the reaction and the Kd for complex formation. The errors which are listed in the text are standard errors of the fits.

$$k_{obs} = k_{ET} \frac{[\text{Amicaynin(CuI)}]}{[\text{Amicyanin(CuI)}] + K_d} + k_{-ET} \qquad (4.4.1)$$

4.4.2.3 *Analysis of k_{ET} by ET theory*

Data for the temperature-dependence of k_{ET} was analyzed using ET theory (eq 4.4.2) [142]. The terms in the equation are temperature (T), free energy (ΔG°), electronic coupling (H_{AB}), the reorganization energy (λ), Planck's constant (h) and the gas constant (R). ΔG° is calculated by eq 4.4.3, where n is equal to the number of electrons transferred, F is Faraday's constant, and ΔEm is the difference in the oxidation-reduction midpoint potential value of the electron donor and acceptor sites. Data were also analyzed by eq 4.4.4 where Ea is the activation energy and A is the pre-exponential factor.

$$k_{ET} = \left[\frac{4\pi^2 HAB^2}{h\sqrt{(4\pi\lambda RT)}}\right] e^{\left[-\frac{(\Delta G^\circ + \lambda)2}{4\lambda RT}\right]} \quad (4.4.2)$$

$$\Delta G^\circ = -nF\Delta Em \quad (4.4.3)$$

$$\ln(k) = \left(\frac{-E_a}{RT}\right) + \ln(A) \quad (4.4.4)$$

4.4.2.4 *In Silico Docking of amicyanin and Y294MauG*

A docking model of amicyanin with Y294H MauG was constructed by using the ZDOCK utility and server (http://zdock.umassmed.edu) [163]. The PDB files of amicyanin (PDB ID: 2OV0) and Y294H MauG (PDB ID: 3ORV, chain A) were used in model building.

4.4.3 Results

4.4.3.1 Determination of k_{ET} for of the reaction of Y294H MauG with reduced amicyanin.

The formation of the high-valent species in Y294H MauG is accompanied by a decrease in intensity of the Soret peak, which occurs immediately after addition of H_2O_2. Subsequent addition of reduced amicyanin results in an increase in intensity of the Soret peak and return of the absorbance spectrum to that of the diferric state (Figure 4.4.2A). The kinetics of this reaction fit well to a single exponential transition. The kinetic plot derived from the global fit of the SVD-reduced three-dimensional data set is shown in Figure 4.4.2B. Analysis of the time course of the reaction at a single wavelength (404 nm) also fit well to a single exponential (Figure 4.4.2C). The reaction of the high-valent state of Y294H MauG with varied concentrations of reduced amicyanin at pH 7.5 at 25° C exhibited saturation behavior (Figure 4.4.2D). The fit of this data to eq 1 yielded a limiting first-order rate constant (k_{ET}) of 33 ± 4 s-1 and a K_d of 300 ± 128 μM. For comparison, the reaction of *bis*-Fe(IV) WT MauG with reduced amicyanin fit exhibited a k_{ET} of 22 s-1 and a K_d of 165 μM [182]. Similar monophasic kinetics was observed for the reaction of *bis*-Fe(IV) WT MauG with reduced amicyanin. It should be noted that the reduction of either high-valent MauG species, *bis*-Fe(IV) or compound I, requires two electrons whereas the oxidation of Cu(I) amicyanin requires one electron. Thus, two molecules of Cu(I) amicyanin must be oxidized to observe the complete reaction. In each reaction, the change in absorbance fit best to a single exponential. The monophasic kinetics means that the reaction of the first Cu(I) amicyanin is followed by dissociation of the complex and reaction with a second Cu(I) amicyanin. If the dissociation/association steps are very rapid relative to k_{ET} and excess Cu(I) amicyanin is present, rebinding of the Cu(II) amicyanin after the single turnover is not a factor and monophasic kinetics is observed

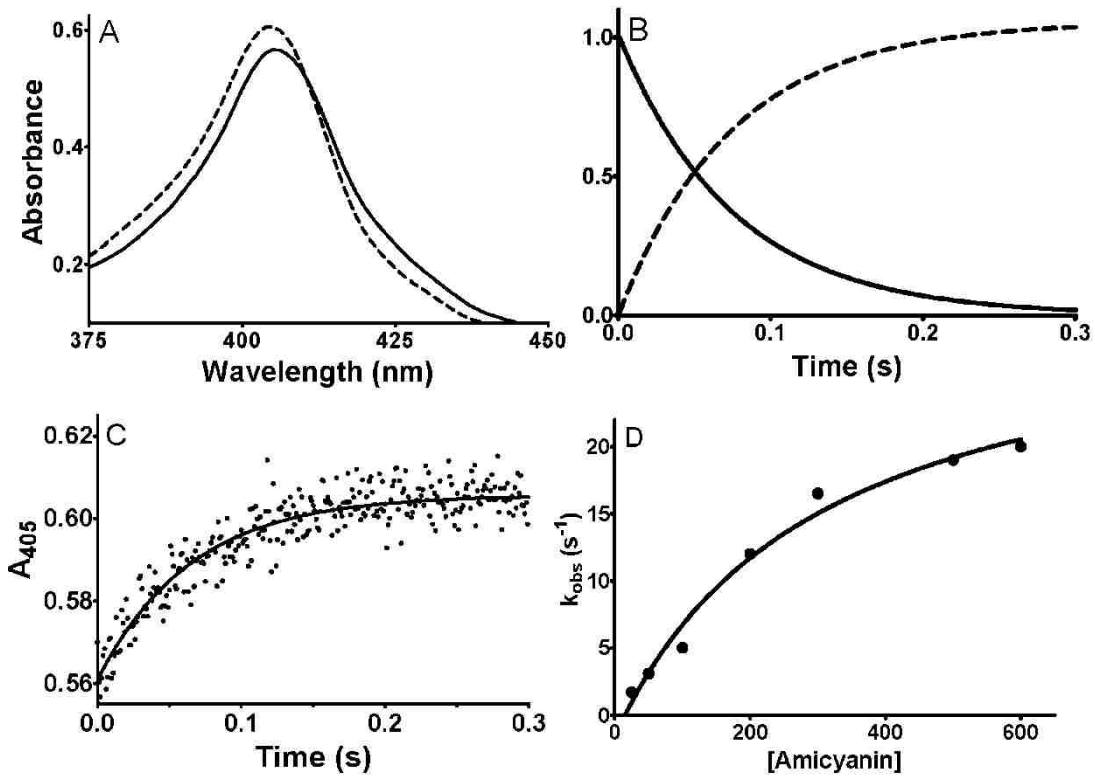

Figure 4.4.2 The reduction of compound I Y294H MauG by reduced amicyanin. A. Spectral changes associated with the ET reaction. The visible spectrum of the Soret region of Y294H MauG is shown immediately after formation of the compound I state (solid line) and after (dashed line) reaction with reduced amicyanin. B. The kinetic plots depict global fits of the most statistically significant eigenvector of the SVD reduced three-dimensional data. The time courses for the disappearance of the initial species (solid line) and appearance of the final species (dashed line) are displayed. C. The time course for the change in absorbance at 404 nm after formation of the compound I state. The solid line is the fit of the data by a single exponential transition. D. The dependence on amicyanin concentration of observed rate of ET from reduced amicyanin to compound I. The line is a fit of the data by eq. 1. Each data point is the average of at least three measurements which vary by less than 10%.

4.4.3.2 *Temperature-dependence of k_{ET} for the reaction of Y294H MauG with reduced amicyanin.*

The k_{ET} for the ET reaction from reduced amicyanin to the compound I Y294H MauG was determined at temperatures from 10º C to 27 ºC (Figure 4.4.3A). The high-valent state of Y294H MauG was unstable at higher temperatures, and so this limited the range that could be studied. The E_m value for the compound I/diferric couple of Y294H MauG is unknown. E_m values have been determined for the compound I/FeIII couple in soybean ascorbate peroxidase [183], Arthromyces ramosus peroxidase [57], yeast cytochrome c peroxidase [184], and horseradish peroxidase type A_2 [185] and type C [185-188]. These E_m values range from 717 to 954 mV, with an average of 887 mV. As such, for the analysis of the temperature-dependence of the ET rates by eqs 4.4.2 the E_m value of 887 mV was used for Y294H MauG. That value and the known E_m value of amicyanin at pH 7.5 of 265 mV[7] were used to determine the ΔGº for the ET reaction from the ΔE_m. The fit of the data to eq 4.4.2 yielded values of $\lambda = 1.95 \pm 0.08$ eV and $H_{AB} = 0.03 \pm 0.01$ cm-1. For comparison, the reaction of *bis*-Fe(IV) WT MauG with reduced amicyanin exhibited values of $\lambda = 2.34 \pm 0.16$ eV and $H_{AB} = 0.6 \pm 0.1$ cm-1 [182]. Thus, the mutation decreased the magnitudes of both λ and H_{AB}. These data were also analyzed by eq 3 (Figure 4.4.3B). This yielded values of E_a of 8.2 ± 0.3 kcal/mol for the reaction with WT MauG and 4.6 ± 0.3 kcal/mol for the reaction with Y294H MauG.

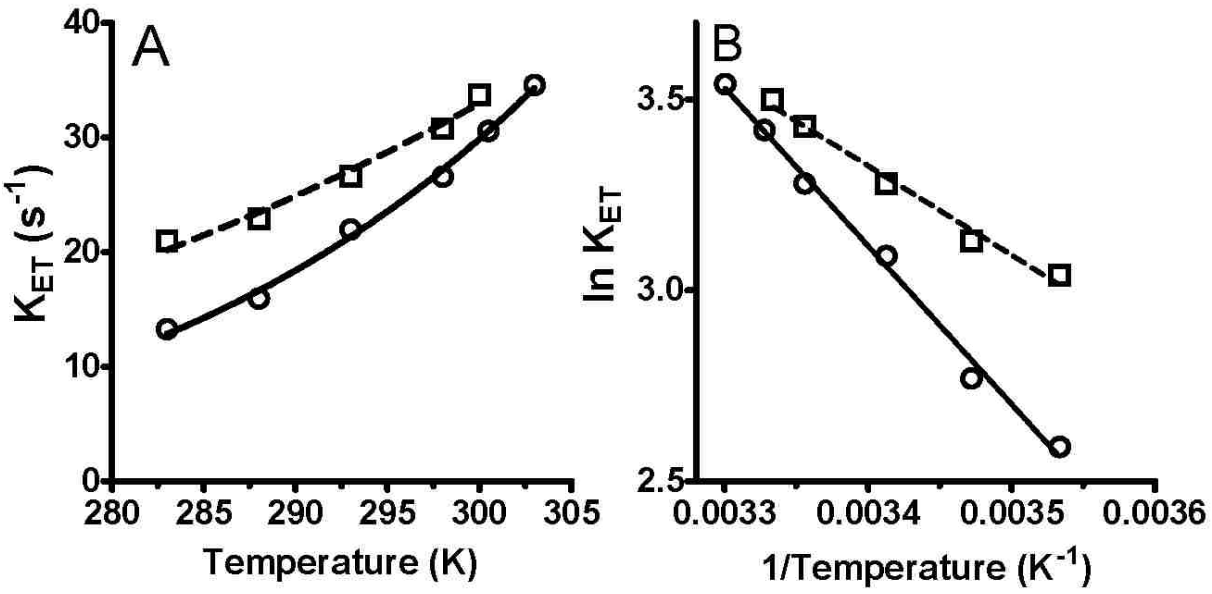

Figure 4.4.3. The temperature dependence of k_{ET} from reduced amicyanin to *bis*-Fe(IV) WT MauG and compound I Y294H MauG. A. The lines are a fit of the data by eq 2. *bis*-Fe(IV) WT MauG is shown in circles, and Compound-I Y294H MauG is shown in squares. B. The lines are a fit of the data by eq 4. The reactions with *bis*-Fe(IV) WT MauG are shown as circles with solid lines and the reactions with compound I Y294H MauG are shown as squares with dashed lines.

4.4.3.3 *Docking model of the complex of Y294H MauG and Amicyanin*

A protein docking model was constructed using the ZDOCK server and utility [163] from the crystal structures of amicyanin and Y294H MauG (Figure 4.4.4). The relative orientations of the redox centers in this complex were similar to those in the docking model of the WT MauG-amicyanin [182].

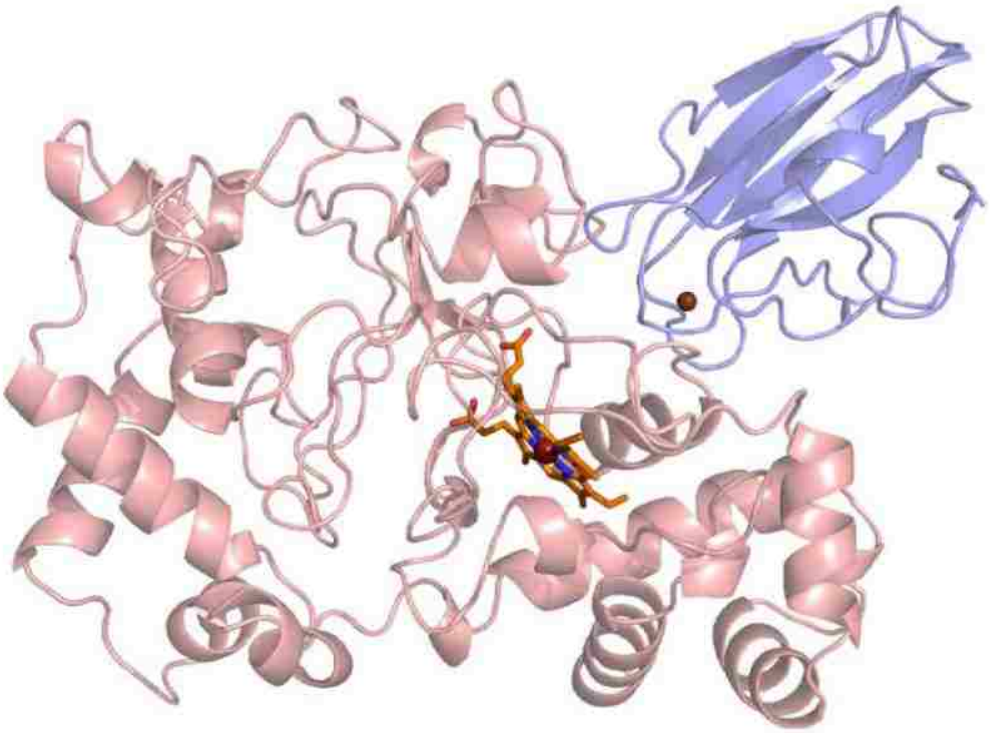

Figure 4.4.4. Docking model of amicyanin-Y294H MauG complex. MauG is colored pink with the heme shown as sticks and amicyanin is colored purple with the copper shown as a sphere.

4.4.4 Discussion

The value of λ reflects the amount of energy needed to optimize the system for ET, or in other words the energy required to bring the reactant and product states to the state in which the ET event occurs. The value of λ is composed of an inner sphere λ_{in}, which derives from optimization bond lengths and bond angles of the inner shell of atoms of the redox center for the ET event, and an outer sphere λ_{out}, which reflects reorientation of solvent molecules that that is associated with the ET event. In small molecules, these two parameters are fairly well distinguishable. However, in protein ET reactions, the line between these two terms can become blurred as electron density is distributed asymmetrically about the redox cofactor or metal-ligating residues. Computational methods have been used to predict λ which reflects reorientation of solvent molecules that that is associated with the medium [73, 189]. λ values have also been determined for ET reactions between native redox cofactors and redox-active active tags such as Ruthenium complexes [75, 168]. ET reactions between the copper of azurin a disulfide radical anion were used to determine λ [76]. The proteins used in the present study are among the few for which λ values have been experimentally determined for the reactions with their natural redox partners; the reactions of amicyanin with MADH [157] and cytochrome *c*-551i [149], and the reactions between MauG and preMADH and MADH [70]. λ values have also been determined for some other ET reactions between quinoprotein dehydrogenases redox protein partners [190]. However, in general there have been relatively few studies in which λ values have been experimentally determined for an ET reaction between two protein-bound redox cofactors.

The structures of WT and Y294H MauG suggest that there should be little difference in the value of λ_{out} during ET into the high-valent hemes since the only solvent accessible portion of the diheme site is the Fe(IV)=O of the five-coordinate heme [66, 191]. The six-coordinate heme is shielded from solvent by the protein. Therefore, the 0.39 eV decrease in the experimentally-determined λ that was caused by the Y294H mutation is most likely a consequence of a decrease in λ_{in}. It was previously suggested that the relatively large λ values

associated the ET reactions of WT *bis*-Fe(IV) MauG with preMADH [70] and amicyanin [182] could be attributed to the fact that λ_{in}

associated with the *bis*-Fe(IV) state could require alterations in lengths and angles of multiple bonds within the two hemes and intervening Trp93. In Y294H MauG, the ET reaction associated with the high-valent compound I redox state would only require such changes in bond lengths and angles of the five-coordinate heme, as there is no change in the redox state of the six-coordinate heme. This would explain the decrease in λ that was caused by the Y294H mutation.

The Y294H mutation also caused a decrease in H_{AB}. Comparison of the docking models of the complexes of amicyanin with WT MauG and Y294MauG does not provide a clear explanation for this. H_{AB} is dependent upon the ET distance and the nature of the intervening medium. ET through amino acid bonds in proteins will exhibit a larger H_{AB} than for ET through empty space [71, 72]. For interprotein ET reactions, a through-space segment of the ET pathway is required to get from one protein to the other. As such, the nature of the protein-protein interface in the ET protein complex can be a critical determinant of the overall H_{AB}. An increase of less than an angstrom in the length of the through-space jump can significantly decrease the overall H_{AB} [93]. Such distances cannot be reliably ascertained from docking models. It should be noted that while the structures of the diheme sites of WT amicyanin and Y294H amicyanin are indistinguishable, there were some other changes in structure of the protein. In order for His294 to replace Tyr294 as a heme axial ligand, residues 291-314 in the C-terminal region of the Y294H MauG are displaced relative to WT MauG [181]. While this region is not at the interface with amicyanin, it does leave open the possibility that the mutation may have also caused subtle changes in structure at the protein surface that affect the interface. The fact that the Y294H mutation increased the Kd for complex formation with amicyanin from 165 μM to 265 μM supports the notion that subtle changes have occurred at the protein-protein interface. These could account for the decrease in H_{AB}.

Analysis of the temperature-dependence of k_{ET} by eq 4 (Figure 4.4.3B) also clearly illustrates the effect of the Y294H mutation on λ and H_{AB} as both the slope and y-intercept of the lines are altered. The change in slope reflects the decrease in Ea for the ET reaction. Since this is an ET reaction, the term in eq 2 which corresponds to Ea in eq 4 is $(\Delta G° + \lambda)2/4\lambda$. Thus, using the experimentally-determined values of λ for the two reactions, it is calculated that the ΔEa caused by the mutation of -3.6 kcal/mol corresponds to -0.156 eV. This describes the overall effect on the reaction of the 0.39 eV decrease in λ that was caused by the mutation. The change in the y-intercept caused by the mutation reflects the change in H_{AB}, which is present in the pre-exponential term in eq 2.

In addition to providing some insights into the factors which contribute to the magnitude of λ for ET reactions involving hemes, as well as other cofactors, these results provide some insight into why nature uses alternative mechanisms by which to stabilize and use utilize high-valent Fe(V) equivalent heme species. These results clearly indicate that compound I is a more efficient electron acceptor in redox reactions than *bis*-Fe(IV) by virtue of the lower λ associated with the ET reaction. Single-heme enzymes which function as oxygenases utilize the compound I species catalyze enzymatic reactions requiring a strong oxidant in which the substrate is in close proximity to the heme. In this case, it makes sense to not delocalize the oxidizing potential but to keep it centered on the heme. The results presented herein further suggest that this also minimizes the energy barrier for the short range ET that is part of the catalytic mechanism in the active site. In contrast, the diheme redox center of MauG catalyzes a reaction at the surface of the protein that is distant from the heme site. The ability to delocalize the oxidizing potential over two hemes which are themselves separated by several angstroms significantly reduces the distance for the long range ET required for catalysis. While this delocalization results in a significant increase in the λ associated with the reaction, that deficiency is more than made up for by the decrease in ET distance by approximately 20 Å. The importance of this

consideration is evidenced by that fact that Y294H MauG, which forms the compound I state instead of the *bis*-Fe(IV), was unable to oxidize the natural substrate preMADH over the longer distance [181].

4.5 Section II Conclusion

By using a non-physiologic complex with amicyanin and MauG, it has been possible to work around certain problems, such as the potential unreliability of studying the temperature dependence of k_{ET}, to study different aspects of ET that are not able to be studied, when amicyanin and MauG are used in complex with their respective natural redox partners. Using this novel complex, it has been possible to use the free energy and temperature dependence of k_{ET} between the Cu(I) of WT and P94A amicyanin and the two different redox centers in WT and Y294H MauG, *bis*-Fe(IV) diheme and compound I heme, respectively, to study the ET parameters of their respective reactions.

In general, specific tuning of the redox potential is not possible to do in proteins due to the limited technologies available to specifically modify the redox potential of cofactors and coenzymes. For example, one of the most widely used ways to do this is by site-directed mutagenesis of specific residues near the redox site in an attempt to modify the redox potential. However, typically it is not possible to use mutagenesis to change redox potential without affecting the conformation of the protein or other parameters of the ET reaction, such as the electronic coupling. In the amicyanin-MauG complex, the redox potential was able to be adjusted precisely and accurately by taking advantage of the pH-dependence of the redox potential of the copper site. With amicyanin's natural redox partner, MADH, this is not possible due to the pH-independence of the redox potential of amicyanin when in complex with MADH. Thus, the amicyanin-MauG complex provides a unique opportunity to study this aspect of interprotein ET.

Using the free energy dependence of the reaction, the ET parameters determined by using the temperature dependence of the reaction were confirmed. This is important because temperature

differences have been shown to affect the free energy of the reaction by affecting the redox potentials of the electron donor and/or acceptor site(s) and also the reorganization energy. Temperature also has the ability to affect any preceding adiabatic reaction steps enough so that the ET step is no longer the rate limiting step. In this case, k_{ET} may either be gated by or kinetically coupled to a preceding adiabatic reaction step. Thus, while the temperature dependence is the easier, and, in many cases, the only way to experimentally determine the ET parameters, it may not be the most accurate method to determine the ET parameters of a reaction and the properties of its respective electron donating and accepting sites. Confirmation of the ET parameters derived from temperature dependence experiments sets an important precedent to be able to confidently use temperature-dependence to further study ET using this specific complex.

Since the free energy dependence of the ET reaction confirmed the parameters determined from the temperature dependence of the reaction, the properties of the P94A amicyanin and Y294H MauG were able to be studied using the temperature dependence of their respective ET reactions. Amicyanin has the shortest and most conformationally constrained ligand loop of all the cupredoxins. The P94A mutation was made in an effort to further test the idea of "rack-induced" bonding at the copper site and determine the effects of relaxation of the ligand loop on the ET and redox properties of the copper redox site. The idea of "rack-induced" bonding suggests that the large number of intraprotein stabilizing forces can create a preformed metal binding site with little flexibility[192]. However, this mutation was not able to be studied with its natural electron acceptor, cytochrome *c*-551i, because the reaction was found to follow a kinetically coupled ET mechanism. By using the novel amicyanin-MauG complex, the ET properties of the reduced P94A amicyanin copper site were able to be studied, and it was found that this mutation had no effect on the ET properties of the copper site other than increasing the intrinsic redox potential and shifting the pKa of the pH-dependence of the redox potential. In addition, the experimentally determined reorganization energy suggests that the loose interprotein interface provided by the MauG, as opposed to MADH, does not influence the equilibrium

between the two alternate conformations of the copper ion in reduced P94A amicyanin. Thus the "rack-induced" bonding concept should be expanded to include the interprotein stabilizing and hindering forces provided by other proteins in the complex.

Y294H MauG is another example of a mutant redox protein that was not able to be studied with its natural redox partner, but it was able to be studied with the amicyanin-MauG complex. The Y294H mutation in MauG caused an inactivation of the six-coordinate heme and converted the five-coordinate heme into a compound I type heme. Compound I hemes are involved in a wide range of reaction mechanisms and are implicated in the pathogenesis of several disease states. This highly reactive heme species is very transient, and it has been very hard to study. One example to illustrate this is that until recently the nature of the ferryl heme and its protonation state was unknown[193]. One method used to determine the nature of such transient redox states is to use crystallographic approaches such as cryocrystallography and multicrystal crystallography[193, 194]. However, as with all crystallographic approaches, it is a concern that the crystallized complex and its respective conformation may not reflect the actual nature of the complex in solution. By using MauG and the amicyanin-MauG complex, these problems can be circumvented. The high valent redox state of MauG and Y294H MauG is unusually stable and lasts for several minutes, as opposed to a second-scale timeframe for other heme-dependent peroxidases. This unusual stability allows it to be studied in solution with a redox partner, such as amicyanin, to determine the ET properties of its high valent redox state cofactor. In addition, the relevant ET parameters, such as reorganization energy, studied in a non-physiologic enzyme complex in solution are not affected by complex orientation.

Through ET studies of Y294H MauG with amicyanin, it has been possible to incrementally increase our knowledge and understanding of redox sites used for long-range ET versus short range ET for catalysis. The redox site in Y294H MauG mutant represents a compound I heme, which is a typical reactive intermediate in many catalytic heme dependent enzymes. Comparison of this redox site with that of the *bis*-

Fe(IV) redox site in MauG show that compared to the compound Iheme, the diheme center is optimal for long range ET despite its larger reorganization energy. This is due to its novel charge delocalization mechanisms, which effectively decreases the ET distance. The compound I site however is better for catalysis, and this is shown its higher potential per unit of reorganization energy as compared to the diheme site in WT MauG. This is the first time the reorganization energy and the nature of a redox site in a heme dependent enzyme has been changed by site-directed mutagenesis.

This incremental increase in understanding of cofactor design, reaction mechanisms, and their relation to reorganization energy has implications for future protein engineering and application. For example, future studies may use this knowledge for "designer" proteins by changing the coordinating ligands of cofactors in existing proteins to modify its reaction mechanism and enzymatic properties. An alternative would be to use this as a method to lower reorganization energy to optimize ET with the cofactor of a redox partner that has a high intrinsic reorganization energy, long ET distance, or low electronic coupling.

5 GENERAL DISCUSSION

Cupredoxins were one of the first families of metalloproteins used to study interprotein electron transfer in depth. Azurin and amicyanin have been studied extensively, and this has led to a better understanding of various types of copper centers, tuning the potential of the copper site, and understanding how electron transfer occurs through various protein secondary structures. However, these are the first studied to our knowledge that utilize amicyanin to further probe stabilizing mechanisms of beta barrel proteins and to examine the nature of a *bis*-Fe(IV) and compound I redox center.

Site-directed mutagenesis was used to convert the sole tryptophan of amicyanin to phenylalanine, lysine, leucine, and tyrosine in order to study the contribution of the tryptophan on the structure, function, and stability of the protein. Of these mutants, only the tyrosine mutant was tolerated. The tyrosine mutation resulted in no significant change in the function or structure of the protein. However, the thermal stability of the copper site was significantly decreased. Further analysis by CD revealed that the overall protein structure was significantly destabilized in the oxidized, reduced, and apo forms of the protein. This indicates that this residue is involved in a bonding network that stabilizes the protein. Analysis of the crystal structure revealed the loss of an interior, cross-barrel hydrogen bond in the mutant protein between the indole nitrogen of Trp45 and the hydroxyl group of Tyr90. Trp45 is part of a sequence of paired hydrophobic residues. This pattern of paired residues is a conserved feature in the core of cupredoxins. This interaction and stabilizing mechanism may be a general feature of beta barrel proteins.

Attempts to incorporate a homologous bond into a structurally similar protein, V_L, were not successful. This bond engineering was attempted by using site-directed mutagenesis to incorporate a residue that has a side chain capable of hydrogen bonding into the core of the protein at specified locations. Specifically, tryptophan, tyrosine, serine, and threonine mutations were attempted as a means of directly adding an interior hydrogen bond. However, none of these mutations were tolerated. As a result of these

failed mutations, it can be surmised that although the V_L is very structurally similar to amicyanin, its core is such that it cannot tolerate large or polar residues. This may be a result of the bulkiness of a tryptophan caused a perturbation in the structure of the protein which led to destabilization or that polar residues were not able to be stabilized within the hydrophobic core.

Since the reactivity and redox characteristics of amicyanin have been so extensively studied, it was possible to use amicyanin to study the diheme cofactor of MauG, particularly in its high valent oxidation state. The *bis*-Fe(IV) diheme cofactor of MauG is not well understood for a variety of reasons. Like other high valent heme cofactors, the *bis*-Fe(IV) cofactor in MauG is highly reactive and spontaneously decays. In addition, the electron density and electron holes alike are shared across a large area composed of two hemes and an intermediate tryptophan residue, and are present in an ever changing ensemble of high valent states. As a result, the true redox site of the cofactor becomes delocalized across the entire cofactor, and the electron density becomes even more blurred at the "boundary" of the cofactor. This further complicates the reorganization energy term because as the electronic boundary of the cofactor blurs, more of the protein and/or solvent matrix is accounted for in the reorganization energy.

One particular advantage of reacting reduced amicyanin with the *bis*-Fe(IV) cofactor of MauG is that in this complex, the redox potential of amicyanin is pH-dependent. Thus, the free energy dependence of the rate of electron transfer between the two proteins was able to be observed. As mentioned earlier, this is not easily nor commonly done in proteins. Thus this shows that this approach could possibly be used with other systems in which the electron donor or acceptor site has a pH-dependent redox potential in order to gain information regarding the associated ET event and its parameters. The results obtained from this particular complex are interesting in that the obtained reorganization energy was equal to that of the amicyanin-MADH complex. While the respective cofactors of MADH and MauG may seem different, they have many similarities. MauG has two hemes which are electronically linked to each other, and the TTQ of MADH

consists of two covalently bound tryptophans which share charge. The large number of bond angles and lengths are likely reflected in the relatively large value for reorganization energy that was obtained. The optimization of these bonds was kinetically indistinguishable from the ET event in both the temperature and free energy dependence studies.

Further support for this is garnered from the analysis of the rate of electron transfer in the amicyanin-Y294H MauG complex. In the high valent state of Y294H MauG, the six-coordinate heme is not redox active due to its inability to stabilize the high valent state. Thus both of the oxidizing equivalents that would normally be delocalized amongst both hemes in WT MauG are now located on the five-coordinate heme. This heme is now equal to a traditional "compound I" heme. In a compound I heme, the iron is in the Fe(IV) state and there is a cation radical on the porphyrin ring. Analysis of k_{ET} showed that the associated reorganization energy was nearly twenty percent lower as compared to the reaction with WT MauG. As a result, the compound I heme is a more efficient electron acceptor due to its lower intrinsic reorganization energy. Thus, it makes sense that catalytic reactions should proceed quicker in a heme-dependent enzyme with a single heme versus a diheme system like that of WT MauG. The diheme system of WT MauG, even though it has a larger relative reorganization energy, is more efficient electron at transferring electrons over long distances due to the delocalization of the diheme redox center. This delocalization decreases the distance the electron must travel, and this decrease in distance more than compensates for the increases reorganization energy relative to that of a single heme cofactor.

Due to their relative simplicity in structure and function, cupredoxins have long been studied to understand biological ET, including the design of copper sites and how electrons travel through different secondary structures. Presented in this dissertation are examples of how the cupredoxin amicyanin can be used to further the study of other proteins and cofactors. Amicyanin is used as a structural model and also as an enzymatic tool to probe reaction chemistries of other, more complicated metallocofactors.

APPENDIX
COPYRIGHT PERMISSIONS

ELSEVIER LICENSE
TERMS AND CONDITIONS

Nov 30, 2015

This is an Agreement between Brian Dow ("You") and Elsevier ("Elsevier"). It consists of your order details, the terms and conditions provided by Elsevier, and the payment terms and conditions.

All payments must be made in full to CCC. For payment instructions, please see information listed at the bottom of this form.

Supplier	Elsevier Limited The Boulevard,Langford Lane Kidlington,Oxford,OX5 1GB,UK
Registered Company Number	1982084
Customer name	Brian Dow
Customer address	8234 Sulston St ORLANDO, FL 32827
License number	3758490658519
License date	Nov 29, 2015
Licensed content publisher	Elsevier
Licensed content publication	Archives of Biochemistry and Biophysics
Licensed content title	The sole tryptophan of amicyanin enhances its thermal stability but does not influence the electronic properties of the type 1 copper site
Licensed content author	Brian A. Dow,Narayanasami Sukumar,Jason O. Matos,Moonsung Choi,Alfons Schulte,Suren A. Tatulian,Victor L. Davidson
Licensed content date	15 May 2014
Licensed content volume number	550
Licensed content issue number	n/a
Number of pages	8
Start Page	20
End Page	27
Type of Use	reuse in a thesis/dissertation
Portion	full article
Format	both print and electronic
Are you the author of this Elsevier article?	Yes
Will you be translating?	No
Title of your thesis/dissertation	THE MAUC GENE ENCODES A VERSATILE SIGNAL SEQUENCE AND REDOX PROTEIN THAT CAN BE UTILIZED IN NATIVE AND NON-NATIVE PROTEIN EXPRESSION AND ELECTRON TRANSFER SYSTEMS
Expected completion date	Jan 2016
Estimated size (number of pages)	150
Elsevier VAT number	GB 494 6272 12

Price	0.00 USD
VAT/Local Sales Tax	0.00 USD / 0.00 GBP
Total	**0.00 USD**

Terms and Conditions

INTRODUCTION

1. The publisher for this copyrighted material is Elsevier. By clicking "accept" in connection with completing this licensing transaction, you agree that the following terms and conditions apply to this transaction (along with the Billing and Payment terms and conditions established by Copyright Clearance Center, Inc. ("CCC"), at the time that you opened your Rightslink account and that are available at any time at http://myaccount.copyright.com).

GENERAL TERMS

2. Elsevier hereby grants you permission to reproduce the aforementioned material subject to the terms and conditions indicated.

3. Acknowledgement: If any part of the material to be used (for example, figures) has appeared in our publication with credit or acknowledgement to another source, permission must also be sought from that source. If such permission is not obtained then that material may not be included in your publication/copies. Suitable acknowledgement to the source must be made, either as a footnote or in a reference list at the end of your publication, as follows:
"Reprinted from Publication title, Vol /edition number, Author(s), Title of article / title of chapter, Pages No., Copyright (Year), with permission from Elsevier [OR APPLICABLE SOCIETY COPYRIGHT OWNER]." Also Lancet special credit - "Reprinted from The Lancet, Vol. number, Author(s), Title of article, Pages No., Copyright (Year), with permission from Elsevier."

4. Reproduction of this material is confined to the purpose and/or media for which permission is hereby given.

5. Altering/Modifying Material: Not Permitted. However figures and illustrations may be altered/adapted minimally to serve your work. Any other abbreviations, additions, deletions and/or any other alterations shall be made only with prior written authorization of Elsevier Ltd. (Please contact Elsevier at permissions@elsevier.com)

6. If the permission fee for the requested use of our material is waived in this instance, please be advised that your future requests for Elsevier materials may attract a fee.

7. Reservation of Rights: Publisher reserves all rights not specifically granted in the combination of (i) the license details provided by you and accepted in the course of this licensing transaction, (ii) these terms and conditions and (iii) CCC's Billing and Payment terms and conditions.

8. License Contingent Upon Payment: While you may exercise the rights licensed immediately upon issuance of the license at the end of the licensing process for the transaction, provided that you have disclosed complete and accurate details of your proposed use, no license is finally effective unless and until full payment is received from you (either by publisher or by CCC) as provided in CCC's Billing and Payment terms and conditions. If full payment is not received on a timely basis, then any license preliminarily granted shall be deemed automatically revoked and shall be void as if never granted. Further, in the event that you breach any of these terms and conditions or any of CCC's Billing and Payment terms and conditions, the license is automatically revoked and shall be void as if never granted. Use of materials as described in a revoked license, as well as any use of the materials beyond the scope of an unrevoked license, may constitute copyright infringement and publisher reserves the right to take any and all action to protect its copyright in the materials.

9. Warranties: Publisher makes no representations or warranties with respect to the licensed material.

10. Indemnity: You hereby indemnify and agree to hold harmless publisher and CCC, and their respective officers, directors, employees and agents, from and against any and all claims arising out of your use of the licensed material other than as specifically authorized pursuant to this license.

11. No Transfer of License: This license is personal to you and may not be sublicensed, assigned, or transferred by you to any other person without publisher's written permission.

12. No Amendment Except in Writing: This license may not be amended except in a writing signed by both parties (or, in the case of publisher, by CCC on publisher's behalf).

13. Objection to Contrary Terms: Publisher hereby objects to any terms contained in any purchase order, acknowledgment, check endorsement or other writing prepared by you, which terms are inconsistent with these terms and conditions or CCC's Billing and Payment terms and conditions. These terms and conditions, together with CCC's Billing and Payment terms and conditions (which are incorporated herein), comprise the entire agreement between you and publisher (and CCC) concerning this licensing transaction. In the event of any conflict between your obligations established by these terms and conditions and those established by CCC's Billing and Payment terms and conditions, these terms and conditions shall control.

14. Revocation: Elsevier or Copyright Clearance Center may deny the permissions described in this License at their sole discretion, for any reason or no reason, with a full refund payable to you. Notice of such denial will be made using the

contact information provided by you. Failure to receive such notice will not alter or invalidate the denial. In no event will Elsevier or Copyright Clearance Center be responsible or liable for any costs, expenses or damage incurred by you as a result of a denial of your permission request, other than a refund of the amount(s) paid by you to Elsevier and/or Copyright Clearance Center for denied permissions.

LIMITED LICENSE

The following terms and conditions apply only to specific license types:

15. **Translation**: This permission is granted for non-exclusive world **English** rights only unless your license was granted for translation rights. If you licensed translation rights you may only translate this content into the languages you requested. A professional translator must perform all translations and reproduce the content word for word preserving the integrity of the article.

16. **Posting licensed content on any Website**: The following terms and conditions apply as follows: Licensing material from an Elsevier journal: All content posted to the web site must maintain the copyright information line on the bottom of each image; A hyper-text must be included to the Homepage of the journal from which you are licensing at http://www.sciencedirect.com/science/journal/xxxxx or the Elsevier homepage for books at http://www.elsevier.com; Central Storage: This license does not include permission for a scanned version of the material to be stored in a central repository such as that provided by Heron/XanEdu.

Licensing material from an Elsevier book: A hyper-text link must be included to the Elsevier homepage at http://www.elsevier.com . All content posted to the web site must maintain the copyright information line on the bottom of each image.

Posting licensed content on Electronic reserve: In addition to the above the following clauses are applicable: The web site must be password-protected and made available only to bona fide students registered on a relevant course. This permission is granted for 1 year only. You may obtain a new license for future website posting.

17. **For journal authors:** the following clauses are applicable in addition to the above:

Preprints:

A preprint is an author's own write-up of research results and analysis, it has not been peer-reviewed, nor has it had any other value added to it by a publisher (such as formatting, copyright, technical enhancement etc.).

Authors can share their preprints anywhere at any time. Preprints should not be added to or enhanced in any way in order to appear more like, or to substitute for, the final versions of articles however authors can update their preprints on arXiv or RePEc with their Accepted Author Manuscript (see below).

If accepted for publication, we encourage authors to link from the preprint to their formal publication via its DOI. Millions of researchers have access to the formal publications on ScienceDirect, and so links will help users to find, access, cite and use the best available version. Please note that Cell Press, The Lancet and some society-owned have different preprint policies. Information on these policies is available on the journal homepage.

Accepted Author Manuscripts: An accepted author manuscript is the manuscript of an article that has been accepted for publication and which typically includes author-incorporated changes suggested during submission, peer review and editor-author communications.

Authors can share their accepted author manuscript:

- immediately
  - via their non-commercial person homepage or blog
  - by updating a preprint in arXiv or RePEc with the accepted manuscript
  - via their research institute or institutional repository for internal institutional uses or as part of an invitation-only research collaboration work-group
  - directly by providing copies to their students or to research collaborators for their personal use
  - for private scholarly sharing as part of an invitation-only work group on commercial sites with which Elsevier has an agreement
- after the embargo period
  - via non-commercial hosting platforms such as their institutional repository
  - via commercial sites with which Elsevier has an agreement

In all cases accepted manuscripts should:

- link to the formal publication via its DOI
- bear a CC-BY-NC-ND license - this is easy to do
- if aggregated with other manuscripts, for example in a repository or other site, be shared in alignment with our hosting policy not be added to or enhanced in any way to appear more like, or to substitute for, the published journal article.

Published journal article (JPA): A published journal article (PJA) is the definitive final record of published research that appears or will appear in the journal and embodies all value-adding publishing activities including peer review co-ordination, copy-editing, formatting, (if relevant) pagination and online enrichment.
Policies for sharing publishing journal articles differ for subscription and gold open access articles:
Subscription Articles: If you are an author, please share a link to your article rather than the full-text. Millions of researchers have access to the formal publications on ScienceDirect, and so links will help your users to find, access, cite, and use the best available version.
Theses and dissertations which contain embedded PJAs as part of the formal submission can be posted publicly by the awarding institution with DOI links back to the formal publications on ScienceDirect.
If you are affiliated with a library that subscribes to ScienceDirect you have additional private sharing rights for others' research accessed under that agreement. This includes use for classroom teaching and internal training at the institution (including use in course packs and courseware programs), and inclusion of the article for grant funding purposes.
Gold Open Access Articles: May be shared according to the author-selected end-user license and should contain a CrossMark logo, the end user license, and a DOI link to the formal publication on ScienceDirect.
Please refer to Elsevier's posting policy for further information.
18. **For book authors** the following clauses are applicable in addition to the above: Authors are permitted to place a brief summary of their work online only. You are not allowed to download and post the published electronic version of your chapter, nor may you scan the printed edition to create an electronic version. **Posting to a repository:** Authors are permitted to post a summary of their chapter only in their institution's repository.
19. **Thesis/Dissertation**: If your license is for use in a thesis/dissertation your thesis may be submitted to your institution in either print or electronic form. Should your thesis be published commercially, please reapply for permission. These requirements include permission for the Library and Archives of Canada to supply single copies, on demand, of the complete thesis and include permission for Proquest/UMI to supply single copies, on demand, of the complete thesis. Should your thesis be published commercially, please reapply for permission. Theses and dissertations which contain embedded PJAs as part of the formal submission can be posted publicly by the awarding institution with DOI links back to the formal publications on ScienceDirect.

Elsevier Open Access Terms and Conditions
You can publish open access with Elsevier in hundreds of open access journals or in nearly 2000 established subscription journals that support open access publishing. Permitted third party re-use of these open access articles is defined by the author's choice of Creative Commons user license. See our open access license policy for more information.
Terms & Conditions applicable to all Open Access articles published with Elsevier:
Any reuse of the article must not represent the author as endorsing the adaptation of the article nor should the article be modified in such a way as to damage the author's honour or reputation. If any changes have been made, such changes must be clearly indicated.
The author(s) must be appropriately credited and we ask that you include the end user license and a DOI link to the formal publication on ScienceDirect.
If any part of the material to be used (for example, figures) has appeared in our publication with credit or acknowledgement to another source it is the responsibility of the user to ensure their reuse complies with the terms and conditions determined by the rights holder.
Additional Terms & Conditions applicable to each Creative Commons user license:
CC BY: The CC-BY license allows users to copy, to create extracts, abstracts and new works from the Article, to alter and revise the Article and to make commercial use of the Article (including reuse and/or resale of the Article by commercial entities), provided the user gives appropriate credit (with a link to the formal publication through the relevant DOI), provides a link to the license, indicates if changes were made and the licensor is not represented as endorsing the use made of the work. The full details of the license are available at http://creativecommons.org/licenses/by/4.0.
CC BY NC SA: The CC BY-NC-SA license allows users to copy, to create extracts, abstracts and new works from the Article, to alter and revise the Article, provided this is not done for commercial purposes, and that the user gives appropriate credit (with a link to the formal publication through the relevant DOI), provides a link to the license, indicates if changes were made and the licensor is not represented as endorsing the use made of the work. Further, any new works must be made available on the same conditions. The full details of the license are available at http://creativecommons.org/licenses/by-nc-sa/4.0.
CC BY NC ND: The CC BY-NC-ND license allows users to copy and distribute the Article, provided this is not done for commercial purposes and further does not permit distribution of the Article if it is changed or edited in any way, and provided the user gives appropriate credit (with a link to the formal publication through the relevant DOI), provides a link to the license, and that the licensor is not represented as endorsing the use made of the work. The full details of the license

ELSEVIER LICENSE
TERMS AND CONDITIONS

Nov 29, 2015

This is an Agreement between Brian Dow ("You") and Elsevier ("Elsevier"). It consists of your order details, the terms and conditions provided by Elsevier, and the payment terms and conditions.

All payments must be made in full to CCC. For payment instructions, please see information listed at the bottom of this form.

Supplier	Elsevier Limited The Boulevard,Langford Lane Kidlington,Oxford,OX5 1GB,UK
Registered Company Number	1982084
Customer name	Brian Dow
Customer address	8234 Sulston St ORLANDO, FL 32827
License number	3758490918852
License date	Nov 29, 2015
Licensed content publisher	Elsevier
Licensed content publication	Protein Expression and Purification
Licensed content title	Use of the amicyanin signal sequence for efficient periplasmic expression in E. coli of a human antibody light chain variable domain
Licensed content author	Brian A. Dow,Suren A. Tatulian,Victor L. Davidson
Licensed content date	April 2015
Licensed content volume number	108
Licensed content issue number	n/a
Number of pages	4
Start Page	9
End Page	12
Type of Use	reuse in a thesis/dissertation
Intended publisher of new work	other
Portion	full article
Format	both print and electronic
Are you the author of this Elsevier article?	Yes
Will you be translating?	No
Title of your thesis/dissertation	THE MAUC GENE ENCODES A VERSATILE SIGNAL SEQUENCE AND REDOX PROTEIN THAT CAN BE UTILIZED IN NATIVE AND NON-NATIVE PROTEIN EXPRESSION AND ELECTRON TRANSFER SYSTEMS
Expected completion date	Jan 2016
Estimated size (number of pages)	150

Elsevier VAT number	GB 494 6272 12
Price	0.00 USD
VAT/Local Sales Tax	0.00 USD / 0.00 GBP
Total	**0.00 USD**

Terms and Conditions

INTRODUCTION

1. The publisher for this copyrighted material is Elsevier. By clicking "accept" in connection with completing this licensing transaction, you agree that the following terms and conditions apply to this transaction (along with the Billing and Payment terms and conditions established by Copyright Clearance Center, Inc. ("CCC"), at the time that you opened your Rightslink account and that are available at any time at http://myaccount.copyright.com).

GENERAL TERMS

2. Elsevier hereby grants you permission to reproduce the aforementioned material subject to the terms and conditions indicated.

3. Acknowledgement: If any part of the material to be used (for example, figures) has appeared in our publication with credit or acknowledgement to another source, permission must also be sought from that source. If such permission is not obtained then that material may not be included in your publication/copies. Suitable acknowledgement to the source must be made, either as a footnote or in a reference list at the end of your publication, as follows:
"Reprinted from Publication title, Vol /edition number, Author(s), Title of article / title of chapter, Pages No., Copyright (Year), with permission from Elsevier [OR APPLICABLE SOCIETY COPYRIGHT OWNER]." Also Lancet special credit - "Reprinted from The Lancet, Vol. number, Author(s), Title of article, Pages No., Copyright (Year), with permission from Elsevier."

4. Reproduction of this material is confined to the purpose and/or media for which permission is hereby given.

5. Altering/Modifying Material: Not Permitted. However figures and illustrations may be altered/adapted minimally to serve your work. Any other abbreviations, additions, deletions and/or any other alterations shall be made only with prior written authorization of Elsevier Ltd. (Please contact Elsevier at permissions@elsevier.com)

6. If the permission fee for the requested use of our material is waived in this instance, please be advised that your future requests for Elsevier materials may attract a fee.

7. Reservation of Rights: Publisher reserves all rights not specifically granted in the combination of (i) the license details provided by you and accepted in the course of this licensing transaction, (ii) these terms and conditions and (iii) CCC's Billing and Payment terms and conditions.

8. License Contingent Upon Payment: While you may exercise the rights licensed immediately upon issuance of the license at the end of the licensing process for the transaction, provided that you have disclosed complete and accurate details of your proposed use, no license is finally effective unless and until full payment is received from you (either by publisher or by CCC) as provided in CCC's Billing and Payment terms and conditions. If full payment is not received on a timely basis, then any license preliminarily granted shall be deemed automatically revoked and shall be void as if never granted. Further, in the event that you breach any of these terms and conditions or any of CCC's Billing and Payment terms and conditions, the license is automatically revoked and shall be void as if never granted. Use of materials as described in a revoked license, as well as any use of the materials beyond the scope of an unrevoked license, may constitute copyright infringement and publisher reserves the right to take any and all action to protect its copyright in the materials.

9. Warranties: Publisher makes no representations or warranties with respect to the licensed material.

10. Indemnity: You hereby indemnify and agree to hold harmless publisher and CCC, and their respective officers, directors, employees and agents, from and against any and all claims arising out of your use of the licensed material other than as specifically authorized pursuant to this license.

11. No Transfer of License: This license is personal to you and may not be sublicensed, assigned, or transferred by you to any other person without publisher's written permission.

12. No Amendment Except in Writing: This license may not be amended except in a writing signed by both parties (or, in the case of publisher, by CCC on publisher's behalf).

13. Objection to Contrary Terms: Publisher hereby objects to any terms contained in any purchase order, acknowledgment, check endorsement or other writing prepared by you, which terms are inconsistent with these terms and conditions or CCC's Billing and Payment terms and conditions. These terms and conditions, together with CCC's Billing and Payment terms and conditions (which are incorporated herein), comprise the entire agreement between you and publisher (and CCC) concerning this licensing transaction. In the event of any conflict between your obligations established by these terms and conditions and those established by CCC's Billing and Payment terms and conditions, these terms and conditions shall control.

14. Revocation: Elsevier or Copyright Clearance Center may deny the permissions described in this License at their sole

discretion, for any reason or no reason, with a full refund payable to you. Notice of such denial will be made using the contact information provided by you. Failure to receive such notice will not alter or invalidate the denial. In no event will Elsevier or Copyright Clearance Center be responsible or liable for any costs, expenses or damage incurred by you as a result of a denial of your permission request, other than a refund of the amount(s) paid by you to Elsevier and/or Copyright Clearance Center for denied permissions.

LIMITED LICENSE

The following terms and conditions apply only to specific license types:

15. **Translation**: This permission is granted for non-exclusive world **English** rights only unless your license was granted for translation rights. If you licensed translation rights you may only translate this content into the languages you requested. A professional translator must perform all translations and reproduce the content word for word preserving the integrity of the article.

16. **Posting licensed content on any Website**: The following terms and conditions apply as follows: Licensing material from an Elsevier journal: All content posted to the web site must maintain the copyright information line on the bottom of each image; A hyper-text must be included to the Homepage of the journal from which you are licensing at http://www.sciencedirect.com/science/journal/xxxxx or the Elsevier homepage for books at http://www.elsevier.com; Central Storage: This license does not include permission for a scanned version of the material to be stored in a central repository such as that provided by Heron/XanEdu.

Licensing material from an Elsevier book: A hyper-text link must be included to the Elsevier homepage at http://www.elsevier.com . All content posted to the web site must maintain the copyright information line on the bottom of each image.

Posting licensed content on Electronic reserve: In addition to the above the following clauses are applicable: The web site must be password-protected and made available only to bona fide students registered on a relevant course. This permission is granted for 1 year only. You may obtain a new license for future website posting.

17. **For journal authors:** the following clauses are applicable in addition to the above:

Preprints:

A preprint is an author's own write-up of research results and analysis, it has not been peer-reviewed, nor has it had any other value added to it by a publisher (such as formatting, copyright, technical enhancement etc.).

Authors can share their preprints anywhere at any time. Preprints should not be added to or enhanced in any way in order to appear more like, or to substitute for, the final versions of articles however authors can update their preprints on arXiv or RePEc with their Accepted Author Manuscript (see below).

If accepted for publication, we encourage authors to link from the preprint to their formal publication via its DOI. Millions of researchers have access to the formal publications on ScienceDirect, and so links will help users to find, access, cite and use the best available version. Please note that Cell Press, The Lancet and some society-owned have different preprint policies. Information on these policies is available on the journal homepage.

Accepted Author Manuscripts: An accepted author manuscript is the manuscript of an article that has been accepted for publication and which typically includes author-incorporated changes suggested during submission, peer review and editor-author communications.

Authors can share their accepted author manuscript:

- immediately
  - via their non-commercial person homepage or blog
  - by updating a preprint in arXiv or RePEc with the accepted manuscript
  - via their research institute or institutional repository for internal institutional uses or as part of an invitation-only research collaboration work-group
  - directly by providing copies to their students or to research collaborators for their personal use
  - for private scholarly sharing as part of an invitation-only work group on commercial sites with which Elsevier has an agreement
- after the embargo period
  - via non-commercial hosting platforms such as their institutional repository
  - via commercial sites with which Elsevier has an agreement

In all cases accepted manuscripts should:

- link to the formal publication via its DOI
- bear a CC-BY-NC-ND license - this is easy to do
- if aggregated with other manuscripts, for example in a repository or other site, be shared in alignment with our hosting policy not be added to or enhanced in any way to appear more like, or to substitute for, the published

journal article.

Published journal article (JPA): A published journal article (PJA) is the definitive final record of published research that appears or will appear in the journal and embodies all value-adding publishing activities including peer review co-ordination, copy-editing, formatting, (if relevant) pagination and online enrichment.
Policies for sharing publishing journal articles differ for subscription and gold open access articles:
Subscription Articles: If you are an author, please share a link to your article rather than the full-text. Millions of researchers have access to the formal publications on ScienceDirect, and so links will help your users to find, access, cite, and use the best available version.
Theses and dissertations which contain embedded PJAs as part of the formal submission can be posted publicly by the awarding institution with DOI links back to the formal publications on ScienceDirect.
If you are affiliated with a library that subscribes to ScienceDirect you have additional private sharing rights for others' research accessed under that agreement. This includes use for classroom teaching and internal training at the institution (including use in course packs and courseware programs), and inclusion of the article for grant funding purposes.
Gold Open Access Articles: May be shared according to the author-selected end-user license and should contain a CrossMark logo, the end user license, and a DOI link to the formal publication on ScienceDirect.
Please refer to Elsevier's posting policy for further information.
18. **For book authors** the following clauses are applicable in addition to the above: Authors are permitted to place a brief summary of their work online only. You are not allowed to download and post the published electronic version of your chapter, nor may you scan the printed edition to create an electronic version. **Posting to a repository:** Authors are permitted to post a summary of their chapter only in their institution's repository.
19. **Thesis/Dissertation**: If your license is for use in a thesis/dissertation your thesis may be submitted to your institution in either print or electronic form. Should your thesis be published commercially, please reapply for permission. These requirements include permission for the Library and Archives of Canada to supply single copies, on demand, of the complete thesis and include permission for Proquest/UMI to supply single copies, on demand, of the complete thesis. Should your thesis be published commercially, please reapply for permission. Theses and dissertations which contain embedded PJAs as part of the formal submission can be posted publicly by the awarding institution with DOI links back to the formal publications on ScienceDirect.

Elsevier Open Access Terms and Conditions
You can publish open access with Elsevier in hundreds of open access journals or in nearly 2000 established subscription journals that support open access publishing. Permitted third party re-use of these open access articles is defined by the author's choice of Creative Commons user license. See our open access license policy for more information.
Terms & Conditions applicable to all Open Access articles published with Elsevier:
Any reuse of the article must not represent the author as endorsing the adaptation of the article nor should the article be modified in such a way as to damage the author's honour or reputation. If any changes have been made, such changes must be clearly indicated.
The author(s) must be appropriately credited and we ask that you include the end user license and a DOI link to the formal publication on ScienceDirect.
If any part of the material to be used (for example, figures) has appeared in our publication with credit or acknowledgement to another source it is the responsibility of the user to ensure their reuse complies with the terms and conditions determined by the rights holder.
Additional Terms & Conditions applicable to each Creative Commons user license:
CC BY: The CC-BY license allows users to copy, to create extracts, abstracts and new works from the Article, to alter and revise the Article and to make commercial use of the Article (including reuse and/or resale of the Article by commercial entities), provided the user gives appropriate credit (with a link to the formal publication through the relevant DOI), provides a link to the license, indicates if changes were made and the licensor is not represented as endorsing the use made of the work. The full details of the license are available at http://creativecommons.org/licenses/by/4.0.
CC BY NC SA: The CC BY-NC-SA license allows users to copy, to create extracts, abstracts and new works from the Article, to alter and revise the Article, provided this is not done for commercial purposes, and that the user gives appropriate credit (with a link to the formal publication through the relevant DOI), provides a link to the license, indicates if changes were made and the licensor is not represented as endorsing the use made of the work. Further, any new works must be made available on the same conditions. The full details of the license are available at http://creativecommons.org/licenses/by-nc-sa/4.0.
CC BY NC ND: The CC BY-NC-ND license allows users to copy and distribute the Article, provided this is not done for commercial purposes and further does not permit distribution of the Article if it is changed or edited in any way, and

ELSEVIER LICENSE
TERMS AND CONDITIONS

Nov 29, 2015

This is an Agreement between Brian Dow ("You") and Elsevier ("Elsevier"). It consists of your order details, the terms and conditions provided by Elsevier, and the payment terms and conditions.

All payments must be made in full to CCC. For payment instructions, please see information listed at the bottom of this form.

Supplier	Elsevier Limited The Boulevard,Langford Lane Kidlington,Oxford,OX5 1GB,UK
Registered Company Number	1982084
Customer name	Brian Dow
Customer address	8234 Sulston St ORLANDO, FL 32827
License number	3758491029505
License date	Nov 29, 2015
Licensed content publisher	Elsevier
Licensed content publication	Biochimica et Biophysica Acta (BBA) - Bioenergetics
Licensed content title	Characterization of the free energy dependence of an interprotein electron transfer reaction by variation of pH and site-directed mutagenesis
Licensed content author	Brian A. Dow,Victor L. Davidson
Licensed content date	October 2015
Licensed content volume number	1847
Licensed content issue number	10
Number of pages	6
Start Page	1181
End Page	1186
Type of Use	reuse in a thesis/dissertation
Intended publisher of new work	other
Portion	full article
Format	both print and electronic
Are you the author of this Elsevier article?	Yes
Will you be translating?	No
Title of your thesis/dissertation	THE MAUC GENE ENCODES A VERSATILE SIGNAL SEQUENCE AND REDOX PROTEIN THAT CAN BE UTILIZED IN NATIVE AND NON-NATIVE PROTEIN EXPRESSION AND ELECTRON TRANSFER SYSTEMS
Expected completion date	Jan 2016
Estimated size (number of pages)	150

Elsevier VAT number	GB 494 6272 12
Price	0.00 USD
VAT/Local Sales Tax	0.00 USD / 0.00 GBP
Total	**0.00 USD**

Terms and Conditions

INTRODUCTION

1. The publisher for this copyrighted material is Elsevier. By clicking "accept" in connection with completing this licensing transaction, you agree that the following terms and conditions apply to this transaction (along with the Billing and Payment terms and conditions established by Copyright Clearance Center, Inc. ("CCC"), at the time that you opened your Rightslink account and that are available at any time at http://myaccount.copyright.com).

GENERAL TERMS

2. Elsevier hereby grants you permission to reproduce the aforementioned material subject to the terms and conditions indicated.

3. Acknowledgement: If any part of the material to be used (for example, figures) has appeared in our publication with credit or acknowledgement to another source, permission must also be sought from that source. If such permission is not obtained then that material may not be included in your publication/copies. Suitable acknowledgement to the source must be made, either as a footnote or in a reference list at the end of your publication, as follows:
"Reprinted from Publication title, Vol /edition number, Author(s), Title of article / title of chapter, Pages No., Copyright (Year), with permission from Elsevier [OR APPLICABLE SOCIETY COPYRIGHT OWNER]." Also Lancet special credit - "Reprinted from The Lancet, Vol. number, Author(s), Title of article, Pages No., Copyright (Year), with permission from Elsevier."

4. Reproduction of this material is confined to the purpose and/or media for which permission is hereby given.

5. Altering/Modifying Material: Not Permitted. However figures and illustrations may be altered/adapted minimally to serve your work. Any other abbreviations, additions, deletions and/or any other alterations shall be made only with prior written authorization of Elsevier Ltd. (Please contact Elsevier at permissions@elsevier.com)

6. If the permission fee for the requested use of our material is waived in this instance, please be advised that your future requests for Elsevier materials may attract a fee.

7. Reservation of Rights: Publisher reserves all rights not specifically granted in the combination of (i) the license details provided by you and accepted in the course of this licensing transaction, (ii) these terms and conditions and (iii) CCC's Billing and Payment terms and conditions.

8. License Contingent Upon Payment: While you may exercise the rights licensed immediately upon issuance of the license at the end of the licensing process for the transaction, provided that you have disclosed complete and accurate details of your proposed use, no license is finally effective unless and until full payment is received from you (either by publisher or by CCC) as provided in CCC's Billing and Payment terms and conditions. If full payment is not received on a timely basis, then any license preliminarily granted shall be deemed automatically revoked and shall be void as if never granted. Further, in the event that you breach any of these terms and conditions or any of CCC's Billing and Payment terms and conditions, the license is automatically revoked and shall be void as if never granted. Use of materials as described in a revoked license, as well as any use of the materials beyond the scope of an unrevoked license, may constitute copyright infringement and publisher reserves the right to take any and all action to protect its copyright in the materials.

9. Warranties: Publisher makes no representations or warranties with respect to the licensed material.

10. Indemnity: You hereby indemnify and agree to hold harmless publisher and CCC, and their respective officers, directors, employees and agents, from and against any and all claims arising out of your use of the licensed material other than as specifically authorized pursuant to this license.

11. No Transfer of License: This license is personal to you and may not be sublicensed, assigned, or transferred by you to any other person without publisher's written permission.

12. No Amendment Except in Writing: This license may not be amended except in a writing signed by both parties (or, in the case of publisher, by CCC on publisher's behalf).

13. Objection to Contrary Terms: Publisher hereby objects to any terms contained in any purchase order, acknowledgment, check endorsement or other writing prepared by you, which terms are inconsistent with these terms and conditions or CCC's Billing and Payment terms and conditions. These terms and conditions, together with CCC's Billing and Payment terms and conditions (which are incorporated herein), comprise the entire agreement between you and publisher (and CCC) concerning this licensing transaction. In the event of any conflict between your obligations established by these terms and conditions and those established by CCC's Billing and Payment terms and conditions, these terms and conditions shall control.

14. Revocation: Elsevier or Copyright Clearance Center may deny the permissions described in this License at their sole

discretion, for any reason or no reason, with a full refund payable to you. Notice of such denial will be made using the contact information provided by you. Failure to receive such notice will not alter or invalidate the denial. In no event will Elsevier or Copyright Clearance Center be responsible or liable for any costs, expenses or damage incurred by you as a result of a denial of your permission request, other than a refund of the amount(s) paid by you to Elsevier and/or Copyright Clearance Center for denied permissions.

LIMITED LICENSE

The following terms and conditions apply only to specific license types:

15. **Translation**: This permission is granted for non-exclusive world **English** rights only unless your license was granted for translation rights. If you licensed translation rights you may only translate this content into the languages you requested. A professional translator must perform all translations and reproduce the content word for word preserving the integrity of the article.

16. **Posting licensed content on any Website**: The following terms and conditions apply as follows: Licensing material from an Elsevier journal: All content posted to the web site must maintain the copyright information line on the bottom of each image; A hyper-text must be included to the Homepage of the journal from which you are licensing at http://www.sciencedirect.com/science/journal/xxxxx or the Elsevier homepage for books at http://www.elsevier.com; Central Storage: This license does not include permission for a scanned version of the material to be stored in a central repository such as that provided by Heron/XanEdu.

Licensing material from an Elsevier book: A hyper-text link must be included to the Elsevier homepage at http://www.elsevier.com . All content posted to the web site must maintain the copyright information line on the bottom of each image.

Posting licensed content on Electronic reserve: In addition to the above the following clauses are applicable: The web site must be password-protected and made available only to bona fide students registered on a relevant course. This permission is granted for 1 year only. You may obtain a new license for future website posting.

17. **For journal authors:** the following clauses are applicable in addition to the above:

Preprints:

A preprint is an author's own write-up of research results and analysis, it has not been peer-reviewed, nor has it had any other value added to it by a publisher (such as formatting, copyright, technical enhancement etc.).

Authors can share their preprints anywhere at any time. Preprints should not be added to or enhanced in any way in order to appear more like, or to substitute for, the final versions of articles however authors can update their preprints on arXiv or RePEc with their Accepted Author Manuscript (see below).

If accepted for publication, we encourage authors to link from the preprint to their formal publication via its DOI. Millions of researchers have access to the formal publications on ScienceDirect, and so links will help users to find, access, cite and use the best available version. Please note that Cell Press, The Lancet and some society-owned have different preprint policies. Information on these policies is available on the journal homepage.

Accepted Author Manuscripts: An accepted author manuscript is the manuscript of an article that has been accepted for publication and which typically includes author-incorporated changes suggested during submission, peer review and editor-author communications.

Authors can share their accepted author manuscript:

- immediately
  - via their non-commercial person homepage or blog
  - by updating a preprint in arXiv or RePEc with the accepted manuscript
  - via their research institute or institutional repository for internal institutional uses or as part of an invitation-only research collaboration work-group
  - directly by providing copies to their students or to research collaborators for their personal use
  - for private scholarly sharing as part of an invitation-only work group on commercial sites with which Elsevier has an agreement
- after the embargo period
  - via non-commercial hosting platforms such as their institutional repository
  - via commercial sites with which Elsevier has an agreement

In all cases accepted manuscripts should:

- link to the formal publication via its DOI
- bear a CC-BY-NC-ND license - this is easy to do
- if aggregated with other manuscripts, for example in a repository or other site, be shared in alignment with our hosting policy not be added to or enhanced in any way to appear more like, or to substitute for, the published

journal article.

Published journal article (JPA): A published journal article (PJA) is the definitive final record of published research that appears or will appear in the journal and embodies all value-adding publishing activities including peer review co-ordination, copy-editing, formatting, (if relevant) pagination and online enrichment.
Policies for sharing publishing journal articles differ for subscription and gold open access articles:
Subscription Articles: If you are an author, please share a link to your article rather than the full-text. Millions of researchers have access to the formal publications on ScienceDirect, and so links will help your users to find, access, cite, and use the best available version.
Theses and dissertations which contain embedded PJAs as part of the formal submission can be posted publicly by the awarding institution with DOI links back to the formal publications on ScienceDirect.
If you are affiliated with a library that subscribes to ScienceDirect you have additional private sharing rights for others' research accessed under that agreement. This includes use for classroom teaching and internal training at the institution (including use in course packs and courseware programs), and inclusion of the article for grant funding purposes.
Gold Open Access Articles: May be shared according to the author-selected end-user license and should contain a CrossMark logo, the end user license, and a DOI link to the formal publication on ScienceDirect.
Please refer to Elsevier's posting policy for further information.
18. **For book authors** the following clauses are applicable in addition to the above: Authors are permitted to place a brief summary of their work online only. You are not allowed to download and post the published electronic version of your chapter, nor may you scan the printed edition to create an electronic version. **Posting to a repository:** Authors are permitted to post a summary of their chapter only in their institution's repository.
19. **Thesis/Dissertation**: If your license is for use in a thesis/dissertation your thesis may be submitted to your institution in either print or electronic form. Should your thesis be published commercially, please reapply for permission. These requirements include permission for the Library and Archives of Canada to supply single copies, on demand, of the complete thesis and include permission for Proquest/UMI to supply single copies, on demand, of the complete thesis. Should your thesis be published commercially, please reapply for permission. Theses and dissertations which contain embedded PJAs as part of the formal submission can be posted publicly by the awarding institution with DOI links back to the formal publications on ScienceDirect.

Elsevier Open Access Terms and Conditions
You can publish open access with Elsevier in hundreds of open access journals or in nearly 2000 established subscription journals that support open access publishing. Permitted third party re-use of these open access articles is defined by the author's choice of Creative Commons user license. See our open access license policy for more information.
Terms & Conditions applicable to all Open Access articles published with Elsevier:
Any reuse of the article must not represent the author as endorsing the adaptation of the article nor should the article be modified in such a way as to damage the author's honour or reputation. If any changes have been made, such changes must be clearly indicated.
The author(s) must be appropriately credited and we ask that you include the end user license and a DOI link to the formal publication on ScienceDirect.
If any part of the material to be used (for example, figures) has appeared in our publication with credit or acknowledgement to another source it is the responsibility of the user to ensure their reuse complies with the terms and conditions determined by the rights holder.
Additional Terms & Conditions applicable to each Creative Commons user license:
CC BY: The CC-BY license allows users to copy, to create extracts, abstracts and new works from the Article, to alter and revise the Article and to make commercial use of the Article (including reuse and/or resale of the Article by commercial entities), provided the user gives appropriate credit (with a link to the formal publication through the relevant DOI), provides a link to the license, indicates if changes were made and the licensor is not represented as endorsing the use made of the work. The full details of the license are available at http://creativecommons.org/licenses/by/4.0.
CC BY NC SA: The CC BY-NC-SA license allows users to copy, to create extracts, abstracts and new works from the Article, to alter and revise the Article, provided this is not done for commercial purposes, and that the user gives appropriate credit (with a link to the formal publication through the relevant DOI), provides a link to the license, indicates if changes were made and the licensor is not represented as endorsing the use made of the work. Further, any new works must be made available on the same conditions. The full details of the license are available at http://creativecommons.org/licenses/by-nc-sa/4.0.
CC BY NC ND: The CC BY-NC-ND license allows users to copy and distribute the Article, provided this is not done for commercial purposes and further does not permit distribution of the Article if it is changed or edited in any way, and

REFERENCES

1. Durley, R., Chen, L., Lim, L. W., Mathews, F. S., and Davidson, V. L. (1993) Crystal structure analysis of amicyanin and apoamicyanin from *Paracoccus denitrificans* at 2.0 A and 1.8 A resolution, *Protein Sci 2*, 739-752.

2. Hart, P. J., Nersissian, A. M., Herrmann, R. G., Nalbandyan, R. M., Valentine, J. S., and Eisenberg, D. (1996) A missing link in cupredoxins: crystal structure of cucumber stellacyanin at 1.6 A resolution, *Protein Sci 5*, 2175-2183.

3. Nar, H., Messerschmidt, A., Huber, R., van de Kamp, M., and Canters, G. W. (1991) Crystal structure analysis of oxidized Pseudomonas aeruginosa azurin at pH 5.5 and pH 9.0. A pH-induced conformational transition involves a peptide bond flip, *J Mol Biol 221*, 765-772.

4. Holm, R. H., Kennepohl, P., and Solomon, E. I. (1996) Structural and Functional Aspects of Metal Sites in Biology, *Chem Rev 96*, 2239-2314.

5. Solomon, E. I., Szilagyi, R. K., DeBeer George, S., and Basumallick, L. (2004) Electronic structures of metal sites in proteins and models: contributions to function in blue copper proteins, *Chem Rev 104*, 419-458.

6. Zaitseva, E. I., Titova, O. V., Melekhova, L. S., Makarenko, T. G., and Sosina, T. E. (1996) [New data on clinical response to therapeutic effects of gastrozepin], *Klinicheskaia meditsina 74*, 49-50.

7. Zhu, Z., Cunane, L. M., Chen, Z., Durley, R. C., Mathews, F. S., and Davidson, V. L. (1998) Molecular basis for interprotein complex-dependent effects on the redox properties of amicyanin, *Biochemistry 37*, 17128-17136.

8. Machczynski, M. C., Gray, H. B., and Richards, J. H. (2002) An outer-sphere hydrogen-bond network constrains copper coordination in blue proteins, *J Inorg Biochem 88*, 375-380.

9. Libeu, C. A., Kukimoto, M., Nishiyama, M., Horinouchi, S., and Adman, E. T. (1997) Site-directed mutants of pseudoazurin: explanation of increased redox potentials from X-ray structures and from calculation of redox potential differences, *Biochemistry 36*, 13160-13179.

10. Marshall, N. M., Garner, D. K., Wilson, T. D., Gao, Y. G., Robinson, H., Nilges, M. J., and Lu, Y. (2009) Rationally tuning the reduction potential of a single cupredoxin beyond the natural range, *Nature 462*, 113-116.

11. Reinhammar, B. R. (1972) Oxidation-reduction potentials of the electron acceptors in laccases and stellacyanin, *Biochim Biophys Acta 275*, 245-259.

12. Van Pouderoyen, G., Cigna, G., Rolli, G., Cutruzzola, F., Malatesta, F., Silvestrini, M. C., Brunori, M., and Canters, G. W. (1997) Electron-transfer properties of Pseudomonas aeruginosa [Lys44, Glu64]azurin, *European journal of biochemistry / FEBS 247*, 322-331.

13. Kukimoto, M., Nishiyama, M., Ohnuki, T., Turley, S., Adman, E. T., Horinouchi, S., and Beppu, T. (1995) Identification of interaction site of pseudoazurin with its redox partner, copper-containing nitrite reductase from Alcaligenes faecalis S-6, *Protein engineering 8*, 153-158.

14. Gray, K. A., Knaff, D. B., Husain, M., and Davidson, V. L. (1986) Measurement of the oxidation-reduction potentials of amicyanin and c-type cytochromes from Paracoccus denitrificans, *FEBS letters 207*, 239-242.

15. Anderson, G. P., Sanderson, D. G., Lee, C. H., Durell, S., Anderson, L. B., and Gross, E. L. (1987) The effect of ethylenediamine chemical modification of plastocyanin on the rate of cytochrome f oxidation and P-700+ reduction, *Biochim Biophys Acta 894*, 386-398.

16. Hall, J. F., Kanbi, L. D., Harvey, I., Murphy, L. M., and Hasnain, S. S. (1998) Modulating the redox potential and acid stability of rusticyanin by site-directed mutagenesis of Ser86, *Biochemistry 37*, 11451-11458.

17. Lee, W. T. (2004) An interactive introduction to protein structure, *Biochemistry and molecular biology education : a bimonthly publication of the International Union of Biochemistry and Molecular Biology 32*, 170-172.

18. Forst, D., Welte, W., Wacker, T., and Diederichs, K. (1998) Structure of the sucrose-specific porin ScrY from Salmonella typhimurium and its complex with sucrose, *Nature structural biology 5*, 37-46.

19. Newcomer, M. E., and Ong, D. E. (2000) Plasma retinol binding protein: structure and function of the prototypic lipocalin, *Biochim Biophys Acta 1482*, 57-64.

20. Getzoff, E. D., Tainer, J. A., Stempien, M. M., Bell, G. I., and Hallewell, R. A. (1989) Evolution of CuZn superoxide dismutase and the Greek key beta-barrel structural motif, *Proteins 5*, 322-336.

21. Hemmingsen, J. M., Gernert, K. M., Richardson, J. S., and Richardson, D. C. (1994) The tyrosine corner: a feature of most Greek key beta-barrel proteins, *Protein Sci 3*, 1927-1937.

22. Hendrix, R. W. (1999) Evolution: the long evolutionary reach of viruses, *Current biology : CB 9*, R914-917.

23. Perona, J. J., and Craik, C. S. (1997) Evolutionary divergence of substrate specificity within the chymotrypsin-like serine protease fold, *The Journal of biological chemistry 272*, 29987-29990.

24. Hutchinson, E. G., and Thornton, J. M. (1993) The Greek key motif: extraction, classification and analysis, *Protein engineering 6*, 233-245.

25. Choi, M., and Davidson, V. L. (2011) Cupredoxins--a study of how proteins may evolve to use metals for bioenergetic processes, *Metallomics 3*, 140-151.

26. Taanman, J. W. (1997) Human cytochrome c oxidase: structure, function, and deficiency, *Journal of bioenergetics and biomembranes 29*, 151-163.

27. Gough, J., and Chothia, C. (2004) The linked conservation of structure and function in a family of high diversity: the monomeric cupredoxins, *Structure 12*, 917-925.

28. Sukumar, N., Mathews, F. S., Langan, P., and Davidson, V. L. (2010) A joint x-ray and neutron study on amicyanin reveals the role of protein dynamics in electron transfer, *Proc Natl Acad Sci U S A 107*, 6817-6822.

29. Delfino, I., and Cannistraro, S. (2009) Optical investigation of the electron transfer protein azurin-gold nanoparticle system, *Biophys Chem 139*, 1-7.

30. Petrich, J. W., Longworth, J. W., and Fleming, G. R. (1987) Internal motion and electron transfer in proteins: a picosecond fluorescence study of three homologous azurins, *Biochemistry 26*, 2711-2722.

31. Padlan, E. A. (1994) Anatomy of the antibody molecule, *Molecular immunology 31*, 169-217.

32. Ye, Y., and Godzik, A. (2003) Flexible structure alignment by chaining aligned fragment pairs allowing twists, *Bioinformatics 19 Suppl 2*, ii246-255.

33. Baden, E. M., Owen, B. A., Peterson, F. C., Volkman, B. F., Ramirez-Alvarado, M., and Thompson, J. R. (2008) Altered dimer interface decreases stability in an amyloidogenic protein, *The Journal of biological chemistry 283*, 15853-15860.

34. Lowe, D., Dudgeon, K., Rouet, R., Schofield, P., Jermutus, L., and Christ, D. (2011) Aggregation, stability, and formulation of human antibody therapeutics, *Advances in protein chemistry and structural biology 84*, 41-61.

35. Barthelemy, P. A., Raab, H., Appleton, B. A., Bond, C. J., Wu, P., Wiesmann, C., and Sidhu, S. S. (2008) Comprehensive analysis of the factors contributing to the stability and solubility of autonomous human VH domains, *The Journal of biological chemistry 283*, 3639-3654.

36. Riechmann, L. (1996) Rearrangement of the former VL interface in the solution structure of a camelised, single antibody VH domain, *Journal of molecular biology 259*, 957-969.

37. Dudgeon, K., Rouet, R., Kokmeijer, I., Schofield, P., Stolp, J., Langley, D., Stock, D., and Christ, D. (2012) General strategy for the generation of human antibody variable domains with increased aggregation resistance, *Proc Natl Acad Sci U S A 109*, 10879-10884.

38. Brockmann, E. C., Cooper, M., Stromsten, N., Vehniainen, M., and Saviranta, P. (2005) Selecting for antibody scFv fragments with improved stability using phage display with denaturation under reducing conditions, *Journal of immunological methods 296*, 159-170.

39. Famm, K., Hansen, L., Christ, D., and Winter, G. (2008) Thermodynamically stable aggregation-resistant antibody domains through directed evolution, *Journal of molecular biology 376*, 926-931.

40. Chennamsetty, N., Voynov, V., Kayser, V., Helk, B., and Trout, B. L. (2009) Design of therapeutic proteins with enhanced stability, *Proceedings of the National Academy of Sciences of the United States of America 106*, 11937-11942.

41. Lowe, D., Dudgeon, K., Rouet, R., Schofield, P., Jermutus, L., and Christ, D. (2011) Aggregation, Stability, and Formulation of Human Antibody Therapeutics, *Adv Protein Chem Str 84*, 41-61.

42. Demarest, S. J., and Glaser, S. M. (2008) Antibody therapeutics, antibody engineering, and the merits of protein stability, *Curr Opin Drug Disc 11*, 675-687.

43. Lee, C. C., Perchiacca, J. M., and Tessier, P. M. (2013) Toward aggregation-resistant antibodies by design, *Trends in biotechnology 31*, 612-620.

44. Waldmann, H. (2014) Human monoclonal antibodies: the residual challenge of antibody immunogenicity, *Methods in molecular biology 1060*, 1-8.

45. Buxbaum, J. N., Chuba, J. V., Hellman, G. C., Solomon, A., and Gallo, G. R. (1990) Monoclonal immunoglobulin deposition disease: light chain and light and heavy chain deposition diseases and their relation to light chain amyloidosis. Clinical features, immunopathology, and molecular analysis, *Annals of internal medicine 112*, 455-464.

46. Poulos, T. L. (2014) Heme enzyme structure and function, *Chem Rev 114*, 3919-3962.

47. Orii, Y., Yoshida, S., and Iizuka, T. (1976) Heme a and copper environments in cytochrome oxidase, *Advances in experimental medicine and biology 74*, 228-239.

48. Bruice, T. C. (1986) Chemical studies pertaining to the chemistry of cytochrome P-450 and the peroxidases, *Annals of the New York Academy of Sciences 471*, 83-98.

49. Obinger, C. (2006) Chemistry and biology of human peroxidases, *Archives of biochemistry and biophysics 445*, 197-198.

50. Gray, H. B., and Winkler, J. R. (2003) Electron tunneling through proteins, *Quarterly reviews of biophysics 36*, 341-372.

51. Battistuzzi, G., Borsari, M., Cowan, J. A., Ranieri, A., and Sola, M. (2002) Control of cytochrome C redox potential: axial ligation and protein environment effects, *Journal of the American Chemical Society 124*, 5315-5324.

52. Reedy, C. J., and Gibney, B. R. (2004) Heme protein assemblies, *Chem Rev 104*, 617-649.

53. Battistuzzi, G., Bellei, M., Casella, L., Bortolotti, C. A., Roncone, R., Monzani, E., and Sola, M. (2007) Redox reactivity of the heme Fe3+/Fe 2+ couple in native myoglobins and mutants with peroxidase-like activity, *Journal of biological inorganic chemistry : JBIC : a publication of the Society of Biological Inorganic Chemistry 12*, 951-958.

54. Varadarajan, R., Zewert, T. E., Gray, H. B., and Boxer, S. G. (1989) Effects of buried ionizable amino acids on the reduction potential of recombinant myoglobin, *Science 243*, 69-72.

55. Farhangrazi, Z. S., Fossett, M. E., Powers, L. S., and Ellis, W. R., Jr. (1995) Variable-temperature spectroelectrochemical study of horseradish peroxidase, *Biochemistry 34*, 2866-2871.

56. Mondal, M. S., and Mitra, S. (1996) Kinetic studies of the two-step reactions of H2O2 with manganese-reconstituted myoglobin, *Biochim Biophys Acta 1296*, 174-180.

57. Farhangrazi, Z. S., Copeland, B. R., Nakayama, T., Amachi, T., Yamazaki, I., and Powers, L. S. (1994) Oxidation-reduction properties of compounds I and II of Arthromyces ramosus peroxidase, *Biochemistry 33*, 5647-5652.

58. Munro, A. W., Girvan, H. M., and McLean, K. J. (2007) Variations on a (t)heme--novel mechanisms, redox partners and catalytic functions in the cytochrome P450 superfamily, *Natural product reports 24*, 585-609.

59. Jones, D. K., Dalton, D. A., Rosell, F. I., and Raven, E. L. (1998) Class I heme peroxidases: characterization of soybean ascorbate peroxidase, *Archives of biochemistry and biophysics 360*, 173-178.

60. Conroy, C. W., Tyma, P., Daum, P. H., and Erman, J. E. (1978) Oxidation-reduction potential measurements of cytochrome c peroxidase and pH dependent spectral transitions in the ferrous enzyme, *Biochim Biophys Acta 537*, 62-69.

61. Zhang, Z., Chouchane, S., Magliozzo, R. S., and Rusling, J. F. (2002) Direct voltammetry and catalysis with Mycobacterium tuberculosis catalase-peroxidase, peroxidases, and catalase in lipid films, *Anal Chem 74*, 163-170.

62. Battistuzzi, G., Bellei, M., De Rienzo, F., and Sola, M. (2006) Redox properties of the Fe3+/Fe2+ couple in Arthromyces ramosus class II peroxidase and its cyanide adduct, *Journal of biological inorganic chemistry : JBIC : a publication of the Society of Biological Inorganic Chemistry 11*, 586-592.

63. Ciaccio, C., Rosati, A., De Sanctis, G., Sinibaldi, F., Marini, S., Santucci, R., Ascenzi, P., Welinder, K. G., and Coletta, M. (2003) Relationships of ligand binding, redox properties, and protonation in Coprinus cinereus peroxidase, *The Journal of biological chemistry 278*, 18730-18737.

64. Yamada, H., Makino, R., and Yamazaki, I. (1975) Effects of 2,4-substituents of deuteropheme upon redox potentials of horseradish peroxidases, *Archives of biochemistry and biophysics 169*, 344-353.

65. Harbury, H. A. (1957) Oxidation-reduction potentials of horseradish peroxidase, *The Journal of biological chemistry 225*, 1009-1024.

66. Jensen, L. M., Sanishvili, R., Davidson, V. L., and Wilmot, C. M. (2010) In crystallo posttranslational modification within a MauG/pre-methylamine dehydrogenase complex, *Science 327*, 1392-1394.

67. Li, X., Jones, L. H., Pearson, A. R., Wilmot, C. M., and Davidson, V. L. (2006) Mechanistic possibilities in MauG-dependent tryptophan tryptophylquinone biosynthesis, *Biochemistry 45*, 13276-13283.

68. Wang, Y., Li, X., Jones, L. H., Pearson, A. R., Wilmot, C. M., and Davidson, V. L. (2005) MauG-dependent in vitro biosynthesis of tryptophan tryptophylquinone in methylamine dehydrogenase, *Journal of the American Chemical Society 127*, 8258-8259.

69. Li, X., Feng, M., Wang, Y., Tachikawa, H., and Davidson, V. L. (2006) Evidence for redox cooperativity between c-type hemes of MauG which is likely coupled to oxygen activation during tryptophan tryptophylquinone biosynthesis, *Biochemistry 45*, 821-828.

70. Choi, M., Shin, S., and Davidson, V. L. (2012) Characterization of electron tunneling and hole hopping reactions between different forms of MauG and methylamine dehydrogenase within a natural protein complex, *Biochemistry 51*, 6942-6949.

71. Onuchic, J. N., Beratan, D. N., Winkler, J. R., and Gray, H. B. (1992) Pathway analysis of protein electron-transfer reactions, *Annual review of biophysics and biomolecular structure 21*, 349-377.

72. Moser, C. C., Keske, J. M., Warncke, K., Farid, R. S., and Dutton, P. L. (1992) Nature of biological electron transfer, *Nature 355*, 796-802.

73. Sharp, K. A. (1998) Calculation of electron transfer reorganization energies using the finite difference Poisson-Boltzmann model, *Biophys J 74*, 1241-1250.

74. Scott, J. R., Willie, A., Mclean, M., Stayton, P. S., Sligar, S. G., Durham, B., and Millett, F. (1993) Intramolecular Electron-Transfer in Cytochrome-B(5) Labeled with Ruthenium(Ii) Polypyridine Complexes - Rate Measurements in the Marcus Inverted Region, *J Am Chem Soc 115*, 6820-6824.

75. Meade, T. J., Gray, H. B., and Winkler, J. R. (1989) Driving-Force Effects on the Rate of Long-Range Electron-Transfer in Ruthenium-Modified Cytochrome-C, *J Am Chem Soc 111*, 4353-4356.

76. Farver, O., Hosseinzadeh, P., Marshall, N. M., Wherland, S., Lu, Y., and Pecht, I. (2015) Long-range electron transfer in engineered azurins exhibits Marcus inverted region behavior, *J Phys Chem Lett 6*, 100-105.

77. Brooks, H. B., and Davidson, V. L. (1994) Free-Energy Dependence of the Electron-Transfer Reaction between Methylamine Dehydrogenase and Amicyanin, *J Am Chem Soc 116*, 11201-11202.

78. Davidson, V. L., and Jones, L. H. (1996) Electron transfer from copper to heme within the methylamine dehydrogenase-amicyanin-cytochrome c-551i complex, *Biochemistry 35*, 8120-8125.

79. Choi, M., Shin, S., and Davidson, V. L. (2012) Characterization of Electron Tunneling and Hole Hopping Reactions between Different Forms of MauG and Methylamine Dehydrogenase within a Natural Protein Complex, *Biochemistry 51*, 6942-6949.

80. Davidson, V. L. (2002) Chemically gated electron transfer. A means of accelerating and regulating rates of biological electron transfer, *Biochemistry 41*, 14633-14636.

81. Carrell, C. J., Sun, D., Jiang, S., Davidson, V. L., and Mathews, F. S. (2004) Structural studies of two mutants of amicyanin from *Paracoccus denitrificans* that stabilize the reduced state of the copper, *Biochemistry 43*, 9372-9380.

82. Davidson, V. L. (2000) Effects of kinetic coupling on experimentally determined electron transfer parameters, *Biochemistry 39*, 4924-4928.

83. Kuznetsova, S., Zauner, G., Schmauder, R., Mayboroda, O. A., Deelder, A. M., Aartsma, T. J., and Canters, G. W. (2006) A Forster-resonance-energy transfer-based method for fluorescence detection of the protein redox state, *Analytical biochemistry 350*, 52-60.

84. Dennison, C. (2005) Investigating the structure and function of cupredoxins, *Coord. Chem. Rev. 249*, 3025-3054.

85. Husain, M., and Davidson, V. L. (1985) An inducible periplasmic blue copper protein from *Paracoccus denitrificans*. Purification, properties, and physiological role, *The Journal of biological chemistry 260*, 14626-14629.

86. Cunane, L. M., Chen, Z. W., Durley, R. C., and Mathews, F. S. (1996) X-ray structure of the cupredoxin amicyanin, from Paracoccus denitrificans, refined at 1.31 A resolution, *Acta Crystallogr D Biol Crystallogr 52*, 676-686.

87. Husain, M., and Davidson, V. L. (1987) Purification and properties of methylamine dehydrogenase from Paracoccus denitrificans, *J Bacteriol 169*, 1712-1717.

88. Husain, M., and Davidson, V. L. (1986) Characterization of two inducible periplasmic c-type cytochromes from Paracoccus denitrificans, *The Journal of biological chemistry 261*, 8577-8580.

89. Chen, L., Durley, R. C., Mathews, F. S., and Davidson, V. L. (1994) Structure of an electron transfer complex: methylamine dehydrogenase, amicyanin, and cytochrome c551i, *Science 264*, 86-90.

90. Chen, L., Durley, R., Poliks, B. J., Hamada, K., Chen, Z., Mathews, F. S., Davidson, V. L., Satow, Y., Huizinga, E., Vellieux, F. M., and et al. (1992) Crystal structure of an electron-transfer complex between methylamine dehydrogenase and amicyanin, *Biochemistry 31*, 4959-4964.

91. Choi, M., Sukumar, N., Liu, A., and Davidson, V. L. (2009) Defining the role of the axial ligand of the type 1 copper site in amicyanin by replacement of methionine with leucine, *Biochemistry 48*, 9174-9184.

92. Davidson, V. L., Jones, L. H., Graichen, M. E., Mathews, F. S., and Hosler, J. P. (1997) Factors which stabilize the methylamine dehydrogenase-amicyanin electron transfer protein complex revealed by site-directed mutagenesis, *Biochemistry 36*, 12733-12738.

93. Davidson, V. L., Jones, L. H., and Zhu, Z. (1998) Site-directed mutagenesis of Phe 97 to Glu in amicyanin alters the electronic coupling for interprotein electron transfer from quinol methylamine dehydrogenase, *Biochemistry 37*, 7371-7377.

94. Ma, J. K., Mathews, F. S., and Davidson, V. L. (2007) Correlation of rhombic distortion of the type 1 copper site of M98Q amicyanin with increased electron transfer reorganization energy, *Biochemistry 46*, 8561-8568.

95. Ma, J. K., Wang, Y., Carrell, C. J., Mathews, F. S., and Davidson, V. L. (2007) A single methionine residue dictates the kinetic mechanism of interprotein electron transfer from methylamine dehydrogenase to amicyanin, *Biochemistry 46*, 11137-11146.

96. Sun, D., and Davidson, V. L. (2003) Effects of engineering uphill electron transfer into the methylamine dehydrogenase-amicyanin-cytochrome c-551i complex, *Biochemistry 42*, 1772-1776.

97. Sun, D., Li, X., Mathews, F. S., and Davidson, V. L. (2005) Site-directed mutagenesis of proline 94 to alanine in amicyanin converts a true electron transfer reaction into one that is kinetically coupled, *Biochemistry 44*, 7200-7206.

98. Husain, M., Davidson, V. L., and Smith, A. J. (1986) Properties of *Paracoccus denitrificans* amicyanin, *Biochemistry 25*, 2431-2436.

99. Baker, E. N. (1988) Structure of azurin from Alcaligenes denitrificans refinement at 1.8 A resolution and comparison of the two crystallographically independent molecules, *J Mol Biol 203*, 1071-1095.

100. Morpurgo, L., Finazzi-Agro, A., Rotilio, G., and Mondovi, B. (1972) Studies of the metal sites of copper proteins. IV. Stellacyanin: preparation of apoprotein and involvement of sulfhydryl and tryptophan in the copper chromophore, *Biochim Biophys Acta 271*, 292-299.

101. Szabo, A. G., Stepanik, T. M., Wayner, D. M., and Young, N. M. (1983) Conformational heterogeneity of the copper binding site in azurin. A time-resolved fluorescence study, *Biophysical Journal 41*, 233-244.

102. Sweeney, J. A., Harmon, P. A., Asher, S. A., Hutnik, C. M., and Szabo, A. G. (1991) Uv Resonance Raman Examination of the Azurin Tryptophan Environment and Energy Relaxation Pathways, *J Am Chem Soc 113*, 7531-7537.

103. Shih, C., Museth, A. K., Abrahamsson, M., Blanco-Rodriguez, A. M., Di Bilio, A. J., Sudhamsu, J., Crane, B. R., Ronayne, K. L., Towrie, M., Vlcek, A., Jr., Richards, J. H., Winkler, J. R., and Gray, H. B. (2008) Tryptophan-accelerated electron flow through proteins, *Science 320*, 1760-1762.

104. Engman, K. C., Sandberg, A., Leckner, J., and Karlsson, B. G. (2004) Probing the influence on folding behavior of structurally conserved core residues in P. aeruginosa apo-azurin, *Protein Sci 13*, 2706-2715.

105. Davidson, V. L. (1990) Methylamine dehydrogenases from methylotrophic bacteria, *Methods Enzymol 188*, 241-246.

106. Chistoserdov, A. Y., Boyd, J., Mathews, F. S., and Lidstrom, M. E. (1992) The genetic organization of the mau gene cluster of the facultative autotroph Paracoccus denitrificans, *Biochem Biophys Res Commun 184*, 1181-1189.

107. Carrell, C. J., Ma, J. K., Antholine, W. E., Hosler, J. P., Mathews, F. S., and Davidson, V. L. (2007) Generation of novel copper sites by mutation of the axial ligand of amicyanin. Atomic resolution structures and spectroscopic properties, *Biochemistry 46*, 1900-1912.

108. Lim, L. W., Mathews, F. S., Husain, M., and Davidson, V. L. (1986) Preliminary X-ray crystallographic study of amicyanin from Paracoccus denitrificans, *J Mol Biol 189*, 257-258.

109. Otwinowski, Z., and Minor, W. (1997) Processing of x-ray diffraction data collected by oscillation methods., *Methods Enzymol. 276*, 307-326.

110. McCoy, A. J., Grosse-Kunstleve, R.W., Adams, P.D., Winn, M.D., Storoni, L.C. and Read, R.J. (2007) Phaser crystallographic software, *J. Appl. Cryst. 40*, 658-674.

111. Adams, P. D., Grosse-Kunstleve, R. W., Hung, L. W., Ioerger, T. R., McCoy, A. J., Moriarty, N. W., Read, R. J., Sacchettini, J. C., Sauter, N. K., and Terwilliger, T. C. (2002) PHENIX: building new software for automated crystallographic structure determination, *Acta Crystallogr D Biol Crystallogr 58*, 1948-1954.

112. Emsley, P., and Cowtan, K. (2004) Coot: model-building tools for molecular graphics, *Acta Crystallogr D Biol Crystallogr 60*, 2126-2132.

113. Brunger, A. T. (1992) Free R value: a novel statistical quantity for assessing the accuracy of crystal structures, *Nature 355*, 472-475.

114. Laskowski, R., Thornton, J., Moss, D., and MacArthur, M. (1993) PROCHECK: a program to check the stereochemical quality of protein structures., *J. Appl. Cryst. 26*, 283-291.

115. Potterton, L., McNicholas, S., Krissinel, E., Gruber, J., Cowtan, K., Emsley, P., Murshudov, G. N., Cohen, S., Perrakis, A., and Noble, M. (2004) Developments in the CCP4 molecular-graphics project, *Acta Crystallogr D Biol Crystallogr 60*, 2288-2294.

116. CCP4. (1994) Collaborative Computational Project Number 4, *Acta Crystallogr. Sect. D Biol. Crystallogr. 50*, 760-763.

117. Cammack, R. (1995) In *Bioenergetics: A Practical Approach* (Brown, G. C., and Cooper, C. E., Eds.), pp 85-109, IRL Press, New York.

118. Brooks, H. B., Jones, L. H., and Davidson, V. L. (1993) Deuterium kinetic isotope effect and stopped-flow kinetic studies of the quinoprotein methylamine dehydrogenase, *Biochemistry 32*, 2725-2729.

119. Davidson, V. L., and Jones, L. H. (1991) Intermolecular electron transfer from quinoproteins and its relevance to biosensor technology, *Anal Chim Acta 249*, 235-240.

120. La Rosa, C., Milardi, D., Grasso, D. M., Verbeet, M. P., Canters, G. W., Sportelli, L., and Guzzi, R. (2002) A model for the thermal unfolding of amicyanin, *Eur Biophys J 30*, 559-570.

121. Davidson, V. L., Graichen, M. E., and Jones, L. H. (1993) Binding constants for a physiologic electron-transfer protein complex between methylamine dehydrogenase and amicyanin. Effects of ionic strength and bound copper on binding, *Biochim Biophys Acta 1144*, 39-45.

122. Sreerama, N., and Woody, R. W. (2000) Circular dichroism of peptides and proteins, In *Circular Dichroism: Principles and Applications* (Berova, N., Nakanishi, K., and Woody, R. W., Eds.) 2nd ed., pp 601-620, John Wiley & Sons, New York.

123. Sharma, K. D., Loehr, T. M., Sanders-Loehr, J., Husain, M., and Davidson, V. L. (1988) Resonance Raman spectroscopy of amicyanin, a blue copper protein from Paracoccus denitrificans, *The Journal of biological chemistry 263*, 3303-3306.

124. Woodruff, W. H., Dyer, R. B., and Schoonover, J. R. (1988) In *Biological Applications of Raman Spectroscopy* (Spiro, T. G., Ed.), p 413, John Wiley and Sons, New York.

125. Krissinel, E., and Henrick, K. (2004) Secondary-structure matching (SSM), a new tool for fast protein structure alignment in three dimensions, *Acta Crystallogr D Biol Crystallogr 60*, 2256-2268.

126. Ma, J. K., Bishop, G. R., and Davidson, V. L. (2005) The ligand geometry of copper determines the stability of amicyanin, *Arch. Biochem. Biophys. 444*, 27-33.

127. Woody, R. W., and Dunker, A. K. (1996) Aromatic and cysteine side-chain circular dichroism in proteins, In *Circular Dichroism and the Conformational Analysis of Biomolecules* (Fasman, G. D., Ed.), pp 109-157, Plenum Press, New York.

128. Kumar, M. A., and Davidson, V. L. (1992) Methods to identify and avoid artifactual formation of interchain disulfide bonds when analyzing proteins by SDS-PAGE, *Biotechniques 12*, 198, 200, 202.

129. Battistuzzi, G., Borsari, M., Canters, G. W., di Rocco, G., de Waal, E., Arendsen, Y., Leonardi, A., Ranieri, A., and Sola, M. (2005) Ligand loop effects on the free energy change of redox and pH-dependent equilibria in cupredoxins probed on amicyanin variants, *Biochemistry 44*, 9944-9949.

130. Paltrinieri, L., Borsari, M., Battistuzzi, G., Sola, M., Dennison, C., de Groot, B. L., Corni, S., and Bortolotti, C. A. (2013) How the dynamics of the metal-binding loop region controls the acid transition in cupredoxins, *Biochemistry 52*, 7397-7404.

131. Hira, D., Nojiri, M., and Suzuki, S. (2009) Atomic resolution structure of pseudoazurin from the methylotrophic denitrifying bacterium Hyphomicrobium denitrificans: structural insights into its spectroscopic properties, *Acta Crystallogr D Biol Crystallogr 65*, 85-92.

132. Wilson, C. J., and Wittung-Stafshede, P. (2005) Role of structural determinants in folding of the sandwich-like protein Pseudomonas aeruginosa azurin, *Proc Natl Acad Sci U S A 102*, 3984-3987.

133. Chothia, C., Gelfand, I., and Kister, A. (1998) Structural determinants in the sequences of immunoglobulin variable domain, *J Mol Biol 278*, 457-479.

134. Davidson, V. L., and Sun, D. (2002) Lysozyme-osmotic shock methods for localization of periplasmic redox proteins in bacteria, *Methods Enzymol 353*, 121-130.

135. Pace, C. N., Vajdos, F., Fee, L., Grimsley, G., and Gray, T. (1995) How to measure and predict the molar absorption coefficient of a protein, *Protein Sci 4*, 2411-2423.

136. Stevens, F. J. (2008) Meta-specific vaccine, method for treating patients immunized with meta-specific vaccine, Google Patents.

137. Ewert, S., Huber, T., Honegger, A., and Pluckthun, A. (2003) Biophysical properties of human antibody variable domains, *J Mol Biol 325*, 531-553.

138. Jespers, L., Schon, O., Famm, K., and Winter, G. (2004) Aggregation-resistant domain antibodies selected on phage by heat denaturation, *Nature biotechnology 22*, 1161-1165.

139. Nilson, B. H. K., Logdberg, L., Kastern, W., Bjorck, L., and Akerstrom, B. (1993) Purification of antibodies using protein-L-binding framework structures in the light-chain variable domain, *J Immunol Methods 164*, 33-40.

140. Woody, R. W. (1996) In *Circular Dichroism and the Conformational Analysis of Biomolecules* (Fasman, G. D., Ed.), pp 25-67, Plenum Press, New York.

141. Ma, J. K., Lee, S., Choi, M., Bishop, G. R., Hosler, J. P., and Davidson, V. L. (2008) The axial ligand and extent of protein folding determine whether Zn or Cu binds to amicyanin, *J Inorg Biochem 102*, 342-346.

142. Marcus, R. A., and Sutin, N. (1985) Electron transfers in chemistry and biology, *Biochim. Biophys. Acta 811*, 265-322.

143. Page, C. C., Moser, C. C., Chen, X., and Dutton, P. L. (1999) Natural engineering principles of electron tunnelling in biological oxidation-reduction, *Nature 402*, 47-52.

144. Davidson, V. L. (1996) Unraveling the kinetic complexity of interprotein electron transfer reactions, *Biochemistry 35*, 14035-14039.

145. Davidson, V. L. (2008) Protein control of true, gated and coupled electron transfer reactions, *Acc. Chem. Res. 41*, 730-738.

146. McIntire, W. S., Wemmer, D. E., Chistoserdov, A., and Lidstrom, M. E. (1991) A new cofactor in a prokaryotic enzyme: tryptophan tryptophylquinone as the redox prosthetic group in methylamine dehydrogenase, *Science 252*, 817-824.

147. Davidson, V. L. (2001) Pyrroloquinoline quinone (PQQ) from methanol dehydrogenase and tryptophan tryptophylquinone (TTQ) from methylamine dehydrogenase, *Advances in Protein Chemistry 58*, 95-140.

148. Husain, M., and Davidson, V. L. (1986) Characterization of two inducible periplasmic *c*-type cytochromes from *Paracoccus denitrificans*, *J Biol Chem 261*, 8577-8580.

149. Davidson, V. L., and Jones, L. H. (1996) Electron transfer from copper to heme within the methylamine dehydrogenase--amicyanin--cytochrome *c*-551i complex, *Biochemistry 35*, 8120-8125.

150. Chen, L., Durley, R., Poliks, B. J., Hamada, K., Chen, Z., Mathews, F. S., Davidson, V. L., Satow, Y., Huizinga, E., and Vellieux, F. M. (1992) Crystal structure of an electron-transfer complex between methylamine dehydrogenase and amicyanin, *Biochemistry 31*, 4959-4964.

151. Ferrari, D., Di Valentin, M., Carbonera, D., Merli, A., Chen, Z.-W., Mathews, F. S., Davidson, V. L., and Rossi, G.-L. (2004) Electron transfer in crystals of the binary and ternary complexes of methylamine dehydrogenase with amicyanin and cytochrome *c*551i as detected by EPR spectroscopy, *J. Biol. Inorg. Chem. 9*, 231-237.

152. Ferrari, D., Merli, A., Peracchi, A., Di Valentin, M., Carbonera, D., and Rossi, G. L. (2003) Catalysis and electron transfer in protein crystals: the binary and ternary complexes of methylamine dehydrogenase with electron acceptors, *Biochimica et Biophysica Acta 1647*, 337-342.

153. Merli, A., Brodersen, D. E., Morini, B., Chen, Z., Durley, R. C., Mathews, F. S., Davidson, V. L., and Rossi, G. L. (1996) Enzymatic and electron transfer activities in crystalline protein complexes, *Journal of Biological Chemistry 271*, 9177-9180.

154. Bishop, G. R., and Davidson, V. L. (1995) Intermolecular electron transfer from substrate-reduced methylamine dehydrogenase to amicyanin is linked to proton transfer, *Biochemistry 34*, 12082-12086.

155. Bishop, G. R., and Davidson, V. L. (1998) Electron transfer from the aminosemiquinone reaction intermediate of methylamine dehydrogenase to amicyanin, *Biochemistry 37*, 11026-11032.

156. Brooks, H. B., and Davidson, V. L. (1994) Kinetic and thermodynamic analysis of a physiologic intermolecular electron-transfer reaction between methylamine dehydrogenase and amicyanin, *Biochemistry 33*, 5696-5701.

157. Brooks, H. B., and Davidson, V. L. (1994) Free energy dependence of the electron transfer reaction between methylamine dehydrogenase and amicyanin, *J. Am. Chem. Soc. 116*, 11202-11202.

158. Davidson, V. L., and Jones, L. H. (1995) Complex formation with methylamine dehydrogenase affects the pathway of electron transfer from amicyanin to cytochrome *c*-551i, *Journal of Biological Chemistry 270*, 23941-23943.

159. Wang, Y. T., Graichen, M. E., Liu, A. M., Pearson, A. R., Wilmot, C. M., and Davidson, V. L. (2003) MauG, a novel diheme protein required for tryptophan tryptophylquinone biogenesis, *Biochemistry 42*, 7318-7325.

160. Hoffman, B. M., and Ratner, M. A. (1987) Gated electron-transfer - When are observed rates controlled by conformational interconversion, *J Am Chem Soc 109*, 6237-6243.

161. Leferink, N. G., Pudney, C. R., Brenner, S., Heyes, D. J., Eady, R. R., Samar Hasnain, S., Hay, S., Rigby, S. E., and Scrutton, N. S. (2012) Gating mechanisms for biological electron transfer: integrating structure with biophysics reveals the nature of redox control in cytochrome P450 reductase and copper-dependent nitrite reductase, *FEBS letters 586*, 578-584.

162. Li, X., Fu, R., Lee, S., Krebs, C., Davidson, V. L., and Liu, A. (2008) A catalytic di-heme bis-Fe(IV) intermediate, alternative to an Fe(IV)=O porphyrin radical, *Proc Natl Acad Sci U S A 105*, 8597-8600.

163. Pierce, B. G., Wiehe, K., Hwang, H., Kim, B. H., Vreven, T., and Weng, Z. (2014) ZDOCK server: interactive docking prediction of protein-protein complexes and symmetric multimers, *Bioinformatics 30*, 1771-1773.

164. Battistuzzi, G., Bellei, M., Bortolotti, C. A., and Sola, M. (2010) Redox properties of heme peroxidases, *Arch Biochem Biophys 500*, 21-36.

165. DeFelippis, M. R., Murthy, C. P., Faraggi, M., and Klapper, M. H. (1989) Pulse radiolytic measurement of redox potentials: the tyrosine and tryptophan radicals, *Biochemistry 28*, 4847-4853.

166. Tommos, C., Skalicky, J. J., Pilloud, D. L., Wand, A. J., and Dutton, P. L. (1999) De novo proteins as models of radical enzymes, *Biochemistry 38*, 9495-9507.

167. Gunner, M. R., and Dutton, P. L. (1989) Temperature and $-\Delta G^{o}$ dependence of the electron-transfer from $BPh^{\cdot -}$ to Q_a in reaction centerprotein from *Rhodobacter sphaeroides* with different quinones as Q_a, *J Am Chem Soc 111*, 3400-3412.

168. Scott, J. R., Willie, A., Mclean, M., Stayton, P. S., Sligar, S. G., Durham, B., and Millett, F. (1993) Intramolecular electron-transfer in cytochrome-b_5 labeled with Ruthenium(II)

polypyridine complexes - Rate measurements in the Marcus inverted region, *J Am Chem Soc 115*, 6820-6824.

169. Geng, J., Dornevil, K., Davidson, V. L., and Liu, A. (2013) Tryptophan-mediated charge-resonance stabilization in the bis-Fe(IV) redox state of MauG, *Proc Natl Acad Sci U S A 110*, 9639-9644.

170. Silaghi-Dumitrescu, R., Reeder, B. J., Nicholls, P., Cooper, C. E., and Wilson, M. T. (2007) Ferryl haem protonation gates peroxidatic reactivity in globins, *The Biochemical journal 403*, 391-395.

171. Souza, C. E., Maitra, D., Saed, G. M., Diamond, M. P., Moura, A. A., Pennathur, S., and Abu-Soud, H. M. (2011) Hypochlorous acid-induced heme degradation from lactoperoxidase as a novel mechanism of free iron release and tissue injury in inflammatory diseases, *PloS one 6*, e27641.

172. Jerrett, S. A., Jefferson, D., and Mengel, C. E. (1973) Seizures, H 2 O 2 formation and lipid peroxides in brain during exposure to oxygen under high pressure, *Aerospace medicine 44*, 40-44.

173. Cyrklaff, M., Sanchez, C. P., Kilian, N., Bisseye, C., Simpore, J., Frischknecht, F., and Lanzer, M. (2011) Hemoglobins S and C interfere with actin remodeling in Plasmodium falciparum-infected erythrocytes, *Science 334*, 1283-1286.

174. Meunier, B., de Visser, S. P., and Shaik, S. (2004) Mechanism of oxidation reactions catalyzed by cytochrome p450 enzymes, *Chem Rev 104*, 3947-3980.

175. Sono, M., Roach, M. P., Coulter, E. D., and Dawson, J. H. (1996) Heme-Containing Oxygenases, *Chem Rev 96*, 2841-2888.

176. Poulos, T. L. (2010) Thirty years of heme peroxidase structural biology, *Archives of biochemistry and biophysics 500*, 3-12.

177. Gumiero, A., Metcalfe, C. L., Pearson, A. R., Raven, E. L., and Moody, P. C. (2011) Nature of the ferryl heme in compounds I and II, *The Journal of biological chemistry 286*, 1260-1268.

178. Jensen, L. M., Meharenna, Y. T., Davidson, V. L., Poulos, T. L., Hedman, B., Wilmot, C. M., and Sarangi, R. (2012) Geometric and electronic structures of the His-Fe(IV)=O and His-Fe(IV)-Tyr hemes of MauG, *J Biol Inorg Chem 17*, 1241-1255.

179. Geng, J., Davis, I., and Liu, A. (2015) Probing bis-Fe(IV) MauG: experimental evidence for the long-range charge-resonance model, *Angewandte Chemie 54*, 3692-3696.

180. Davidson, V. L., and Wilmot, C. M. (2013) Posttranslational biosynthesis of the protein-derived cofactor tryptophan tryptophylquinone, *Annu Rev Biochem 82*, 531-550.

181. Abu Tarboush, N., Jensen, L. M. R., Feng, M. L., Tachikawa, H., Wilmot, C. M., and Davidson, V. L. (2010) Functional importance of Tyrosine 294 and the catalytic selectivity for the bis-Fe(IV) state of MauG revealed by replacement of this axial heme ligand with Histidine, *Biochemistry 49*, 9783-9791.

182. Dow, B. A., and Davidson, V. L. (2015) Characterization of the free energy dependence of an interprotein electron transfer reaction by variation of pH and site-directed mutagenesis, *Biochim Biophys Acta 1847*, 1181-1186.

183. Efimova, M. G., Jeanny, J., and Guillou, F. (2007) [Immunohistochemical distribution of transferrin receptors of the type 1 (TfR1) in rat seminiferous tubules at different stages of postnatal ontogenesis], *Zhurnal evoliutsionnoi biokhimii i fiziologii 43*, 504-506.

184. Mondal, M. S., Fuller, H. A., and Armstrong, F. A. (1996) Direct measurement of the reduction potential of catalytically active cytochrome c peroxidase compound I: Voltammetric detection of a reversible, cooperative two-electron transfer reaction, *J Am Chem Soc 118*, 263-264.

185. Hayashi, Y., and Yamazaki, I. (1979) Oxidation-Reduction Potentials of Compound-I-Compound-Ii and Compound-Ii-Ferric Couples of Horseradish Peroxidases A2 and C, *Journal of Biological Chemistry 254*, 9101-9106.

186. Farhangrazi, Z. S., Fossett, M. E., Powers, L. S., and Ellis, W. R. (1995) Variable-Temperature Spectroelectrochemical Study of Horseradish-Peroxidase, *Biochemistry 34*, 2866-2871.

187. Nagano, S., Tanaka, M., Ishimori, K., Watanabe, Y., and Morishima, I. (1996) Catalytic roles of the distal site asparagine-histidine couple in peroxidases, *Biochemistry 35*, 14251-14258.

188. Torimura, M., Mochizuki, M., Kano, K., Ikeda, T., and Ueda, T. (1998) Mediator-assisted continuous-flow column electrolytic spectroelectrochemical technique for the measurement of protein redox potentials. Application to peroxidase, *Anal Chem 70*, 4690-4695.

189. Krishtalik, L. I. (2011) The medium reorganization energy for the charge transfer reactions in proteins, *Biochim Biophys Acta 1807*, 1444-1456.

190. Davidson, V. L. (2004) Electron transfer in quinoproteins, *Archives of biochemistry and biophysics 428*, 32-40.

191. Ma, Z., Williamson, H. R., and Davidson, V. L. (2015) Roles of multiple-proton transfer pathways and proton-coupled electron transfer in the reactivity of the *bis*-Fe^{IV} state of MauG, *Proc. Natl. Acad. Sci. U.S.A. 112*, 10896-10901.

192. Malmstrom, B. G. (1994) Rack-induced bonding in blue-copper proteins, *European journal of biochemistry / FEBS 223*, 711-718.

193. Gumiero, A., Metcalfe, C. L., Pearson, A. R., Raven, E. L., and Moody, P. C. (2011) Nature of the ferryl heme in compounds I and II, *The Journal of biological chemistry 286*, 1260-1268.

194. Casadei, C. M., Gumiero, A., Metcalfe, C. L., Murphy, E. J., Basran, J., Concilio, M. G., Teixeira, S. C., Schrader, T. E., Fielding, A. J., Ostermann, A., Blakeley, M. P., Raven, E. L., and Moody, P. C. (2014) Heme enzymes. Neutron cryo-crystallography captures the protonation state of ferryl heme in a peroxidase, *Science 345*, 193-197.